

2014-12-18

# Developing T-type calcium channel blockers as potential therapies for pain.

Bladen, Christopher

---

Bladen, C. (2014). Developing T-type calcium channel blockers as potential therapies for pain. (Doctoral thesis, University of Calgary, Calgary, Canada). Retrieved from <https://prism.ucalgary.ca>. doi:10.11575/PRISM/25630  
<http://hdl.handle.net/11023/1967>  
*Downloaded from PRISM Repository, University of Calgary*

UNIVERSITY OF CALGARY

Developing T-type calcium channel blockers as potential therapies for pain.

by

Christopher Bladen

A THESIS

SUBMITTED TO THE FACULTY OF GRADUATE STUDIES  
IN PARTIAL FULFILMENT OF THE REQUIREMENTS FOR THE  
DEGREE OF DOCTOR OF PHILOSOPHY

GRADUATE PROGRAM IN NEUROSCIENCE

CALGARY, ALBERTA

DECEMBER, 2014

© Christopher Bladen 2014

## Abstract

Low-voltage-activated (T-type) calcium channels play a crucial role in a number of physiological processes, including neuronal and cardiac pacemaker activity and nociception. Therefore, finding specific modulators and/or blockers of T-type channels has become an important field of drug discovery. The aim of this thesis is to look at how different molecules block T-type calcium channels and to look at developing new molecules to expand the limited arsenal of drugs known to modulate this important ion channel family.

First, I examined similarities between T-type channels and their better characterized cousins, the voltage-gated sodium channels (Nav). T-types are thought to be evolutionary related to Navs as they share similar membrane topology and gating kinetics. Simple Multiple Sequence Alignment also revealed several highly conserved regions between T-type and Nav channels that corresponded to drug binding sites known to alter voltage-dependent gating kinetics. I thus reasoned that certain drugs acting on Nav may also modulate T-type channels.

My first experiments determined that a selective Nav1.8 drug (A803467) also bound selectively and potently to T-types in an area of the channel corresponding to the local anesthetic binding site found in Nav channels.

I next examined another well-characterized Nav blocker, spider toxins. Two tarantula toxins, Protoxin I and Protoxin II, had been shown to be potent and selective blockers of Nav channels and my research confirmed that these two toxins also potently and selectively blocked both Cav 3.1 and Cav 3.2 respectively.

The second part of my thesis looked at developing new compounds to block or modulate T-type channels. Studies have suggested that certain dihydropyridines (DHPs), a well known class of L-type blocking drugs, may also block T-type. We therefore synthesized a series of

novel DHP derivatives and our results indicated modifying the ester substituent dramatically increased our compounds' ability to block L-type and T-type calcium channels and furthermore, substituting the ester group with 3-pyridylmethyl, conferred approximately 30-fold selectivity to T-type versus L-type calcium channels. We then took our most effective blocker and structurally similar compounds and demonstrated in-vivo that they were efficacious in reducing pain responses in mice subjected to peripheral inflammation or nerve injury.

Finally, in the last section of my thesis, I examine some novel organic molecules that have structures similar to lipoamino acids, which are endogenous molecules known to interact with T-type calcium channels. We tested their inhibitory effects on T-type channels and then took the most effective inhibitor and demonstrated that it was also efficacious in animal models of pain.

## Acknowledgements

First, I would like to thank my supervisor, Dr. Gerald Zamponi, for giving me the opportunity to pursue a PhD in his lab. I never thought I would be given the chance to achieve this goal and I feel that he showed tremendous faith in me to take on such a task. I also knew that he would be the one person that would help me succeed and allow me to pursue my own ideas, while keeping my work focused and headed in the right direction.

I would like to thank my supervisory committee, Dr. Christophe Altier and Dr. Robert French, for encouraging and supporting my work throughout. In particular, Bob has been a great teacher and mentor in all things “Ephys.” I would also like to thank my internal and external examiners Dr. William Cole and Dr. Terence Hebert for taking the time to read my thesis and provide constructive feedback.

I would like to thank all members of the Zamponi lab, both past and present, for making most days in the lab enjoyable. In particular, I would like to thank Lina Chen for her expertise and patience in providing me with cultures, transfections and cells on demand and Jawed Hamid for being around longer than me and knowing what “Old School” truly means.

I would also like to thank two previous mentors, Dr. Steven Vincent and especially Dr. Susan Dunn, for having the faith in me to do independent research and instilling in me the enthusiasm for science that I have to this day.

I am very grateful to my funding agencies, Alberta Innovates and Health Solutions, Hotchkiss Brain Institute Dr. T. Chen Fong award, as well as the Queen Elizabeth II scholarship from the University of Calgary. Thank you for your financial support. I am also grateful to my graduate coordinators, Dr. Sarah MacFarlane, who also chaired my examination committee, Dr. Cam Teskey and Dr. Richard Wilson, for their support and guidance throughout my thesis.

Finally, I would like to thank my family. First, Tom and Lucas for providing necessary distractions and for reminding me what's really important in life and last but definitely not least, my wife Marion. She not only supported and encouraged me every step of the way, but also kept our real life organized, intact and provided a keen, critical eye for proof reading manuscripts and presentations. I would not be where I am now without you.

## **Dedication**

This thesis is dedicated to my wife Marion, who gave me the time, energy, confidence and support to complete this journey and will always be the smartest one in the family☺. I also dedicate this thesis to the memory of my parents Elizabeth (Betty) Cunningham and William (Bill) Bladen who taught me the most important lessons in life that shaped who I am today.

## Table of Contents

Abstract.....	ii
Acknowledgements.....	iv
Dedication.....	vi
Table of Contents.....	vii
List of Tables.....	x
List of Figures and Illustrations.....	xi
List of Symbols, Abbreviations and Nomenclature.....	xiv
Epigraph.....	xvii
CHAPTER ONE: INTRODUCTION.....	1
1.1 Voltage-gated calcium channels:.....	1
1.2 High-voltage activated (HVA) calcium channels:.....	4
1.2.1 Cav1 (L-type) calcium channels:.....	5
1.2.2 Cav2 (N,P,Q and R-type) calcium channels:.....	5
1.2.3 Auxiliary subunits:.....	6
1.3 Low voltage-activated (LVA) or T-type calcium channels:.....	7
1.3.1 Physiological Function:.....	10
1.3.2 Distribution:.....	13
1.3.3 Inhibition:.....	14
1.3.4 Role of T-type calcium channels in CNS disorders:.....	16
1.4 Pain:.....	17
1.4.1 The role of calcium channels in pain.....	20
1.4.2 The role of LVA calcium channels in pain:.....	20
1.5 Comparing voltage-gated sodium channels and T-type calcium channels:.....	22
1.6 Thesis rationale and significance of work carried out:.....	24
1.6.1 Hypothesis: Similarities between Sodium and T-type channels may extend to similar binding sites:.....	25
1.6.2 Aim 1: To identify common mechanisms of drug interactions with sodium and T-type calcium channels:.....	26
1.6.3 Aim 2: Synthesis and evaluation of DHP derivatives with T-type calcium channel blocking activity and their ability to attenuate inflammatory and neuropathic pain:.....	26
1.6.4 Aim 3: Characterization of novel cannabinoid based selective T-type calcium channel ligands with analgesic effects:.....	27
CHAPTER TWO: MATERIALS AND METHODS.....	30
2.1 Electrophysiology:.....	30
2.2 Data Analysis and Statistics:.....	31
2.3 Molecular Biology:.....	34
2.3.1 Site-Directed Mutagenesis:.....	34
2.3.2 CDNA Constructs:.....	34
2.3 Cell Culture:.....	34
2.3.1 tsA-201 Cell Culture and Transfection:.....	34
2.3.2 Isolation of neurons:.....	35
2.4 Animals:.....	35
2.5 Chemicals:.....	38

2.5.1 Commercial chemicals and drugs:.....	38
2.5.2 Synthesised compounds:.....	38
2.5.2.1 Synthesis of dihydropyridine derivatives: .....	38
2.5.2.2 Synthesis of carbazole derivatives:.....	40
CHAPTER THREE: COMMON MECHANISMS OF DRUG INTERACTIONS WITH SODIUM AND T-TYPE CALCIUM CHANNELS .....	46
3.1 Background:.....	46
3.2 Results and discussion .....	48
3.3 A803467 blocks T-type calcium channels:.....	48
3.4 A803467 block promotes a slow inactivation-like state of hCav3.2 .....	53
3.5 A locus analogous to the Nav local anesthetic binding site controls A803467 block of Cav3.2. ....	55
3.6 Mixed Nav1.8/Cav3.2 inhibitors – a potential strategy to treat pain? .....	64
CHAPTER FOUR: T-TYPE CALCIUM CHANNEL BLOCK BY PROTOXINS I AND II .....	66
4.1 Background:.....	66
4.2 Results.....	69
4.3 ProTx II is a preferential blocker of hCav3.2 .....	69
4.4 ProTx I is a potent and selective blocker of hCav3.1 versus other T-type channels.72	
4.5 The domain IV region of hCav3.1 is important for ProTx I block and function of hCav3.1 .....	75
4.6 Substitution of individual amino acid residues in the putative toxin blocking sites does not affect ProTx I block of hCav3.1 .....	79
4.7 Discussion:.....	82
4.8 Conclusions:.....	83
CHAPTER FIVE: SYNTHESIS AND EVALUATION OF 1,4-DIHYDROPYRIDINE DERIVATIVES WITH T-TYPE CALCIUM CHANNEL BLOCKING ACTIVITY THAT ATTENUATE INFLAMMATORY AND NEUROPATHIC PAIN .....	85
5.1 Background:.....	85
5.2 Results from novel DHP compounds.....	87
5.2.1. Tonic block of L and T-type calcium channels by novel DHP-based compounds.88	
5.2.2 Comparison of dihydropyridine block of L- and T-type calcium channels.....	90
5.4 Potent and selective DHP blockers of T-type calcium channels attenuate inflammatory and neuropathic pain. ....	95
5.4.1 Effects of DHP derivatives on transiently expressed L- and T-type calcium channels .....	95
5.5 Results of potent and selective DHP blockers on animal models of pain. ....	104
5.5.1 Effects of M12, N10 and N12 on inflammatory pain .....	104
5.5.2. Analgesic effects of M12 and N12 are mediated via Cav3.2 calcium channels	109
5.5.3. Effect of compound N12 on neuropathic pain.....	111
5.6 Discussion.....	113
CHAPTER SIX: CHARACTERIZATION OF NOVEL CANNABINOID BASED T-TYPE CALCIUM CHANNEL BLOCKERS WITH ANALGESIC EFFECTS. ....	120

6.1 Background: .....	120
6.2 Results:.....	121
6.2.1 In-vitro characterization of the novel cannabinoid-based compounds .....	121
6.2.2 Effects of Compound 9 in-vivo on acute pain, locomotor activity and Cav3.2 KO mice.....	131
6.2.3 Effect of Compound 9 on chronic neuropathic pain.....	135
6.3 Discussion:.....	137
CHAPTER SEVEN: GENERAL DISCUSSION AND FUTURE DIRECTIONS .....	139
APPENDIX A: PUBLICATIONS OVER THE SPAN OF THIS THESIS .....	170

## List of Tables

Table 1.1 Nomenclature of voltage-gated calcium channel $\alpha$ subunits .....	2
Table 3.1. Biophysical parameters of HVA and LVA calcium channels with or without drug [A803467] <sup>(221)</sup> .....	51
Table 3.2. Biophysical parameters of wild-type and mutant hCav3.2 calcium channels <sup>(221)</sup> .....	58
Table 4.1 Summary of biophysical parameters of various T-type calcium channels in the absence or presence of 1 $\mu$ M ProTx II .....	70
Table 4.2 Summary of biophysical parameters of various T-type calcium channels in the absence or presence of 1 $\mu$ M ProTx I .....	73
Table 4.3 Summary of biophysical parameters of human Cav3.1, rat Cav3.1 and hCav3.1 hCav3.3 chimeras in the absence or presence of 1 $\mu$ M ProTx I .....	78
Table 4.5 Summary of biophysical parameters of wildtype hCav3.1 and hCav3.1 domain IV and domain II mutants in the absence or presence of 1 $\mu$ M ProTx I .....	80
Table 5.2.1 Summary of biophysical parameters of various calcium channels in the absence and the presence of M4 and M12 compounds. ....	92
Table 5.4.1. Summary of biophysical parameters of hCav3.2 calcium channel in the absence and the presence of compounds N10 and N12.....	100
Table 6.2.1.1. Radioligand competitive binding assays (mean $\pm$ SEM) for carbazole-based analogues.....	123
Table 6.2.1.2. Analogues of compound 9: systematic variation in N-alkyl chain length and in the region occupied by the heterocycle.....	127
Table 6.2.1.3. Summary of biophysical parameters of hCav3.2 calcium channel in the absence and the presence of compound 9 and 10. ....	129

## List of Figures and Illustrations

Figure 1.1 Diagram of voltage-gated calcium channel $\alpha 1$ subunit membrane topology.(Modified from Tedford and Zamponi 2006).....	3
Figure 1.2 Diagram of hCav3.2 T-type calcium channel window current. ....	9
Figure 1.3 Current clamp trace showing “rebound burst” of APs (Simms and Zamponi 2014). .	12
Figure 1.5 Diagram of pain pathway (modified from Julius & Basbaum, Nature 2001). ....	19
Figure 2.1 whole cell voltage command protocol used to induce slow inactivation <sup>(221)</sup> .....	33
Figure 2.5.1 The synthetic route for the preparation of the compounds M1-10 <sup>(112)</sup> .....	43
Figure 2.5.2 The synthetic route for the preparation of the compounds N1-12, M12. <sup>(95, 227)</sup> .....	44
Figure 2.5.3 The synthetic route for the preparation of the carbazole-based compounds. ....	45
Figure 3.3.1 Tonic block of voltage-gated calcium channels by A803467 <sup>(221)</sup> .....	49
Figure 3.3.2 Effect of A803467 on activation and inactivation of T-type calcium channels <sup>(221)</sup> .....	52
Figure 3.4.1 A803467 block of Cav3 channel subtypes in a partial slow inactivated state. <sup>(221)</sup> ...	54
Figure 3.5.1 Sequence alignment of the local anesthetic binding regions in Nav channels with the analogous regions in hCav3.2. <sup>(221)</sup> .....	56
Figure 3.5.2 Summary of IC50s for tonic A803467 block of wild-type (Wt) and mutant Cav3.2 channels <sup>(221)</sup> .....	59
Figure 3.5.3. IC50 values for A803467 block of slow inactivated Cav3.2 channels <sup>(221)</sup> .....	60
Figure 3.5.4. Effect of a tyrosine substitution in position 1855 of hCav3.2 <sup>(221)</sup> .....	62
Figure 3.5.5. Summary of IC50s for tonic A803467 block of wild-type (Wt) and mutant Q1848L and Q1848F hCav3.2 channels. ....	63
Figure 4.1.1 Schematic showing various types of toxins and their sites of ion channel interaction (modified from Catterall et al., 2006) <sup>(121)</sup> .....	68
Figure 4.3.1 Tonic block of mouse neuronal or recombinant human Cav3.X (T-type) calcium channels.....	71
Figure 4.4.1 A,B,C, ProTx I Dose response (left), steady state inactivation (middle) and current voltage relations (right) for hCav3.1, hCav3.2 and hCav3.3, respectively. ....	74

Figure 4.5.1. Tonic block of hCav3.1-hCav3.3chimeras by 1 $\mu$ M application of ProTx I.....	77
Figure 4.6.1 Sequence alignment and tonic block of human Cav3.1 and Cav3.1 mutants induced by 1 $\mu$ M application of ProTx I.....	81
Figure 5.2.1 Tonic block of L and T-type calcium channels by novel DHP-based compounds. .	89
Figure 5.2.2.1 Characterization of novel M4 DHP based compound with L and T-type calcium channels.....	91
Figure 5.2.2.2 Characterization of novel M12 DHP-based compound on T-type calcium channels.....	94
Figure 5.4.1 Schematic and table showing series 2 DHP-based compounds .....	96
Figure 5.4.2. Tonic block of L and T-type calcium channels by second series of DHP-based compounds.....	98
Figure 5.4.3 Characterization of novel N10 and N12 DHP-based compounds with hCav3.2. ..	101
Figure 5.4.4 Schematic highlighting structural differences between M12 and N10-12 compounds .....	103
Figure 5.5.1.1 Effects of M12 on inflammatory pain .....	105
Figure 5.5.1.2 Effects of N10 on inflammatory pain.....	107
Figure 5.5.1.3 Effects of N12 on inflammatory pain.....	108
Figure 5.5.2. Data showing M12 and N12 analgesic effects are mediated via Cav3.2 calcium channels and have no side-effects on locomotor activity. ....	110
Figure 5.5.3 Effect of compound N12 on neuropathic pain. ....	112
Figure 5.6.1 Schematic diagram comparing compound M11 versus M12.....	116
Figure 6.2.1.1 Percentage of whole cell current inhibition of human Cav3.2 (T-type) in response to 10 $\mu$ M application of the compound series (n=6 per compound).....	122
Figure 6.2.1.2 Piperidine containing T-type Ca <sup>2+</sup> inhibitors TTA-P1, dual T-type channel blocker/cannabinoid agonist NMP7 and chemical optimization plan 1 to decrease cannabinoid receptor affinities.....	125
Figure 6.2.1.3 Biophysical parameters of hCav3.2 before and after application of compounds 9 and 10.....	130
Figure 6.2.2.1 Effects of Compound 9 in-vivo on acute pain.....	132
Figure 6.2.2.2 Effects of Compound 9 in-vivo on locomotor activity and Cav3.2 KO mice.....	134

Figure 6.2.3 Effect of Compound 9 on chronic neuropathic pain .....	136
Figure 7.1. 3-dimensional structure of NavAB as determined by the lab of W.A. Catterall.....	147

## List of Symbols, Abbreviations and Nomenclature

If you do not have any symbols, abbreviations, or specific nomenclature in your thesis, you do not need to fill out this table. To add another row to the table, with your cursor in the bottom right cell, press the TAB key (beside the letter Q on your keyboard).

Symbol	Definition
APs	Action Potentials
ASDs	Autism Spectrum Disorders
ATP	Adenosine Triphosphate
BaCl <sub>2</sub>	Barium Chloride
BBB	Blood Brain Barrier
CaMKII	Calmodulin-dependent protein kinase II
CAE	Childhood Absence Epilepsy
Cav	Voltage-gated calcium channel (gene)
CB	Cannabinoid
CCR2	Chemokine Receptor 2
cDNA	Complimentary deoxyribonucleic acid
CH <sub>2</sub> Cl <sub>2</sub>	Dichloromethane
CHCl <sub>3</sub>	Chloroform
CNS	Central Nervous System
CsCl	Cesium Chloride
CsMeSO <sub>4</sub>	Cesium Methanesulfonate

CsOH	Cesium Hydroxide
3-D	Three-dimensional
DHPs	Dihydropyridines
DMSO	Dimethyl sulfoxide
DPA	Dynamic Plantar Aesthesiometer
DRG	Dorsal Root Ganglion
GTP	Guanosine Triphosphate
HVA	High-Voltage Activated
HRMS	High Resolution Mass Spectrometry
ICK	Inhibitory Cysteine Knot
Ile	Isoleucines
i.p	Intraperitoneal
i.t	Intrathecally
Kcsa	arterial potassium channel
KO	Knock Out
LTS	Low Threshold Spikes
LVA	Low-Voltage Activated
MgCl <sub>2</sub>	Magnesium Chloride
Nav	Voltage-gated sodium channels
NIMH	National Institute of Mental Health
nRT	Thalamic reticular nucleus
PDSP	Psychoactive Drug Screening Program
Phe	Phenylalanine

PKC	Protein Kinase C
PNS	Peripheral Nervous System
ppm	Parts Per Million
SAR	Structure-Activity Relationships
SNL	Spared Nerve Ligation
SWD	Spike-Wave Discharges
TC	Thalamocortical relay
TLC	Thin Layer Chromatography
T-type	Transient opening calcium channel
TTX-S	tetrodotoxin-sensitive
TTX-R	tetrodotoxin-resistant
Tyr	Tyrosine
VGCCs	Voltage-Gated Calcium Channels
$V_h$	half-inactivation potential
$V_{0.5 \text{ act}}$	half-activation potential

## **Epigraph**

I started this journey not knowing what an “uncompensated transient” was and now I have become one!

## CHAPTER ONE: INTRODUCTION

### 1.1 Voltage-gated calcium channels:

Voltage-gated calcium channels (VGCCs) are important regulators of calcium influx into a variety of cell types<sup>(1-5)</sup>. They open in response to electrical activity to mediate calcium entry across the plasma membrane, which in turn activates a broad variety of intracellular events, ranging from neurotransmitter and hormone release and gene expression, to the contraction of smooth and cardiac muscle<sup>(1, 5-7)</sup>. There are ten members of the VGCC family that can be broadly classified into high-voltage activated (HVA) and low-voltage activated (LVA) channels based on their voltage dependence of activation (Table 1.1). The HVA channels require larger membrane depolarizations to activate and have auxiliary subunits which help regulate gating kinetics and surface expression<sup>(8-10)</sup>. The LVA channels, also known as Cav3 or T-type channels, are activated by more hyperpolarized potentials and were named T-type due to their “transient” or “tiny” current. They have much faster gating kinetics than HVA channels and as yet, have not been found to associate with auxiliary subunits<sup>(1, 11)</sup>.

All calcium channel  $\alpha 1$  subunits share a common transmembrane topology consisting of four transmembrane domains (termed D1-D4), which in turn consist of six membrane-spanning helices (termed S1–S6). A positively charged S4 segment controls voltage-dependent activation<sup>(12)</sup> and a P loop motif between S5 and S6 contains highly conserved negatively charged amino acids (glutamic acids in HVA channels) that form a highly selective permeation pathway for cations such as calcium, barium and strontium<sup>(13-15)</sup>(Figure 1.1).

Intracellular calcium concentrations in most cells are in the 100-200 nM range due to calcium-buffering and sequestration into intracellular calcium stores<sup>(2)</sup>. However, when

**Table 1.1 Nomenclature of voltage-gated calcium channel  $\alpha$  subunits**

<b>Type</b>	<b>Gated by</b>	<b>Protein</b>	<b>Gene</b>
L-type	high voltage	Cav1.1 Cav1.2 Cav1.3 Cav1.4	<i>CACNAIS</i> <i>CACNAIC</i> <i>CACNAID</i> <i>CACNAIF</i>
P-type/ Q-type	high voltage	Cav2.1	<i>CACNAIA</i>
N-type	high voltage	Cav2.2	<i>CACNAIB</i>
R-type	intermediate voltage	Cav2.3	<i>CACNAIE</i>
T-type	low voltage	Cav3.1 Cav3.2 Cav3.3	<i>CACNAIG</i> <i>CACNAIH</i> <i>CACNAII</i>

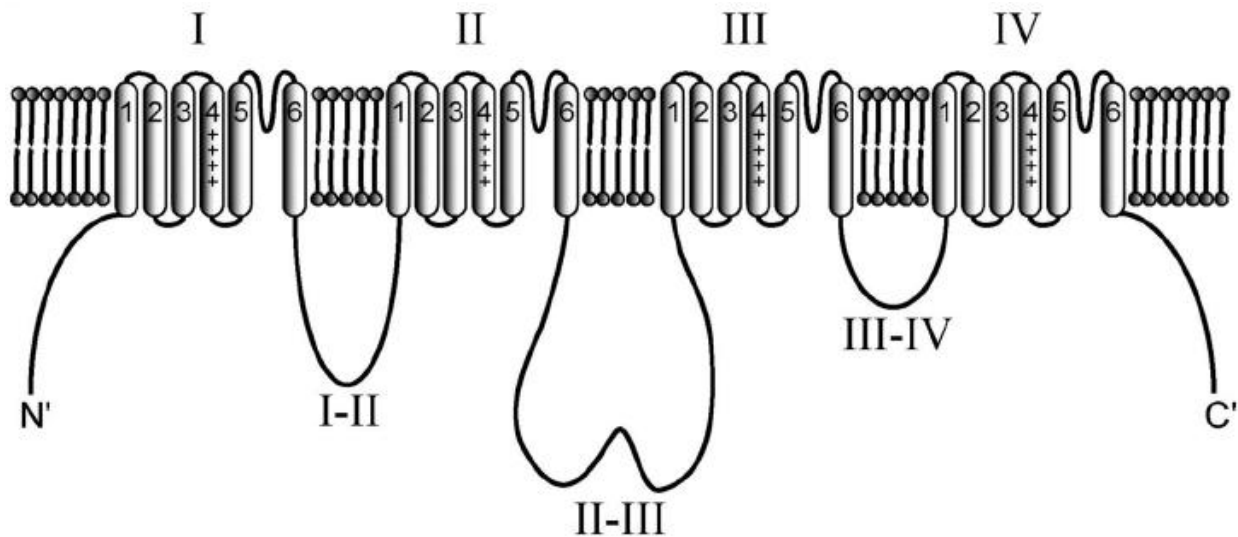


**Figure 1.1 Diagram of voltage-gated calcium channel  $\alpha_1$  subunit membrane topology.**(Modified from Tedford and Zamponi 2006).

All calcium channel  $\alpha$  subunits share a common transmembrane topology consisting of four transmembrane domains (termed D1-D4), which contain six membrane-spanning helices (termed S1–S6). Positively charged S4 segments control the voltage-dependent activation and a P loop motif between S5 and S6 forms a highly selective permeation pathway for cations such as calcium, barium and strontium to pass through.

VGCCs open, the resulting influx of calcium along the electrochemical gradient can elevate intracellular calcium levels to the high micromolar range<sup>(4)</sup>. When this occurs, it triggers a wide range of calcium-dependent processes including gene transcription and neurotransmitter release. It can also cause a calcium dependent cascade of events by activating calcium-dependent enzymes, such as calmodulin-dependent protein kinase II (CaMKII) and protein kinase C (PKC), which in turn, will trigger other signalling pathways<sup>(2, 16-18)</sup>.

Disruption of these processes and/or alterations in calcium channel activity can have detrimental effects and can lead to various neurological disorders, such as epilepsy and chronic pain<sup>(9)</sup>.

Because of this, VGCCs tend to be tightly regulated by intrinsic gating processes and by cell signaling pathways that control calcium channel activity and trafficking to and from the plasma membrane<sup>(8)</sup>. Understandably, finding drugs that can mimic this calcium channel regulation has become increasingly important to the pharmaceutical industry<sup>(19)</sup>.

## **1.2 High-voltage activated (HVA) calcium channels:**

Although not at the center of my research project, it is important to give a brief overview of HVA calcium channels, as they are expressed in some of my experiments for the purpose of examining drug selectivity. HVA calcium channels can be sub-divided into two families by their electrophysiological and pharmacological properties. Cav1 or L-type channels, play a role in muscle contraction and gene transcription and are important for both brain and heart function<sup>(20-24)</sup>. Cav2 channels that encode N,P,Q and R-types, are generally important in rapid synaptic transmission<sup>(4, 25-27)</sup>. Both Cav1 and Cav2 have several family members<sup>(1)</sup>, with the pore forming  $\alpha_1$  subunit being the key determinant of calcium channel subtype. They are heteromeric proteins that consist of a pore forming  $\alpha_1$  subunit that co-assembles with a  $\alpha_2\delta$ ,  $\beta$  and  $\gamma$  subunit to form a functional channel complex<sup>(1, 25, 28, 29)</sup>.

### **1.2.1 Cav1 (L-type) calcium channels:**

The Cav1 channel family encodes three different neuronal L-type channels (termed Cav1.2, Cav1.3, and Cav1.4) and a skeletal muscle-specific isoform, Cav1.1<sup>(30-33)</sup>. Their principle role in the brain is in gene expression, synaptic efficacy and various signalling cascades.<sup>(34)</sup> However, hints of other neurophysiological functions, come from studying Single Nucleotide Polymorphisms (SNPs) in patients with neurological diseases such as Schizophrenia, depression and Parkinson's disease, which show links to both Cav1.2 and Cav1.3 genes (for review see Simms and Zamponi, 2014)<sup>(10)</sup> They display slow voltage-dependent gating characteristics and are among the best characterized calcium channels due to the early discovery that they could be both inhibited and activated by Dihydropyridine (DHP) ligands<sup>(35, 36)</sup>. DHPs are molecules based upon pyridine that have been semi-saturated with two substituents replacing one double bond. They are well known in pharmacology as L-type calcium channel blockers and are now used extensively in the clinical treatment of cardiovascular and hypertensive diseases<sup>(11, 36-39)</sup>. However, the use of DHPs to treat other diseases, including pain and other diseases associated with LVA calcium channels, will be discussed in far greater detail in subsequent chapters<sup>(39-41)</sup>.

### **1.2.2 Cav2 (N,P,Q and R-type) calcium channels:**

Cav2 channels include three family members (Cav2.1, Cav2.2, and Cav2.3), with alternate splicing and different ancillary subunits of Cav2.1 giving rise to P- and Q-type channel isoforms<sup>(7, 10, 42, 43)</sup>. These calcium channel subtypes function predominantly to control evoked neurotransmitter release<sup>(26)</sup>. Both Cav2.1 channel variants are blocked to varying degrees by  $\omega$ -agatoxin IVA, a peptide isolated from American funnel web spider venom<sup>(44)</sup>. The Cav2.2 or N-type calcium channel<sup>(45, 46)</sup> are selectively inhibited by toxins ( $\omega$ -conotoxins GVIA and MVIIA) isolated from the venom of Marine Cone Snails<sup>(47, 48)</sup>. Cav2.3 or R-type channels<sup>(49)</sup>, are

inhibited by a peptide derived from the venom of the Giant Baboon Spider (SNX-482), which is a member of the Tarantula family of spiders<sup>(50, 51)</sup>. Interestingly, peptides derived from another member of the Tarantula family, have been shown to be potent blockers of LVA calcium channels and will be discussed in a later chapter.

### **1.2.3 Auxiliary subunits:**

As noted above, Cav1 and Cav2  $\alpha$ 1 subunits co-assemble with three distinct auxiliary subunits; Cav $\alpha$ 2 $\delta$ , Cav $\beta$  and Cav $\gamma$ ,<sup>(32, 52)</sup>. These auxiliary subunits in turn have multiple members to their protein families and this diversity and differing sub-cellular loci allow them to fulfill highly specialized roles in various cells. Proper assembly and expression of all calcium channel subunits is critical for normal channel function, as inappropriate expression, assembly and dysfunction, gives rise to a variety of disorders, including pain, epilepsy, arrhythmia, migraine and ataxia<sup>(10, 53-55)</sup>.

The Cav $\alpha$ 2 $\delta$  subunit family has four members with additional splice variants. Cav $\alpha$ 2 $\delta$  is composed of two peptides Cav $\alpha$ 2 and Cav $\delta$ . They were originally thought to be encoded by two different genes, however it has now been determined that they are encoded by the same gene<sup>(56)</sup>. The principal role of the Cav $\alpha$ 2 $\delta$  subunit is to promote trafficking to the plasma membrane and experiments involving  $\alpha$ 2 $\delta$  knockout mice show functional abnormalities in their cardiovascular system, as well as signs of epilepsy and cerebellar ataxia<sup>(53)</sup>.

To date there are four Cav $\beta$  subunits ( $\beta$ 1,  $\beta$ 2,  $\beta$ 3,  $\beta$ 4) with a number of splice variants that have been identified. They are widely expressed in excitable tissues and are important in regulating HVA calcium channel expression and modulating channel kinetics by shifting the voltage dependence of activation/inactivation to more hyperpolarized potentials<sup>(57-60)</sup>.

The importance of Cav $\beta$ 1 and Cav $\beta$ 2 subunits is highlighted by the fact that mice lacking either of these genes die *in utero* or shortly after birth<sup>(61, 62)</sup>. Cav $\beta$ 3 knockouts however, have relatively mild symptoms such as lowered anxiety and increased aggression<sup>(63)</sup>. Finally, mice lacking the Cav $\beta$ 4 encoding gene have been shown to have seizures, ataxia and paroxysmal dyskinesia, the likely cause being a decrease in expression of P/Q type channels in the cerebellum and the central nervous system (CNS) caused by knocking out this gene<sup>(64, 65)</sup>.

The  $\gamma$  subunit family contains up to eight members, whose primary functions are yet to be fully determined. These 33 kDa proteins have four trans-membrane segments and studies have shown that co-expression of  $\gamma$  subunits with HVA calcium channels can have profound effects on whole-cell current density, but only mild effects on the voltage dependent properties<sup>(66, 67)</sup>.

Given the differing roles that auxilliary subunits have on HVA calcium channel function, it is important to make sure when carrying out pharmacological studies that all subunits are present and/or co-expressed in order to properly understand drug-channel interactions.

### **1.3 Low voltage-activated (LVA) or T-type calcium channels:**

T-type calcium channels are widely expressed in the nervous and cardiovascular systems and are distinguished by their three Cav $\alpha$ 1 subunits (gene names),  $\alpha$ 1G (Cav3.1),  $\alpha$ 1H (Cav3.2) or  $\alpha$ 1I (Cav3.3). In addition, all three T-type calcium channel genes are known to be subject to alternative splicing. In human brain tissue, there are up to fifteen sites of alternative splicing of Cav3.1, fourteen sites in Cav3.2 and two splice sites reported in Cav3.3<sup>(68, 69)</sup>. They are considered LVA channels because they can be activated by relatively small depolarizations of the plasma membrane and they have relatively small single channel conductance (~5–12 pS) compared to HVA channels<sup>(1, 70-72)</sup>.

T-type calcium channels are found in both excitable and non-excitable cells (e.g., muscle, glial cells, neurons, etc.) and at physiological resting membrane potentials, T-type channels are normally closed. However, T-type calcium channels have a small “window current” that permits calcium entry at rest<sup>(72)</sup>. This window current is caused by rapid activation and inactivation kinetics that overlap to form the so called transient or “T-type” current<sup>(1)</sup> (Figure 1.2).

T-type channels are the least understood among the calcium channel families. Although most of the mammalian calcium channel genes were characterized in the late 1980s<sup>(1)</sup>, an additional decade was required for a description of the three T-type genes<sup>(73-75)</sup>. Understanding T-type channel functions continues to be hampered by the lack of selective blockers that discriminate

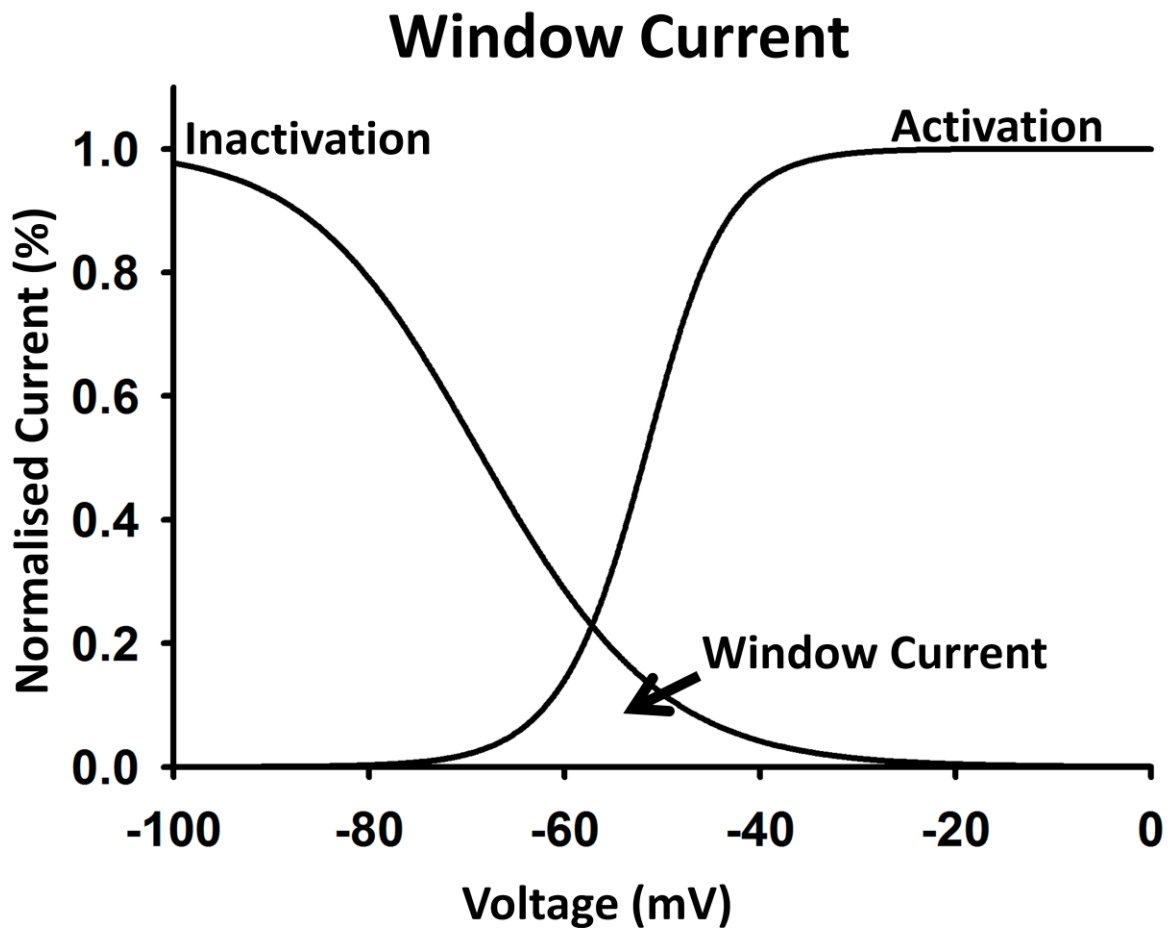


**Figure 1.2 Diagram of hCav3.2 T-type calcium channel window current.**

Window current occurs in the small range of voltage where ion channels can still be open, but also not completely inactivated (The area underneath where Inactivation and Activation intersect). In diseased states or mutant channels, slight alterations of either activation or inactivation shifts the window current, which in turn can cause excess ions to pass through and cells to become over-excited.

between the Cav3 channel sub-types, or separate the LVA calcium channels from the HVA calcium channels<sup>(76)</sup>. Indeed, the primary goal of this thesis is to try and develop more effective blockers of T-type channels in order to better understand their function.

Like HVA calcium channels, Cav3 channels are comprised of 4 domains with 6 transmembrane segments each connected by cytoplasmic linkers and flanked by intracellular N and C termini.

Cav3.1 and Cav3.2 have similar conductance, rates of activation and inactivation, and share 65% sequence identity, whereas Cav3.3 has much slower activation and inactivation kinetics, a slightly greater conductance, and only 50% sequence identity to the other two isoforms<sup>(73-75)</sup>.

### **1.3.1 Physiological Function:**

Cav3 channels activate in response to small membrane depolarizations. As mentioned above, because of their relatively small conductance and ‘window current’, a number of channels can still be open at resting membrane potentials<sup>(71, 72)</sup>. Because of these biophysical characteristics, Cav3 channels play a unique role in cellular excitability and in the generation of rhythmic oscillatory spiking and pacemaker activity.

In the heart, Cav3 channels contribute to pacemaker activity of cardiac cells through their ability to regulate self-generated rhythmic firing in the sinoatrial node<sup>(70, 77)</sup>. Dysregulation of Cav3.2 channels in the heart has been associated with cardiac hypertrophy and congestive heart failure<sup>(70, 78)</sup>.

In neurons, depolarized Cav3 channels open and generate low threshold spikes (LTS), which in turn open voltage gated sodium and potassium channels to generate a set of high frequency action potentials (APs) known as bursts. This bursting behaviour is often observed during seizure activity as well as during sleep<sup>(79, 80)</sup>.

In addition, Cav3 channels play a critical role in the 'rebound bursting' behavior found in many neurons<sup>(81)</sup>, but especially in the thalamocortical relay and thalamic reticular neurons<sup>(82, 83)</sup>. At typical neuronal resting membrane potentials most T-type channels are inactivated<sup>(84)</sup>. However, a small membrane hyperpolarization can be sufficient to recover these T-type channels from their inactivated state so that the ensuing depolarization activates a larger population of T-type channels and hence an increase in whole-cell T-type current amplitude. This increase in T-type current causes a low-threshold calcium potential, that in turn leads to the activation of voltage-gated sodium channels and a subsequent “rebound burst” of APs<sup>(85-87)</sup> (Figure 1.3).

To further understand the physiological function of T-type calcium channels, experiments involving targeted ablation or complete gene knock out (KO) have been conducted with all three genes. In Cav3.1 null mice, signs of bradycardia are apparent due to the slowing of sinoatrial node pacemaking and reduced atrioventricular conduction<sup>(88)</sup>. Cav3.1 KO mice also show resistance to baclofen-induced seizures<sup>(89)</sup>, a finding not surprising given the role of T-type channels in the thalamocortical circuitry and the recent discoveries of T-type channel mutations associated with<sup>(54, 90, 91)</sup> epilepsy. Finally, targeted deletion of Cav3.1 in the thalamus also results in increased arousal and altered sleep/wake patterns, underscoring the importance of Cav3 channels in these neurons<sup>(92)</sup>.

Some of the first experiments involving Cav3.2 KO mice showed compromised coronary function due to a permanent constriction of coronary arterioles<sup>(93)</sup>. However, these results have been overshadowed by the emergence of this channel's role in acute and chronic pain. Previous reports, as well as in experiments described in this thesis, show Cav3.2 KO mice have reduced sensitivity to acute noxious pain (consistent with the expression of these channels in a subset of afferent pain fibers), but somewhat surprisingly they do not show reduced chronic neuropathic

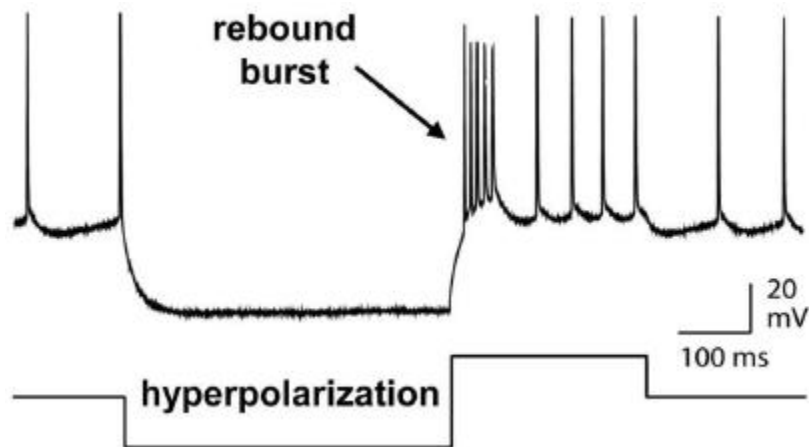


**Figure 1.3** Current clamp trace showing “rebound burst” of APs (Simms and Zamponi 2014).

At typical neuronal resting membrane potentials most T-type channels are inactivated. However, a small membrane hyperpolarization can be sufficient to recover these T-type channels from their inactivated state. The ensuing depolarization activates a larger population of T-type channels and hence an increase in whole-cell T-type current amplitude. This increase in T-type current causes a low-threshold calcium potential that in turn leads to the activation of voltage-gated sodium channels and a subsequent “rebound burst” of APs.

pain<sup>(94)</sup>. This dramatically contrasts with the results of experiments published in this thesis that show potent analgesic actions of intrathecally (i.t.) and intraperitoneal (i.p.) delivered Cav3.2 channel blockers in neuropathic pain models<sup>(95)</sup>. This apparent discrepancy may be in part due to compensation from other types of ion channels (calcium, sodium etc.) in the afferent fibers of Cav3.2 null mice that maintain pain transmission.

The role of Cav3.2 in chronic neuropathic pain is further highlighted in experiments where mice are subjected to nerve injury, colonic inflammation<sup>(96, 97)</sup>, or chronic diabetic conditions<sup>(98)</sup>. Mice in these experiments show increased T-type channel conductance in sensory neurons, which contributes to the development of the chronic pain. However, the underlying mechanisms for this remain unclear but may be due to increased surface expression or some type of posttranslational modification of the channels<sup>(99, 100)</sup>. With this in mind, Cav3.2 serves as a good example of misregulation rather than mutation, causing a disease phenotype and therefore understanding how this channel works at the molecular level is of particular importance. Given that many drugs in clinical use and under development induce state dependent block of ion channels<sup>(101-103)</sup>, finding a specific and selective blocker of Cav3.2 and possibly where and how they might bind, is a primary goal of this thesis.

Finally, little is known about the functional role of the Cav3.3 channel but recent experiments involving Cav3.3 null mice show compromised oscillatory brain wave activity in sleep spindles in thalamic reticular neurons, again underscoring the importance of T-type channels in thalamic neurons<sup>(104)</sup>.

### **1.3.2 Distribution:**

T-type calcium channels are expressed in both the peripheral and central nervous system (PNS and CNS). They are found in the heart, kidney, sperm, retina, cochlea and endocrine glands<sup>(105-</sup>

<sup>107)</sup> as well as in a number of tumor derived cell lines including NG108-15 (neuroblastoma), Y79 (retinoblastoma), U251N (glioma) and LNCaP (prostate carcinoma)<sup>(108, 109)</sup>. In the brain they are found throughout the neocortex, hippocampus, thalamus, and cerebellar neurons<sup>(110, 111)</sup>. At sub-cellular levels all three LVA channels are found within the soma, where as Cav3.1 and Cav3.2 expression has been shown within dendrites and Cav3.3 can be found in the dendritic arbours. As mentioned previously, T-type calcium channels are found throughout the thalamus with Cav3.1 being found predominantly in thalamocortical relay (TC) nuclei, whereas Cav3.2 and to a lesser extent Cav3.3 are found in the thalamic reticular nucleus (nRT)<sup>(80)</sup>. Therefore, several studies involving Cav3 channels are focused on their role in the generation of low threshold spikes (LTS) and oscillation and how this pertains to sleep and sensory perception, as well as the enhanced thalamic neuron excitability that is observed in the various forms of epilepsy<sup>(54, 91)</sup>.

### **1.3.3 Inhibition:**

Although many classes of organic molecules, including derivatives of DHPs, succinimide, diphenylbutylpiperidine and benzodiazepines have been shown to be inhibitors of Cav3 channels<sup>(11, 76, 112-116)</sup>, finding potent and selective blockers of T-type calcium channels remains difficult. Some inorganic compounds, such as divalent and trivalent cations, are known to be T-type calcium channel blockers and to date, the best way to distinguish Cav3 channels from other HVA calcium channels is thought to be by their sensitivity to nickel and their relative resistance to block by cadmium ions<sup>(74, 115, 117, 118)</sup>. Some toxins, in particular a toxin isolated from scorpion venom (kurtoxin), is known to be a potent blocker of T-type calcium channels, but this too has now been shown to also block high-voltage activated calcium channels<sup>(119, 120)</sup>. For a review of effects of toxins on ion channels see Catterall et al.,<sup>(121)</sup>.

Another drug touted to become the drug of choice for most Cav3 studies was Mibefradil, but considerable variability in T-type calcium channel pharmacology for this drug in heterologous expression systems versus native tissues, questions about its selectivity and the fact that it was pulled from clinical use for its interactions with other drugs, has seen the preference for this drug in Cav3 studies decline<sup>(122-124)</sup>.

Classes of drugs that have traditionally been thought of as sodium channel blockers, have now been shown to also block T-type calcium channels. Included in this group are; anesthetics, such as enflurane, halothane and isoflurane<sup>(125)</sup> and anticonvulsants such as phenytoin and lamotrigine<sup>(125, 126)</sup>. Whether T-type calcium channel block by these drugs has any additive or clinical relevance, is yet to be fully determined, but recent work may suggest that mixed sodium and T-type blockers can be beneficial in some models of pain<sup>(127)</sup>. Finally, other antiepileptics such as Ethosuximide, trimethadione and mesuximide inhibit T-type calcium channels and are used for the treatment of seizures, but again whether or not their mode of action is exclusively via LVA channel inhibition, remains to be elucidated<sup>(128, 129)</sup>.

More recently, small organic compounds with structures similar to endogenous lipoamino acids<sup>(113, 114, 130)</sup> and endocannabinoids<sup>(113, 130-132)</sup> have been developed, since these molecules are known to endogenously interact with T-type calcium channels, but they tend to lack selectivity and many have potential undesirable interactions with cannabinoid (CB) receptors. With this in mind, the last part of this thesis looks at developing and synthesizing compounds with similar structures, but with considerably less interaction with CB receptors and therefore potentially less harmful side effects. Indeed the inspiration for many of the experiments described in this thesis is derived from experiments that were conducted using the above “selective T-type calcium channel blockers”.

### **1.3.4 Role of T-type calcium channels in CNS disorders:**

One of the more well known involvements of Cav3 channels in neuronal excitability is the link between Cav3.2 and various forms of epilepsy. Mutations in Cav3.2 have been found in populations suffering from generalized epilepsy and in childhood absence epilepsy (CAE)<sup>(54, 90, 133, 134)</sup>. Although some of these mutations may slightly alter channel gating and membrane expression, the majority have no effect on the biophysical properties of Cav3.2 in heterologous expression systems. This suggests that these mutations may alter protein-protein interactions only found in native cells and/or have splice isoform dependent effects. In addition, mice over-expressing Cav3.1 show an increase in spike-wave discharges (SWD), while Cav3.1 knockout animals show increased resistance to treatments used to generate SWD in wild-type animals<sup>(80, 135)</sup>. Similarly, an over-expression of Cav3.2 mRNA in the hippocampus shifts the spiking mode of pyramidal cells of the hippocampus to the burst firing mode found in temporal lobe epilepsy<sup>(136-138)</sup>.

Other neurological disorders associated with Cav3 channels are Parkinson's disease and Autism Spectrum Disorders (ASDs)<sup>(22, 139)</sup>. Again, Cav3 channels are thought to be involved in generating the oscillatory burst behaviour of sub-thalamic nucleus neurons that are implicated in creating the tremors associated with Parkinson's disease<sup>(140)</sup>. However, perhaps more important is that experiments using rodent models of Parkinson's disease have shown that T-type channel blockers can be efficacious in alleviating the symptoms of this disorder<sup>(141)</sup>.

Finally, ASDs are neuro-developmental disorders that have been linked to all Cav3 channels<sup>(139, 142)</sup>. Mutations associated with autism in the Cav3.2 gene have been examined and shown to reduce T-type calcium currents in heterologous systems<sup>(142)</sup>. How these mutations cause autism, or whether other proteins or autism risk alleles are necessary to manifest this disease, remains to

be determined. Altogether, Cav3 channels play critical roles in regulating neuronal excitability and modulating or blocking T-type calcium current may provide protection from hyper-excitability disorders such as epilepsy, Parkinson's and certain forms of pain.

#### **1.4 Pain:**

Pain can be broadly divided into three categories: 1. Nociceptive pain, which is the ability of a body to sense potential harm caused by peripheral stimuli such as excess heat or a jab, 2. Inflammatory pain, which is a localized reaction that produces redness, warmth, swelling and pain as a result of infection, tissue damage, irritation, or injury (Note: inflammation can be internal or external) and 3. Pathological pain, which is a disease state caused by damage to the nervous system (neuropathic pain) or by its abnormal function (dysfunctional pain, as in fibromyalgia, irritable bowel syndrome, tension type headache, etc.)<sup>(143-148)</sup>. These can be further divided into acute pain, which generally refers to short, painful stimuli and chronic pain, which refers to long term pain such as back pain or the pain associated with illnesses such as cancer<sup>(127, 143, 149-154)</sup>.

Pain can also be thought of as an early alarm system. When the body is subjected to a potentially damaging environmental input such as described above, an electrochemical reaction generates electrical signals in the form of action potentials (APs) to be sent from the site of injury, along nerve fibers (A,  $\delta$  or C), to the dorsal root ganglion (DRG). From there, a second series of APs are generated that travel to the spinal cord dorsal horn, where they release various neurotransmitters depending on the pattern of APs arriving at the axon terminal. The pain signals then travel to the brain, via neo- and paleo-spinothalamic tracts<sup>(146, 152, 155-158)</sup>. The fast A and  $\delta$  type fibers, associated with mechanical and acute thermal pain, are relayed via the neo-spinothalamic tract and terminate in the brainstem or the thalamus with a few fibers reaching the

somatosensory cortex. The slower C fibers, associated with thermal, mechanical and chemical stimuli, connect to the paleo-spinothalamic tract and terminate principally in the medulla, pons and mesencephalon with very few fibers reaching the thalamus or cortex<sup>(158, 159)</sup> (Figure 1.5).

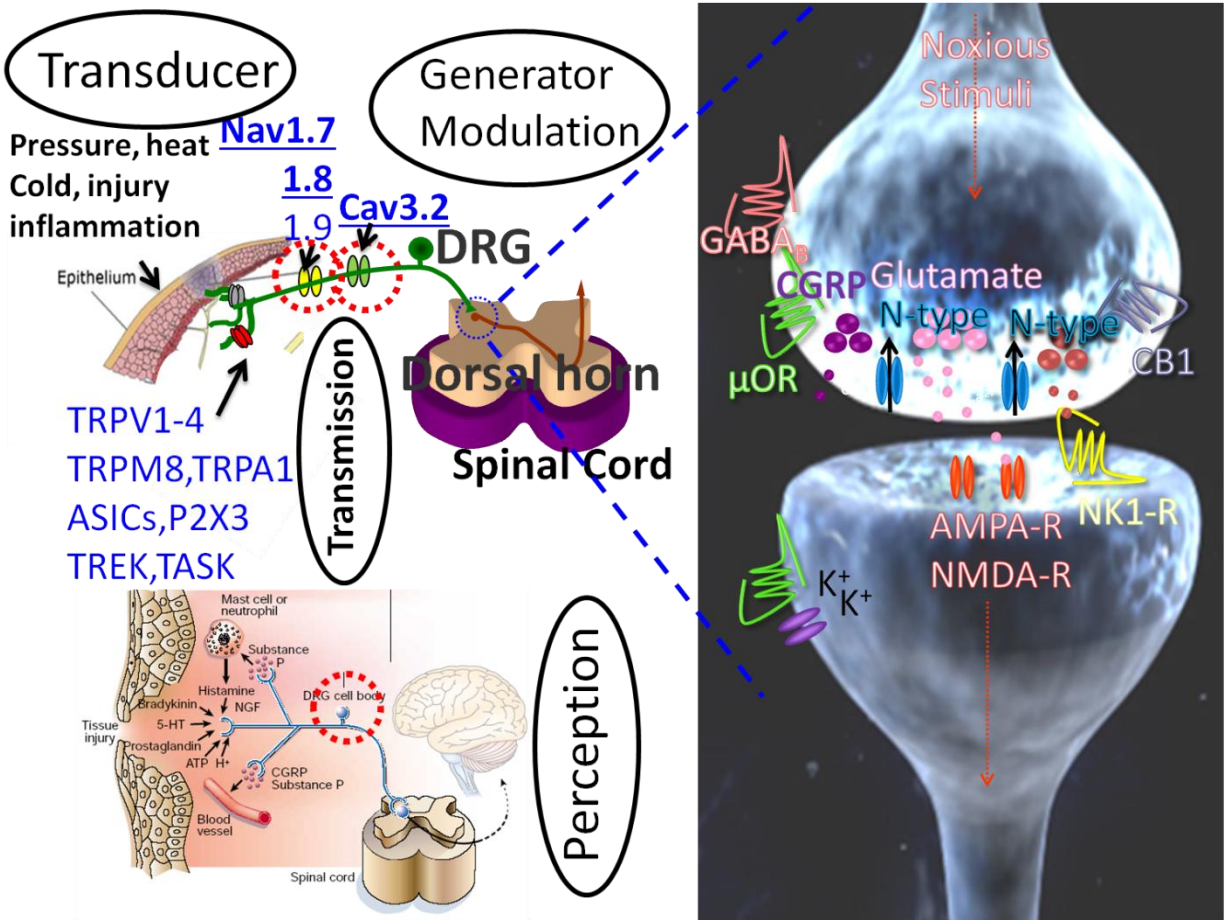


**Figure 1.5 Diagram of pain pathway (modified from Julius & Basbaum, Nature 2001).**

When nociceptors are exposed to products of injury and inflammation, their excitability is altered by a variety of intracellular signalling pathways. This figure underlines Cav3.2, Nav1.7 and Nav1.8 as important downstream targets of modulation. Activation of the nociceptor not only transmits afferent messages (towards) to the spinal cord dorsal horn (and from there to the brain), but also initiates the process of neurogenic inflammation. Neurogenic inflammation is the efferent (away) function of the nociceptor whereby release of neurotransmitters, notably substance P and CGRP from the peripheral terminal induces vasodilation.

### **1.4.1 The role of calcium channels in pain**

Originally, the role of voltage-gated calcium channels in pain was thought to be in controlling fast synaptic transmission and neuronal excitability in peripheral and central pain pathways and the principle player was/is thought to be high voltage-activated N-type calcium channels. N-type VGCCs (Cav2.2) are highly expressed at pre-synaptic nerve terminals and when a painful peripheral stimulus occurs, nociceptive neurons activate and send a train of APs to these pre-synaptic nerve terminals, where they open the Cav2.2 channels and allow calcium entry into the synapse. This cascade of chemical and electrical processes in turn triggers synaptic vesicle release of pro-nociceptive neurotransmitters such as glutamate, substance P and CGRP and further activation of spinothalamic neurons<sup>(9, 10, 94, 122, 154, 156, 160-164)</sup>. These nerve projections to the thalamus are where pain is perceived<sup>(165)</sup>.

To prevent this cascade from happening, a selective and potent N-type channel blocker would be highly desirable and the discovery that  $\omega$ -conotoxins (MVIIA or CVID), produced by fish hunting cone snails, were potent and highly selective inhibitors of N-type VGCCs appeared to be the dawn of a new era in severe chronic pain management<sup>(44, 46-48, 166)</sup>. However, the technically difficult intrathecal administration of a peptide toxin, together with several unwanted side effects, has tempered the enthusiasm for using conotoxins as a pain treatment for all but the most severe and intractable pain found in cancer patients<sup>(167-169)</sup>. Research is ongoing to discover or modify new peptide toxins that are more efficient at blocking N-type calcium channels in the PNS<sup>(170)</sup>.

### **1.4.2 The role of LVA calcium channels in pain:**

More recently another member of the VGCC family, the LVA T-type calcium channels, has been shown to have a critical function in nociception. T-type calcium channels are found in the nerve

endings of afferent fibers where they regulate neuronal excitability by lowering AP thresholds and promote bursting activity and synaptic excitability<sup>(96, 124, 171-174)</sup>. Not surprisingly then, increased T-type activity in this area leads to increased AP firing and therefore increased pain signaling. This scenario is seen in animal models of diabetic and spared nerve ligation (SNL) models of neuropathic pain, where T-type channel current density is dramatically increased<sup>(96, 98)</sup>. Conversely, Cav3.2 KO animals show reduced sensitivity to pain and reduction of neuronal activity in primary afferent fibers<sup>(94, 175-178)</sup>.

Similar to the N-type calcium channels, the functional role of LVA T-type channels in nociception, particular in the PNS, has made them an attractive target for drug discovery teams looking for novel therapies for the treatment of pain. As mentioned earlier, finding a potent and selective blocker has proved elusive (for review see Lory and Chemin, 2007)<sup>(76)</sup>. Many of the starting points for looking at blockers of T-type channels have come from identifying the endogenous modulators (ligands) of these channels and what their functional roles are in native systems. As mentioned earlier, many of the organic molecules that have been shown to modulate T-type calcium channels have structures similar to endogenous lipoamino acids. These bioactive lipids are known to interact with T-type calcium channels and T-type associated conditions such as neuronal excitability, sleep, epilepsy, neuroprotection, inflammation and pain, as well as cardiovascular modulation<sup>(113, 130-132)</sup>.

Another endogenous mechanism associated with T-type channels is Redox modulation. Inorganic divalent cations such as zinc are released from presynaptic vesicles of glutamatergic neurons and the free zinc modulates several membrane receptors, transporters and ion channels, including blockade of T-type channels<sup>(118, 179-181)</sup>. The mechanism by which this is thought to occur, is via the dis-inhibition of endogenous zinc ions<sup>(179)</sup>. The importance of this redox/zinc

regulation of T-type channels was underscored when it was shown that a single-point mutation (H191Q) in Cav3.2 reduced zinc inhibition 40-fold and completely abolished sensitivity of Cav3.2 to reducing and chelating agents<sup>(117)</sup>. In animal pain models, reducing agents and chelators of zinc have been shown to sensitize Cav3.2 containing nociceptors isolated from wild-type mice but not from Cav3.2 KO mice<sup>(98, 118, 179, 180)</sup>. Together, these findings not only emphasize the role of T-type channels in pain perception, but may offer insight and opportunity for developing novel strategies to target them and hence treat some of the pathological conditions of pain.

### **1.5 Comparing voltage-gated sodium channels and T-type calcium channels:**

From an evolutionary standpoint, T-type calcium channels (Cav3) are thought to be an intermediate between high-voltage activated calcium channels and sodium channels<sup>(182, 183)</sup>. They are both comprised of a single polypeptide with four homologous domains. Each domain has six membrane spanning alpha helices (see figure 1). Of these, the S4 segment has several positive charges and functions as the voltage sensor<sup>(184, 185)</sup>. At resting membrane potentials this helix confers channel closure to prevent ion flux. However, membrane depolarization causes this helix to move, inducing a conformational change so that ions may flow through the channels (the open state)<sup>(12, 183, 186-189)</sup>.

In both VGSCs and T-type calcium channels, there are several other putative conformational states, including fast and slow inactivation<sup>(190, 191)</sup>. In VGSCs, fast inactivation is thought to be caused by amino acids in the linker between domains III and IV of the alpha subunit coming together to form a plug or “inactivation gate” that blocks the inside of the channel shortly after it has been activated<sup>(192)</sup>. Fast inactivation mechanisms in T-type calcium channels however appear to be more complex and involve the concerted action of multiple transmembrane domains,

including the I-II linker, as well as other parts of Domain I (I-I loop), III and IV<sup>(193-196)</sup>.

Interestingly, the III-IV linker in Nav1.8, is qualitatively different from other sodium channels and is thought to be the reason why Nav1.8 has relatively slower inactivation kinetics closer to that of the T-type channels<sup>(190)</sup>.

The list of diseases associated with sodium channels is also similar to that of T-type calcium channels. Ventricular fibrillation in the heart and epilepsy in the CNS, represent two groups of diseases that have been associated with both ion channel families<sup>(1, 39, 54, 70, 77, 78, 90, 143, 197)</sup>.

At first, this might seem surprising given that they transport different ions, however, one possible explanation for this is that the mechanism that causes these diseased states may be similar in both types of ion channels. In VGSCs shifts in inactivation can cause muscle stiffness, cardiac arrhythmias and epileptic seizures because of altered transient or “window current”<sup>(143, 198)</sup>. As mentioned previously, window current is the small range of voltage where ion channels can activate but not completely inactivate (see figure 2). In diseased states, alteration of either activation or inactivation shifts the window current, which in turn can cause muscle and/or nerve cells to become over-excited<sup>(143, 198, 199)</sup>.

Likewise, in the Cav3.2 gene, the development of seizures in patients with various forms of epilepsy is thought to be brought on by slight gain-of-function effects that are also predicted to alter the window current of Cav3.2 and therefore result in more available channels at lower membrane potentials. This slight alteration would increase calcium influx and likely result in neuronal hyper-excitability and increased spike and wave discharge<sup>(6, 54, 91, 200)</sup>.

Finally, just as shifts in window current have been associated with sodium and T-type calcium channel diseases, drugs that act on both families of channels tend to preferentially bind in their inactivated or slow inactivated state, possibly explaining their therapeutic efficacy<sup>(127, 190, 201)</sup>.

Given that the structure, kinetics, pharmacology and in some cases function of sodium channels is similar to T-type calcium channels, it is not surprising that cellular localization of these channels also appears to be similar. A specific subtype of T-type channels (Cav3.2b), is highly expressed in nociceptive DRGs and Lamina I, II dorsal horn neurons and is involved in the initiation of AP firing and the generation of burst firing<sup>(81, 110, 118)</sup>. Similarly, both Nav1.7 and Nav1.8 channels are also highly expressed in these two regions and are important for setting the threshold and upstroke of AP firing and they also contribute towards the frequency and sustainability of the firing activity in these neurons<sup>(199, 202-204)</sup>.

The pro-nociceptive roles of all of these channels is confirmed in experiments where knockdown of Cav3.2 T-type channels, or knockout of either Nav1.7 or Nav1.8 channels, reduces pain responses in animal models of both acute and neuropathic pain<sup>(6, 74, 175, 205-207)</sup>. In addition, it has been proposed that the increased AP firing in DRG and dorsal horn neurons associated with chronic pain also drives sodium and calcium channels into a “protective” slow inactivated state<sup>(208-210)</sup>.

The above similarities in these two ion channel families were the starting point for this thesis. The possibility that drugs developed to simultaneously block all of these ion channels and not just selective for one, should be further explored as a potential treatment for both acute and chronic pain<sup>(127)</sup>. Furthermore, developing drugs that target the inactivated and slow-inactivated state of these channels may selectively inhibit hyper-excitabile neurons while sparing normal firing neurons.

### **1.6 Thesis rationale and significance of work carried out:**

Although the pharmaceutical industry has spent decades and enormous amounts of money on developing drugs to treat pain, their success to date has been limited. In particular, attempts to

manage neuropathic pain have proved extremely difficult with morphine and its derivatives proving to be the gold standard and pregabalin and gabapentin being the only effective treatments. Unfortunately, these types of drugs often have severe side effects, including dependency and reduced tolerance over time. In addition, morphine can cause respiratory depression and constipation, while pregabalin and gabapentin can cause dizziness and lethargy. Finding blockers or modulators of T-type calcium channels, especially those in the PNS, would therefore appear to be an effective therapeutic strategy for targeting pain hypersensitivity<sup>(127)</sup> with less potential for negative side effects. However to date, only a few selective T-type channel antagonists have been identified<sup>(11, 39, 114, 116, 127, 131, 176, 211-215)</sup>. Given the scarcity of selective T-type channel inhibitors, this thesis strived to not only better understand the mechanisms behind these inhibitors, but to also try and develop new and more potent selective T-type channel blockers as potential therapies for pain.

### **1.6.1 Hypothesis: Similarities between Sodium and T-type channels may extend to similar binding sites:**

My overall hypothesis is that the similarities in structure, gating kinetics and apparent conservation of drug binding sites of T-type and Nav channels could be exploited to help find treatments for pain and possibly other neuronal hyperexcitability disorders such as epilepsy. In addition, modifying existing T-type calcium channel blockers so that they are more potent and selective will help increase their efficacy and reduce potential side effects when used as treatments for neuropathic and inflammatory pain.

### **1.6.2 Aim 1: To identify common mechanisms of drug interactions with sodium and T-type calcium channels:**

Part one of my thesis examined the blocking kinetics of selective sodium and calcium channel blockers in both their active and inactive states to determine whether there were common mechanisms or common drug interaction sites found in these structurally similar proteins. I examined common determinants of drug action on the T-type calcium channels and the Nav1.8 sodium channel using the Nav1.8 selective Blocker A803467. Secondly, I examined how a toxin derived from Tarantula venom, which potently and selectively blocks the sodium channel Nav1.7, interacted with T-type channels and tried to identify the possible binding sites for this and other toxins.

### **1.6.3 Aim 2: Synthesis and evaluation of DHP derivatives with T-type calcium channel blocking activity and their ability to attenuate inflammatory and neuropathic pain:**

Part two of my thesis looks at developing new compounds to block and modulate T-type calcium channels. Previous studies have shown that some DHPs, normally thought of as classical L-type calcium channel blockers <sup>(216-218)</sup>, may also block LVA calcium channels.

We synthesized ten novel DHP derivatives with a condensed 1,4-DHP ring system (hexahydroquinoline) and determined how different ester groups attached to this backbone affect L- and T-type calcium channel block. By changing the substituents on the phenyl ring of our novel DHP-hexahydroquinoline scaffold, we were able to convert L-type channel blocking compounds into ones that were selective for T-type calcium channels. We then examined the functional effects of the most potent and selective T-type channel blockers on transiently expressed Cav3.2 channels and also in mouse models of inflammatory and neuropathic pain. We

also tested their effects on Cav3.2 null mice, to see if the physiological actions observed, were indeed mediated by T-type calcium channels.

### **1.6.4 Aim 3: Characterization of novel cannabinoid based selective T-type calcium channel ligands with analgesic effects:**

The final part of my thesis focuses on developing novel and selective T-type channel ligands based on structures similar to endogenous cannabinoids (endocannabinoids) called lipoamino acids<sup>(113, 114, 130)</sup>. Lipoamino acids are known to interact with T-type calcium channels and because they are closely related to endocannabinoids<sup>(113, 130-132)</sup>, they can also interact with cannabinoid (CB) receptors<sup>(113, 130-132)</sup>. However, like the interaction of morphine with  $\mu$ -opioid receptors, interactions with CB receptors, particularly CB<sub>1</sub> receptors, can have negative side effects that affect mood and memory in addition to their more well known psychoactive effects<sup>(219, 220)</sup>.

The goal of this study therefore, was to produce a compound that was effective at blocking T-type calcium channels, but had limited CB<sub>1</sub> receptor binding activity.

From previous structure activity relationships (SAR) studies, it was determined that tertiary amines were important for Cav3.2 block and that the length of the linker attaching these amines to the carbazole scaffold, effected cannabinoid receptor binding<sup>(113, 130)</sup>.

We therefore developed a series of compounds where we modified the length of the linker and tested the compounds *in-vitro* for their ability to block transiently expressed human Cav3.2 (hCav3.2) and also their affinities for CB receptors. We then tested the most potent and selective compound *in-vivo* for its ability to attenuate inflammatory and neuropathic pain in mouse models and also in Cav3.2 KO mice to determine whether the effects observed were via its' T-type calcium channel blocking ability.

Note: The data presented in the following chapters were published as papers in the following peer reviewed journals:

**Bladen, Chris;** McDaniel, Steven; Gadotti, Vinicius; Petrov, Ravil; Berger, N.; Diaz, Philippe; Zamponi, Gerald (2014).Characterization of novel cannabinoid based selective T-type calcium channel ligands with analgesic effects." ACS Chem Neurosci 2014. Oct 14. Epub 2014 Oct 14.

**Chris Bladen,** Vinicius M. Gadotti, Miyase G. Gündüz, N. Daniel Berger, Rahime Şimşek, Cihat Şafak and Gerald W. Zamponi. 2014. 1,4-Dihydropyridine derivatives with T-type calcium channel blocking activity attenuate inflammatory and neuropathic pain. Pflügers Archiv 2014. Jul 3. Epub 2014 Jul 3.

**Chris Bladen,** Jawed Hamid, Ivana Assis-Souza, and Gerald W. Zamponi 2014. Block of T-type calcium channels by protoxins I and II. Mol Brain 2014. 9;7:36. Epub 2014 May 9.

**Bladen C,** Gündüz MG, Şimşek R, Şafak C and Zamponi GW. 2013. Synthesis and evaluation of 1,4-Dihydropyridine derivatives with calcium channel blocking activity. Pflügers Archiv 2014. Jul 23;466(7):1355-63. Epub 2013 Oct 23<http://dx.doi.org/10.1007/s00424-013-1376-z>

**Bladen C,** Taking a bite out of pain: Snake venom can be both a curse and a cure when targeting acid sensing ion channels (ASICs) in the pain pathway. Channels 2013 7:1-2.

**Bladen C, Zamponi GW.** Common mechanisms of drug interactions with sodium and T-type calcium channels. *Mol Pharmacol* 2012. 82:481-7.

## CHAPTER TWO: MATERIALS AND METHODS

### 2.1 Electrophysiology:

Whole-cell voltage-clamp recordings from tsA-201 cells were performed at room temperature 2 to 3 days after the transfection. Whole-cell voltage-clamp recordings on Neuronal cells were performed at room temperature, the following day after isolation. For all experiments, the external recording solution contained (in mM): 114 CsCl, 20 BaCl<sub>2</sub>, 1 MgCl<sub>2</sub>, 10 HEPES, 10 Glucose, adjusted to pH 7.4 with CsOH. For voltage-clamp recordings on neuronal cells, 5  $\mu$ M CdCl<sub>2</sub> was also added to the external solution to inhibit high voltage activated calcium channels. The internal patch pipette solution for all experiments contained (in mM): 126.5 CsMeSO<sub>4</sub>, 2 MgCl<sub>2</sub>, 11 EGTA, 10 HEPES adjusted to pH 7.3 with CsOH. Internal solution was also supplemented with 0.6 mM GTP and 2 mM ATP just prior to use. Liquid junction potentials for the above solutions were left uncorrected.

Tested compounds were prepared daily in external solution and were applied locally to cells with the use of a custom built gravity driven micro-perfusion system that permits solution exchanges in less than 1 second<sup>(166)</sup>. A series of vehicle only control experiments were performed to ensure that there were no time dependent shifts in half-activation and half-inactivation potentials, and no such changes were observed (data not shown). Currents were measured using the whole-cell patch clamp technique and an Axopatch 200B amplifier in combination with Clampex 9.2 software (Molecular Devices, Sunnyvale, CA). After establishing whole cell configuration, cellular capacitance was minimized using the amplifier's built-in analog compensation. Cut-off for allowable series resistance was set at <10 M $\Omega$  and was compensated by at least 85% in all experiments. All data were digitized at 10 kHz with a Digidata 1320 interface (Molecular Devices) and filtered at 1 kHz (8-pole Bessel filter). In addition to collecting the raw data, a p/4

online leak-subtraction protocol was used (the p/4 protocol involved 4 very brief hyperpolarizing pulse which should have a negligible effect on drug interactions). Non leak subtracted currents were acquired in parallel for quality control purposes. In current-voltage relation studies, the membrane potential was held at -110 mV and cells were depolarized from -80 to 20 mV in 10 mV increments. For steady-state inactivation studies, the membrane potential was depolarized to 0 mV for rCav1.2 and to -20 mV for all T-type calcium channels, after 3.6-second conditioning pre-pulses of ranging from -110 to 0 mV or -20 mV, respectively (initial holding at -110 mV). Individual sweeps were separated by 12 seconds to permit complete recovery from inactivation between conditioning pulses. The duration of the test pulse was typically 200 ms and the current amplitude obtained from each test pulse was normalized to that observed at the holding potential of -110 mV. For slow inactivation studies, channels were assessed using a test pulse (P2) that followed a 10-s conditioning pre-pulse of between -70 or -80mV to elicit a peak current amplitude that was approximately 50 to 60% of the initial test pulse (P1) (Figure 2.3)<sup>(221)</sup>.

## **2.2 Data Analysis and Statistics:**

Data were analyzed using Clampfit 9.2 (Molecular Devices). Origin 7.5 software (Northampton, MA, USA) was used in the preparation of all figures and curve fittings. Current-voltage relationships were fitted with the modified Boltzmann equation:  $I = [G_{max} * (V_m - E_{rev})] / [1 + \exp((V_{0.5act} - V_m) / k_a)]$ , where  $V_m$  is the test potential,  $V_{0.5act}$  is the half-activation potential,  $E_{rev}$  is the reversal potential,  $G_{max}$  is the maximum slope conductance, and  $k_a$  reflects the slope of the activation curve. Steady-state inactivation curves were fitted using the Boltzmann equation:  $I = 1 / (1 + \exp((V - V_h) / k))$ , where  $V$  is the conditioning potential,  $V_h$  is the half-inactivation potential and  $k$  is the slope factor.

Dose-response curves were fitted with the equation  $y = A2 + (A1-A2)/(1 + ([C]/IC50)^P)$  where  $A1$  is initial current amplitude and  $A2$  is the current amplitude at saturating drug concentrations,  $[C]$  is the drug concentration and  $P$  is the Hill coefficient. Statistical significance was determined by paired or unpaired Student's  $t$ -tests and one-way or repeated measures ANOVA, followed by Dunnett's test or Tukey's Multiple Comparison tests. Significant values were set as indicated in the text and figure legends. All data are given as means  $\pm$  standard errors.

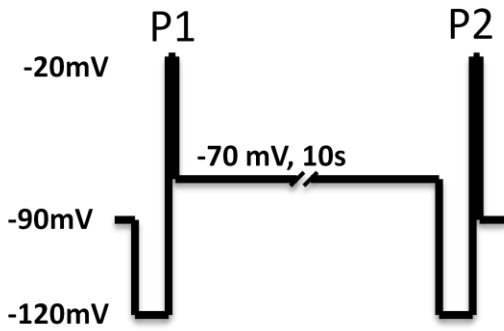


**Figure 2.1 whole cell voltage command protocol used to induce slow inactivation<sup>(221)</sup>.**

A test pulse P1, followed by a 10 second conditioning pulse to -70 mV, then a hyperpolarization step to remove fast inactivation and a second test pulse P2 to determine the fraction of slow inactivated channels.

## **2.3 Molecular Biology:**

### **2.3.1 Site-Directed Mutagenesis:**

Site-Directed Mutagenesis was performed using the QuikChange II™ Site-Directed Mutagenesis Kit and protocols from Agilent Technologies Inc. Mutations were then verified by on-site sequencing of the full length cDNA clone.

### **2.3.2 CDNA Constructs:**

Human Cav3.2, rat Cav1.2, and rat Cav2.1 cDNA constructs, as well as ancillary calcium channel subunit cDNAs were kindly provided by Dr. Terrance Snutch (University of British Columbia, Vancouver, Canada). Human Cav3.3 was obtained from Dr. Arnaud Monteil (CNRS Montpellier, France). Human Cav3.1 was cloned and described previously by our laboratory<sup>(222)</sup> and human Cav3.1 and Cav3.3 chimeras were also described previously<sup>(193)</sup>.

## **2.3 Cell Culture:**

### **2.3.1 tsA-201 Cell Culture and Transfection:**

Human embryonic kidney tsA-201 cells were cultured and transfected using the calcium phosphate method as described previously<sup>(60)</sup>. In experiments involving human Cav3.1, Cav3.2, and Cav3.3,  $\alpha$ 1 subunits were co-transfected (6  $\mu$ g) with enhanced green fluorescent protein (EGFP) DNA (0.5  $\mu$ g of EGFP; Clontech) as a marker. For rat L-type calcium channel experiments, Cav1.2  $\alpha$ 1 subunit (3  $\mu$ g), rat Cav $\alpha$ 1b (3  $\mu$ g) and rat Cav $\alpha$ 2 $\delta$  (3  $\mu$ g) were co-transfected together with EGFP as above. For experiments involving L- and P/Q type calcium channels, rCav1.2 or rCav2.1,  $\alpha$ 1 subunits (3  $\mu$ g), were each co-transfected with rat  $\beta$ 1b (3  $\mu$ g) or rat  $\beta$ 4 (3  $\mu$ g). For experiments involving T-type calcium channels, hCav3.1, hCav3.2, and hCav3.3,  $\alpha$ 1 subunits were transfected. Transfected cells were incubated 48 hours at 37°C and

5% CO<sub>2</sub>, then re-suspended with 0.25% (w/v) trypsin-EDTA (Invitrogen) and plated on glass coverslips a minimum of 3 to 4 hours before patching

### **2.3.2 Isolation of neurons:**

Thalamic neurons were isolated as described previously<sup>(223)</sup>. Briefly, thalami of adult mice were dissected out, cut into small pieces and then digested in papain (Worthington, LS003126) containing culture media. After digestion, the tissue was washed and triturated for neuron dissociation. Thalamic neurons were then seeded at low density onto coverslips pretreated with poly-d-lysine (Sigma, P7280). Dorsal Root Ganglia (DRG) neurons were isolated as described previously<sup>(127)</sup>. Briefly, DRG from adult mice were removed and placed in Ca<sup>2+</sup> and Mg<sup>2+</sup>-free Hank's Balanced Salt Solution, containing (in mM): 140 NaCl, 5.3 KCl, 0.4 KH<sub>2</sub>PO<sub>4</sub>, 0.3 Na<sub>2</sub>HPO<sub>4</sub>, 6 D-glucose, 10 HEPES, and 2 mg/mL collagenase (Type I, Worthington, Lakewood, New Jersey), and 200 units of DNaseI (Worthington, Lakewood, New Jersey). Ganglia were then incubated for 45 min at 37 °C and subsequently placed in media supplemented with 10 % fetal bovine serum to stop digestion. Cells were then dispersed with fire polished Pasteur pipettes and plated on glass coverslips coated with 100 µg/mL poly-L-lysine.

### **2.4 Animals:**

All experiments involving live animals were performed by Vinicius Gadotti with assistance from Daniel Berger. All animal experiments and protocols in this manuscript were approved by the Animal Care Committee of the University of Calgary and comply with the laws of the Canadian Council on Animal Care. During experiments, all efforts were made to minimize animal suffering according to the policies and recommendations of the International Association for the Study of Pain. For all experiments, either adult male C57BL/6J (wild-type) or CACNA1H knockout (Cav3.2 null) mice (20-25g) purchased from Jackson Laboratories were used. There

were a maximum of five mice per cage (30 × 20 × 15 cm) and access to food and water was unlimited. Temperature was kept at 23 ± 1°C on a 12 h light/dark cycle (lights on at 7:00 a.m.). I.p. injections of drugs were a constant volume of 10 ml/kg body weight. I.t. injections used volumes of 10 µl and were performed using the method described previously<sup>(224)</sup> and carried out routinely in our laboratory<sup>(113, 225)</sup>. All drugs were dissolved in DMSO and control animals received PBS + whatever the maximum DMSO concentration was in drug solutions delivered to animals (typically 1% DMSO). For each test, a different group of mice were used and only one experiment per mouse was performed.

#### **2.4.1 Formalin Test:**

Mice were acclimatized in the laboratory for at least 60 minutes prior to experiments. Animals were then injected intraplantarly in the ventral surface of the right hindpaw with 20 µl of a formalin solution (1.25%) made up in PBS. Following intraplantar injection of formalin, individual animals were placed immediately into observation chambers and monitored from 0-5 min (acute nociceptive phase) and 15-30 min (inflammatory phase). The time spent licking or biting the injected paw was then considered as a nociceptive response and recorded with a chronometer. Experimental compounds were delivered by i.t. (20 minutes prior) or by i.p. (30 minutes prior) and their effects on both the nociceptive and inflammatory phases of the formalin test were evaluated.

#### **2.4.2 Open-field test:**

Animals received compounds via intraperitoneal injection (i.p.) (30 mg/kg) 30 minutes before testing and the ambulatory behavior of the treated animals was assessed in an open-field test as described previously<sup>(225)</sup>. Briefly, the apparatus consisted of a wooden box measuring 40 x 60 x 50 cm with a glass front wall. The floor was divided into 12 equal squares and the entire

apparatus was placed in a sound free room. Animals were placed in the rear left square and left to explore freely and the number of squares crossed with all paws (crossing) in a 6 minute timeframe was counted. After each individual mouse session, the apparatus was then cleaned and dried with a 10% alcohol solution.

#### **2.4.3 Partial Sciatic Nerve Injury (PNI)-induced neuropathic pain:**

Before surgery, mice were anaesthetised with isoflurane (5% induction, 2.5% maintenance). Partial ligation of the sciatic nerve was performed by tying the distal 1/3 to 1/2 of the dorsal portion as previously described<sup>(226)</sup>. In sham-operated mice, the sciatic nerve was exposed without ligation and all wounds were closed and treated with iodine solution. Fourteen days post surgery, mice received either Compound (30 mg/kg, i.p.) treatment or vehicle, while sham-operated animals received only vehicle (10 ml/kg, i.p.). The mechanical hyperalgesia responses were then recorded immediately before the surgeries (baselines), 14 days after the surgeries (0), and at various time points (0.5, 1, 2, 3 h) after treatment.

#### **2.4.4 Evaluation of mechanical Hyperalgesia:**

Mechanical hyperalgesia was then measured using a Dynamic Plantar Aesthesiometer (DPA, Ugo Basile, Varese, Italy). Animals were placed individually in small enclosed testing arenas (20 cm × 18.5 cm × 13 cm, length × width × height) on top of a wire mesh floor. Mice were allowed to acclimate for a period of at least 90 minutes. The DPA device was positioned beneath the animal, so that the filament was directly under the plantar surface of the ipsilateral hind paw. Each paw was tested three times per session.

## **2.5 Chemicals:**

### **2.5.1 Commercial chemicals and drugs:**

Unless stated otherwise, all chemicals and reagents were purchased from Sigma (St. Louis, MO). In experiments described in chapter 3, A803467 was purchased from Tocris Bioscience (Ellisville, MO) and was dissolved in dimethyl sulfoxide (DMSO) at the stock concentrations of 10 mM or 30 mM. Working solutions of drug were made in external recording solutions so that the final concentration of DMSO was 0.1% or less. Calcium channel currents were not affected by 0.1% DMSO.

Both ProTx I and ProTx II were purchased from Alomone Labs (Jerusalem, Israel) and were dissolved in external recording solution at the stock concentration of 1 mM. All subsequent dilutions were also made in external recording solution.

### **2.5.2 Synthesised compounds:**

#### **2.5.2.1 Synthesis of dihydropyridine derivatives:**

All synthesis and chemistry used to develop novel DHP-based compounds were performed by Dr. Miyase Gözde Gündüz and the Department of Pharmaceutical Chemistry, Faculty of Pharmacy, Hacettepe University, Ankara, Turkey.

All chemicals used in this study were purchased from Aldrich and Fluka (Steinheim, Germany). Some reactions were carried out using a Discover Microwave Apparatus (CEM). Thin layer chromatography (TLC) was run on Merck aluminium sheets, Silica gel 60 F254 (Darmstadt, Germany), mobile phase ethyl acetate-hexane: (1:1) and ultraviolet (UV) absorbing spots were detected by short-wavelength (254 nm) UV light (Camag UV Cabinet, Wiesloch, Germany). Melting points were determined on a Thomas Hoover Capillary Melting Point Apparatus (Philadelphia, PA, USA) and were uncorrected. <sup>1</sup>H-NMR spectra were obtained in dimethyl

sulfoxide (DMSO) solutions on a Varian Mercury 400, 400 MHz High Performance Digital FT-NMR Spectrometer (Palo Alto, CA, USA). Chemical shifts are reported in parts per million (ppm) relative to tetramethylsilane. Mass spectra were obtained on an Agilent 5973 Network Mass Selective Detector by electron ionization (Philadelphia, PA, USA). Elemental analyses were performed on a Leco CHNS-932 Elemental Analyzer (Philadelphia, PA, USA).

**Synthesis of M-series compounds:** DHP-based compounds were synthesized using a microwave-assisted one-pot method for M-series compounds 1-5. These compounds were achieved by the reaction of 4,4-dimethyl-1,3-cyclohexanedione, 5-nitrosalicylaldehyde, alkyl acetoacetate and ammonium acetate in methanol, according to a modified Hantzsch reaction. The benzoyl moiety was introduced in the 4-phenyl ring of these DHPs by refluxing with benzoyl chloride in acetone in the presence of anhydrous potassium carbonate (Compound 6-10)<sup>(112)</sup>. Synthesis of compounds 11 and 12 has been described previously<sup>(227)</sup> but briefly: 0.001 mol appropriate 1,3-cyclohexanedione (1,3-cyclohexanedione, 4,4-dimethyl-1,3-cyclohexanedione), 2,3-disubstituted benzaldehyde (0,001 mol), 3-pyridylmethyl 3-oxobutanoate (0,001 mol) and ammonium acetate (0,005 mol) were refluxed for 8 h. in 15 mL methanol. The precipitates, which were obtained after cooling the reaction mixture, were filtered to achieve the target compounds.

The general procedure for the preparation of alkyl 4-(2-hydroxy-5-nitrophenyl)-2,6,6-trimethyl-5-oxo-1,4,5,6,7,8-hexahydroquinoline-3-carboxylates (Compound 1-5) was as follows: One-pot four component mixture: 2 mM 4,4-dimethyl-1,3-cyclohexanedione, 2 mM 5-nitrosalicylaldehyde, 2 mM appropriate alkyl acetoacetate and 10 mM ammonium acetate were placed into 35 mL-microwave pressure vial and heated under microwave irradiation (power 50 W, maximum temperature 120 °C) for 10 min in 5 mL methanol. After the reaction was

completed, monitored by TLC, the reaction mixture was poured into ice-water, the obtained precipitate was filtered and crystallized from methanol-water.

The general procedure for the preparation of alkyl 4-(2-(benzoyloxy)-5-nitrophenyl)-2,6,6-trimethyl-5-oxo-1,4,5,6,7,8-hexahydroquinoline-3-carboxylates (Compound 6-10) was as follows: 1mM synthesized 1,4-dihydropyridine derivative (Compound 1-5), 1.5mM benzoyl chloride and 2 g anhydrous potassium carbonate were refluxed in 15 mL acetone for 4 h. The resulting slurry was filtered out and the solvent was removed using a rotary evaporator. The obtained sticky residue was crystallized from ethanol-water to achieve the target compound. The structures of all compounds were elucidated by spectral methods and confirmed by elemental analysis. The synthetic route for the preparation of all the compounds 1-12 have been outlined in Figure 2.1.1<sup>(112)</sup>.

#### **Synthesis of N-series compounds:**

Compounds N1-N12 were synthesized as described previously<sup>(95, 227)</sup>. The synthetic route for the preparation of these compounds has been outlined in Figure 2.1.2.<sup>(95)</sup> The structures of all compounds were elucidated by spectral methods and confirmed by elemental analysis.

DHP-based compounds were dissolved in DMSO at the stock concentrations of 1,10 or 30 mM. Final dilutions were made in external recording solutions so that the final concentration of DMSO was 0.1% or less.

#### **2.5.2.2 Synthesis of carbazole derivatives:**

All synthesis and chemistry used to develop novel carbazole derivatives were performed by Dr. Philippe Diaz and the Core Laboratory for Neuromolecular Production, The University of Montana, Missoula, MT, USA.

All moisture sensitive reactions were performed in an inert, dry atmosphere of argon in flame dried glassware. Air sensitive liquids were transferred via syringe or cannula through rubber septa. Reagent grade solvents were used for extraction and flash chromatography. THF was distilled from Na/benzophenone under argon; dichloromethane ( $\text{CH}_2\text{Cl}_2$ ) and chloroform ( $\text{CHCl}_3$ ) were distilled from  $\text{CaH}_2$  under argon. All other reagents and solvents which were purchased from commercial sources were used directly without further purification. The progress of reactions was checked by analytical thin-layer chromatography (Sorbent Technologies, Silica G TLC plates w/UV 254). The plates were visualized first with UV illumination followed by charring with ninhydrin (0.3% ninhydrin (w/v), 97:3 EtOH-AcOH). Flash column chromatography was performed using prepacked Biotage SNAP cartridges on a Biotage Isolera One instrument. The solvent compositions reported for all chromatographic separations are on a volume/volume (v/v) basis.  $^1\text{H}$ NMR spectra were recorded at 400 or 500 MHz and are reported in parts per million (ppm) on the  $\delta$  scale relative to tetramethylsilane as an internal standard.  $^{13}\text{C}$ NMR spectra were recorded at 100 or 125 MHz and are reported in ppm on the  $\delta$  scale relative to  $\text{CDCl}_3$  ( $\delta$  77.00). Melting points were determined on a Stuart melting point apparatus from Bibby Scientific Limited and are uncorrected. High Resolution mass spectrometry (HRMS) was performed on a Waters/Micromass LCT-TOF instrument. All compounds were more than 95% pure.

The synthesis of the carbazoles derivatives is outline in Figure 2.2 Amidation under standard peptide coupling conditions of previously described N-alkylated carbazole-3-carboxylic derivatives 2 with Boc-protected amines afforded the desired amide derivatives 3 and 6. The resulting coupling products were then de-protected using TFA in dichloromethane to afford compounds 4 and 8 that were then alkylated with N-tert-butyl-2-chloroacetamide to attain the

desired compounds (9, 10, 13, 16, and 19). Compound 20 was prepared by reductive amination of compound 4 using 3,3-dimethylbutyraldehyde. In vitro receptor radioligand CB1 and CB2 binding studies: CB1 and CB2 radioligand binding data were obtained using National Institute of Mental Health (NIMH) Psychoactive Drug Screening Program (PDSP) resources as described earlier<sup>(130, 228, 229)</sup>.

Carbazole-based compounds were dissolved in DMSO at the stock concentrations of 10 mM or 30 mM. Final dilutions were made in external recording solutions so that the final concentration of DMSO was 0.1% or less. Calcium channel currents were not affected by 0.1% DMSO.

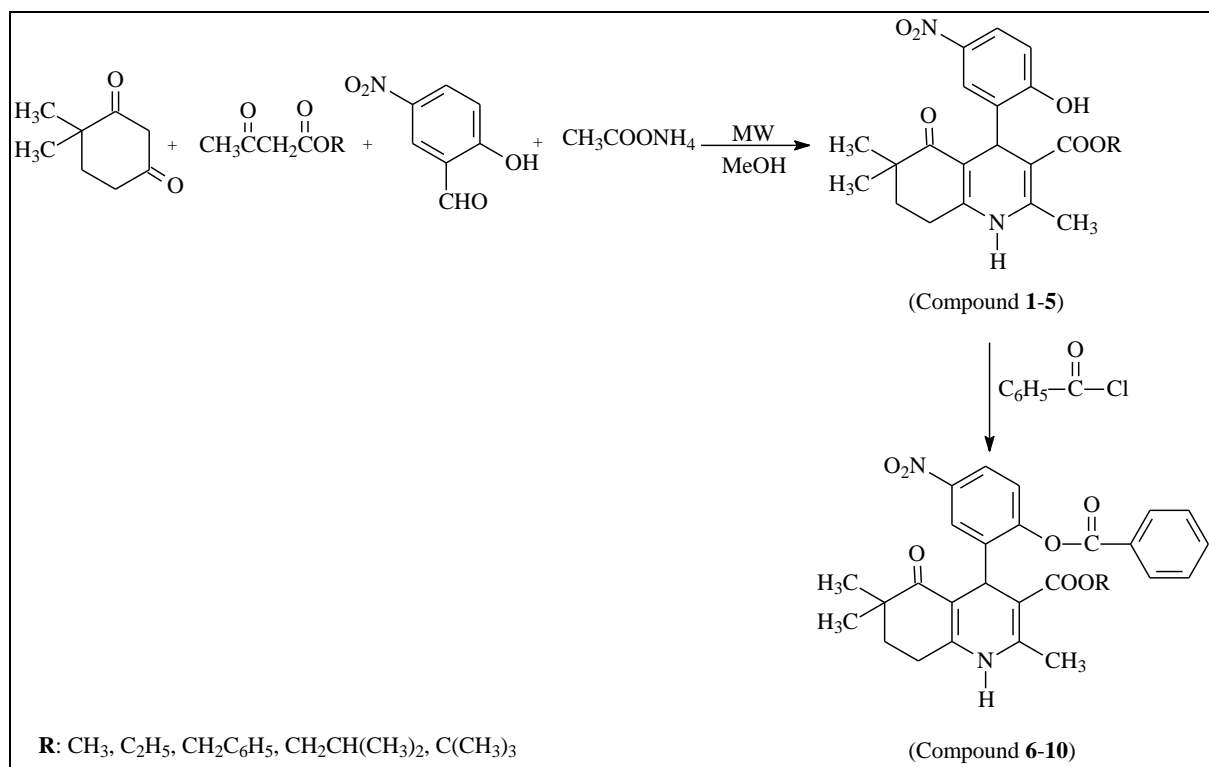


**Figure 2.5.1** The synthetic route for the preparation of the compounds **M1-10**<sup>(112)</sup>.

General procedure for the preparation of alkyl 4-(2-hydroxy-5-nitrophenyl)-2,6,6-trimethyl-5-oxo-1,4,5,6,7,8-hexahydroquinoline-3-carboxylates (Compound 1-5): One-pot four component mixture of 0.002 mol 4,4-dimethyl-1,3-cyclohexanedione, 0.002 mol 5-nitrosalicylaldehyde, 0.002 mol appropriate alkyl acetoacetate and 0.01 mol ammonium acetate was filled into 35 mL-microwave pressure vial and heated under microwave irradiation (power 50 W, maximum temperature 120 °C) for 10 min in 5 mL methanol. After the reaction was completed, monitored by TLC, the reaction mixture was poured into ice-water, the obtained precipitate was filtered and crystallized from methanol-water. General procedure for the preparation of alkyl 4-(2-(benzyloxy)-5-nitrophenyl)-2,6,6-trimethyl-5-oxo-1,4,5,6,7,8-hexahydroquinoline-3-carboxylates (Compound 6-10): 0.001 mol synthesized 1,4-dihydropyridine derivative (Compound 1-5), 0.0015 mol benzoyl chloride and 2 g anhydrous potassium carbonate were refluxed in 15 mL acetone for 4 h. The resulting slurry was filtered out and the solvent was removed using a rotary evaporator. The obtained sticky residue was crystallized from ethanol-water to achieve the target compound.

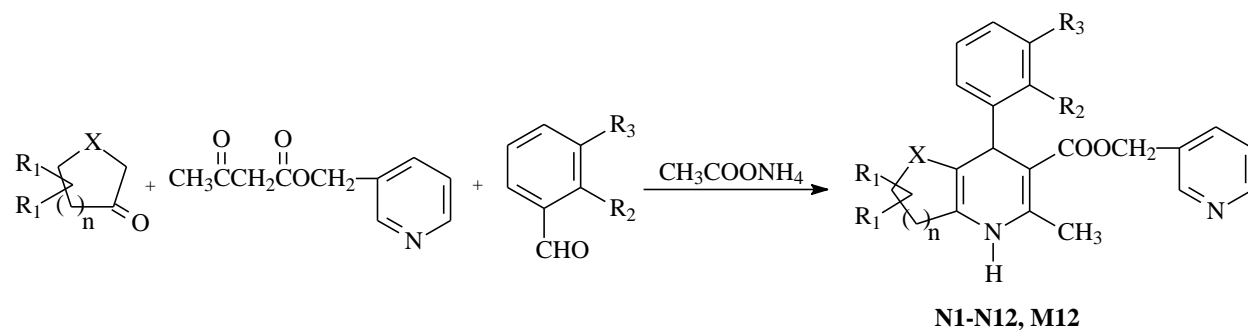


**Figure 2.5.2** The synthetic route for the preparation of the compounds **N1-12, M12**.<sup>(95, 227)</sup>

1 mmol tetrahydrothiophene-3-one-1,1-dioxide (N1-N3) or appropriate cyclic diketone (1,3-cyclohexanedione / 4,4-dimethyl-1,3-cyclohexanedione / 5,5-dimethyl-1,3-cyclohexanedione), 1 mmol 2,3-disubstituted benzaldehyde, 1 mmol 3-pyridylmethyl 3-oxobutanoate and 5 mmol ammonium acetate were refluxed for 8 h. in 15 mL methanol. The precipitates, which were obtained after cooling the reaction mixture, were filtered and crystallized from appropriate solvents to achieve the target compounds.

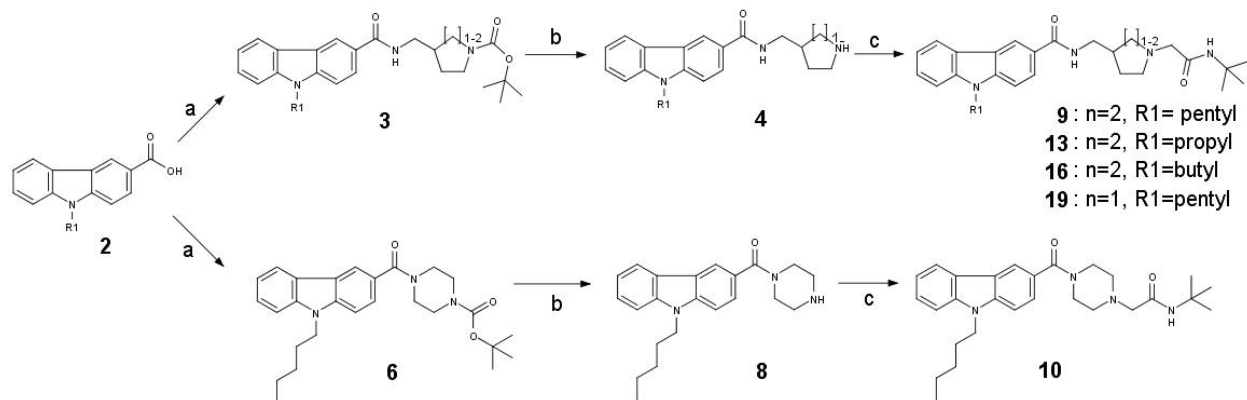


**Figure 2.5.3** The synthetic route for the preparation of the carbazole-based compounds.

Reagents and conditions: (a) corresponding amine, EDAC, HOBt, DMAP, DIPEA, DCM, 0°C to rt.; (b) TFA, CH<sub>2</sub>Cl<sub>2</sub>; (c) N-tert-butyl-2-chloroacetamide, K<sub>2</sub>CO<sub>3</sub>, KI, n-butanol, reflux 3 h.

## CHAPTER THREE: COMMON MECHANISMS OF DRUG INTERACTIONS WITH SODIUM AND T-TYPE CALCIUM CHANNELS

### 3.1 Background:

Voltage-gated sodium (Nav) and calcium channels (Cav) play critical roles in physiological processes, including neuronal and cardiac pacemaker activity, vascular smooth muscle contraction and nociception. They are thought to share a common ancestry and in particular, T-type Cav channels share many structural similarities with Nav channels, both with regard to membrane topology and with regard to gating kinetics, including rapid inactivation.

In the first part of this thesis, using basic on-line sequence alignment tools, I identified several highly conserved regions (~50% shared sequence) between T-type Cav and Nav channels that corresponded to drug binding sites known to alter voltage-dependent gating kinetics. I thus reasoned that certain drugs that act on Nav channels may also modulate the activities of T-type Cav channels.

Nav channels mediate the induction and propagation of APs in most electrically excitable cells<sup>(230)</sup>. The mammalian genome encodes nine different types of Nav  $\alpha$  subunits that are functionally classified as either tetrodotoxin-sensitive (TTX-S) or tetrodotoxin-resistant (TTX-R), with the latter exhibiting slower inactivation kinetics than other sodium channel subtypes<sup>(231, 232)</sup>. The various sodium channel  $\alpha$  subunits share a common transmembrane topology of four homologous domains that each contain six membrane spanning helices plus a p-loop. While the  $\alpha$  subunits define the sodium channel isoform and contain all of the machinery to form a sodium selective voltage activated channel, their functional properties are modulated by association with ancillary  $\beta$ 1 and  $\beta$ 2 subunits<sup>(233)</sup>. Mutations in various sodium channel subunits have been linked to disorders such as paramyotonia congenita, cardiac arrhythmias, epilepsy, and both

hypersensitivity and insensitivity to pain, thus underscoring their importance for nerve, muscle and heart function<sup>(143, 198)</sup>.

Similarly, LVA (i.e., T-type) calcium channels trigger low-threshold depolarizations that in turn lead to the initiation of APs<sup>(6, 206)</sup>. These channels can be activated by small membrane depolarizations and display a small single channel conductance, and compared to other calcium channel subtypes they display rapid activation and inactivation<sup>(74)</sup>.

T-type calcium channels are encoded by one of three different types of Cav3  $\alpha$ 1 subunits (Cav3.1, Cav3.2 and Cav3.3) whose membrane topology is similar to those of sodium channels<sup>(1)</sup>. Moreover, like sodium channels, mutations in T-type channels have been linked to epilepsy<sup>(54, 91)</sup>, upregulation of Cav3.2 T-type channel activity in primary afferent fibers has been linked to the development of chronic pain<sup>(94, 96, 160, 171, 174, 175)</sup> and T-type channel dysfunction contributes to cardiac hypertrophy<sup>(234)</sup>.

Altogether, sodium and T-type calcium channels both contribute to neuronal excitability and contribute to similar disorders such as epilepsy and pain. Indeed, knockout of Nav1.8 and Cav3.2 both result in hyposensitivity to pain<sup>(235, 236)</sup>.

Recently, a new inhibitor of Nav1.8 channels, A803467, had been shown to be efficacious in animal pain models<sup>(237)</sup>. The interaction site of A803467 on the sodium channel complex has not been fully determined, but reports have shown that it overlaps and corresponds to the well characterized local anesthetic binding site in sodium channels<sup>(238, 239)</sup> and its mode of action appears to be preferential binding to the slow inactivated state of this channel<sup>(240)</sup>.

In this chapter, we show that A803467 also inhibits T-type channels in the low micromolar range and mediates a hyperpolarizing shift in the voltage-dependence of activation and inactivation. In addition, the compound promotes a slow inactivation-like phenotype. Furthermore, sequence

alignment between T-type and Nav channels and their local anesthetic interaction site, identified key residues involved in the blocking action of this compound on T-type calcium channels.

Together, these common binding sites and ion channel regulation open up the possibility that these sites may be exploited for the design of mixed T-type and Nav channel blockers that could potentially act synergistically to normalize aberrant neuronal activity<sup>(127)</sup>.

## **3.2 Results and discussion**

### **3.3 A803467 blocks T-type calcium channels:**

A recent study identified a novel compound (A803467) as a specific and potent blocker of TTX-R hNav1.8 channels<sup>(240)</sup>. Given that T-type calcium channels share structural similarities with Nav channels, we examined whether this compound may affect T-type calcium channels at both therapeutic plasma and brain tissue concentrations (10 to 17  $\mu\text{M}$  and 3 to 5  $\mu\text{M}$ , respectively)<sup>(127)</sup>. Figures 3.3.1 A and B illustrate the effect of 5  $\mu\text{M}$  A803467 on human Cav3.2 channels expressed transiently in tsA-201 cells at a holding potential of -110 mV. As evident from the figure, this compound mediated robust peak current inhibition that could be partially reversed upon washout. The concentration dependence of this type of tonic (i.e., resting state) block could be well described by a Hill coefficient close to 1 (Figure 3.3.1C). We then examined the calcium channel subtype selectivity of A803467 (Figure 3.3.1D) and found that all LVA subtypes were blocked with IC<sub>50</sub>s in the low micromolar range, whereas two representative members of the HVA channel family (i.e., L- and P/Q type calcium channels) exhibited lower affinities (i.e., higher IC<sub>50</sub> values).

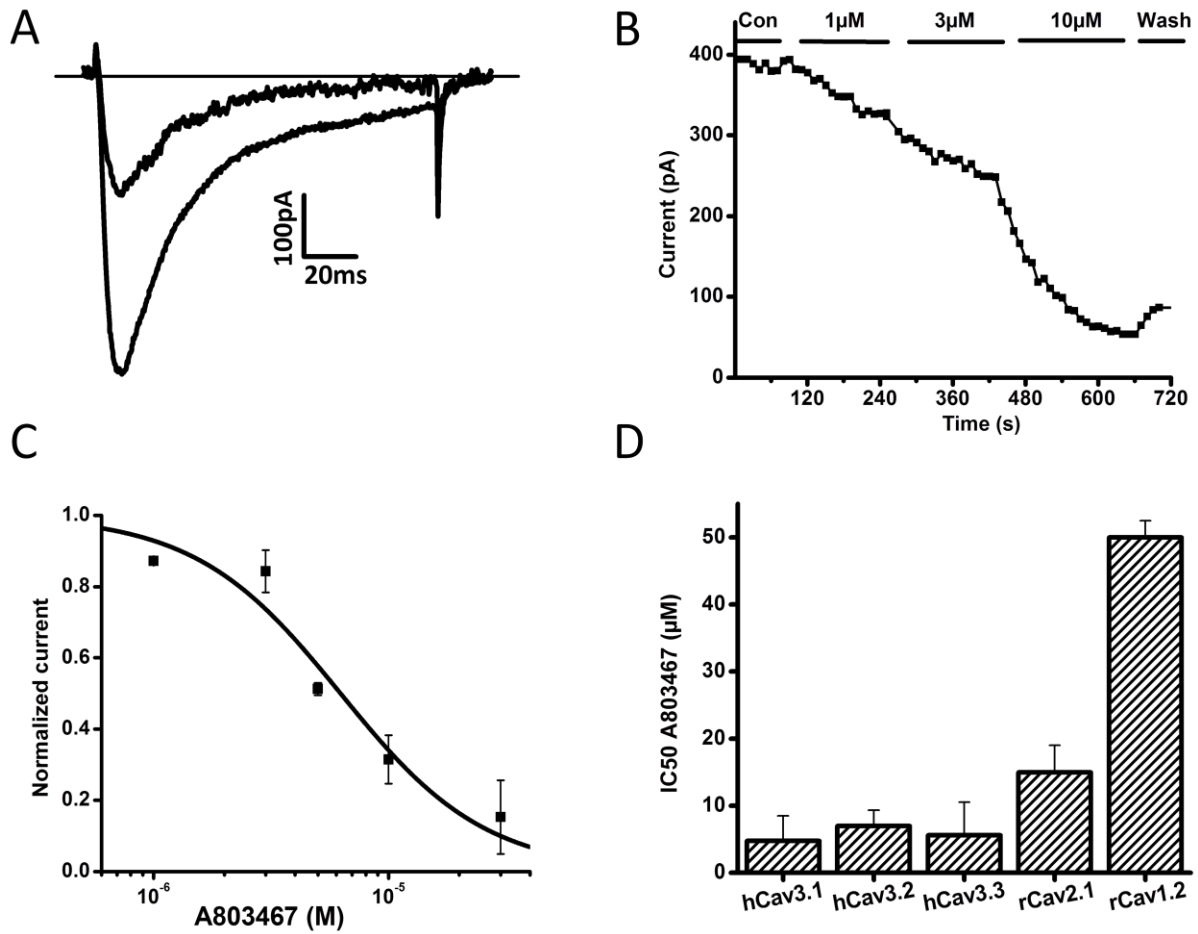


**Figure 3.3.1 Tonic block of voltage-gated calcium channels by A803467<sup>(221)</sup>.**

A. Representative current trace recorded from Cav3.2 channels transiently expressed in tsA-201 cells before and after application of 5  $\mu$ M A803467. Currents were elicited by stepping from a holding potential of -110 mV to a test potential of -30 mV. B. Representative time course of development of and recovery from A803467 block. C. Ensemble dose response curve for tonic Cav3.2 channel inhibition by A803467. The solid line is a fit via the Hill equation. D. IC<sub>50</sub>s for tonic A803467 block of rat HVA and human LVA calcium channels. Data were obtained by fitting dose-response curves for each channel subtype (n=6 per channel). Error bars reflect standard errors.

A study by Jarvis et al., had also shown that this drug did not show significant block of N-type calcium channels, TRPV1, KCNQ2/3 potassium channels and other channels or receptors found in peripheral sensory neurons<sup>(240)</sup>.

Unlike what had been reported for hNav1.8 channels<sup>(240)</sup>, we observed a significant hyperpolarizing shift in the half-activation voltages of both Cav3.1 and Cav3.2 channels (Figure 3.3.2 A,B). There was also a trend towards more hyperpolarized voltages for hCav3.3, however, these did not reach statistical significance (Table 3.1). Application of A803467 to T-type calcium channels also resulted in a significant (~10mV) hyperpolarizing shift in the half-inactivation potentials of hCav3.1 and hCav3.2 (see Figure 3.3.2 C, D) similar to that described previously for hNav1.8 channels<sup>(240)</sup>. The leftward shift in the steady state inactivation curve is consistent with inactivated channel block<sup>(183)</sup>. Altogether, these data indicate that A803467 mediates both resting channel inhibition and inactivated channel block of T-type calcium channels.

Calcium Channel	V <sub>0.5</sub> act (mV) Con	V <sub>0.5</sub> act (mV) Drug	Vh (mV) Con	Vh (mV) Drug	IC50 Tonic (μM)
hCav3.1	-50.3 ±1.6 N=5	-60.0 ±1.6* N=5	-74 ±0.9 N=5	-84 ±1.8* N=5	4.8 N=6
hCav3.2	-44.3 ±1.4 N=7	-52.1 ±1.2* N=7	-64.2 ±0.93 N=5	-71 ±0.45** N=5	7.0 ±0.51 N=6
hCav3.3	-47.8 ±1.6 N=6	-50.0 ±2.7 N.S. N=6	-79 ±1.7 N=9	-83 ±1.6 N.S. N=9	5.6 N=6
rCav2.1	-15.8 ±1.3 N=5	-25 ±1.4 N=5	N.A.	N.A.	15.0 N=6
rCav1.2					50.0 N=6

**Table 3.1. Biophysical parameters of HVA and LVA calcium channels with or without drug [A803467]<sup>(221)</sup>.**

Asterisks denote statistical significance relative to control (\*p<0.05, \*\*p<0.01, N.S. – not significant).

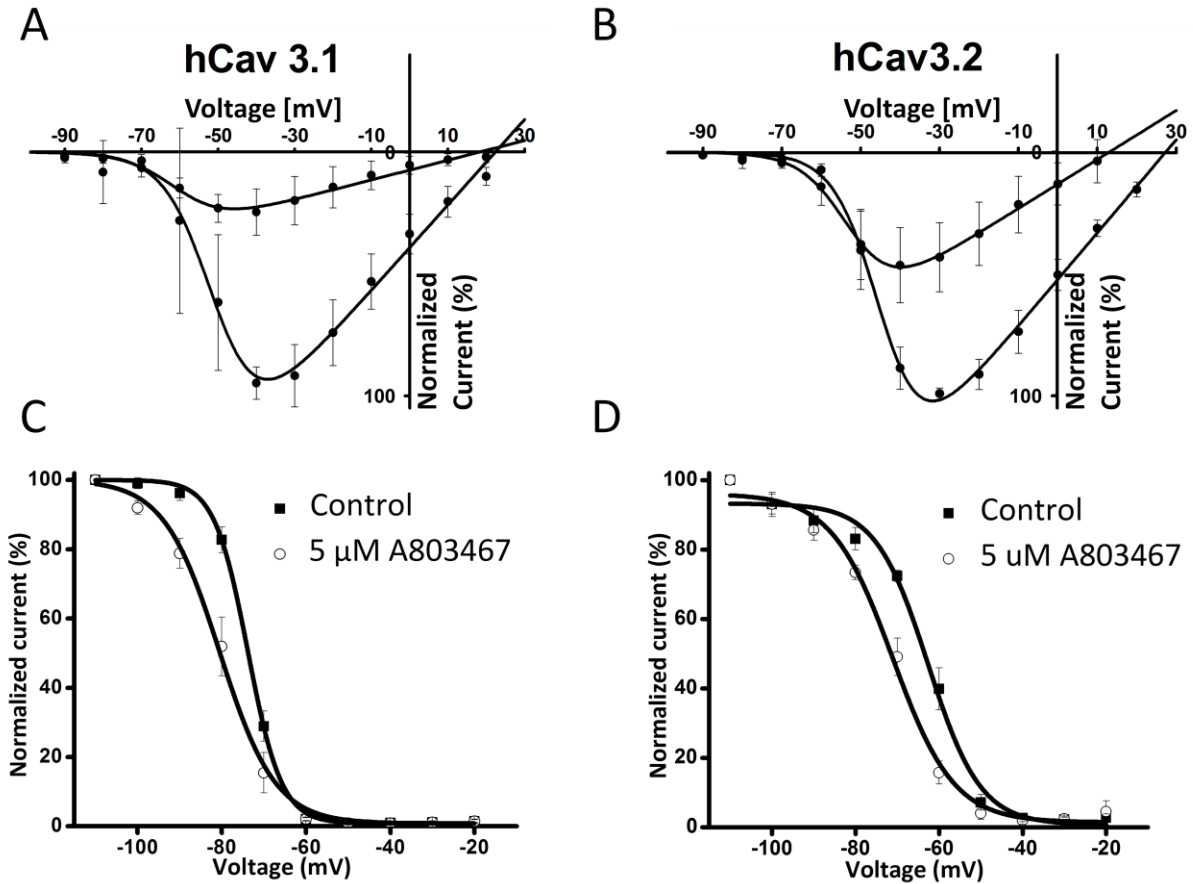


**Figure 3.3.2 Effect of A803467 on activation and inactivation of T-type calcium channels<sup>(221)</sup>.**

A,B, Current voltage relations recorded prior and after application of 5  $\mu\text{M}$  A803467 to hCav3.1 (A) or hCav3.2 (B) channels. Data from multiple paired experiments are included in each figure. C,D, Steady State inactivation curves for hCav3.1 (C) and hCav3.2 (D) channels in the absence (Control) and presence of 5  $\mu\text{M}$  A803467. Note the negative shift in half inactivation potential in the presence of A803467. The data were fitted with the Boltzmann equation, half inactivation potentials obtained from the fits were as follows: hCav3.1: control -74 mV, drug -84 mV; hCav3.2: control -64 mV, drug -71 mV.

### **3.4 A803467 block promotes a slow inactivation-like state of hCav3.2**

Previous studies have identified slow inactivation channel blockers of Navs<sup>(241)</sup>, as well as mixed sodium/T-type channel blockers which stabilize the slow inactivated conformation of these channels<sup>(127)</sup>. To determine whether A803467 may mediate a similar action on T-type calcium channels, we used a slow inactivation protocol to induce a partial slow inactivated-like state of the channel. Specifically, we applied a brief test depolarization (P1) prior to a 10 s conditioning pulse to -70 mV which is expected to induce both fast and slow inactivation (Figure 3.4.1 inset). This was followed by a brief hyperpolarizing step to induce recovery from fast inactivation of non drug-bound channels. A second depolarizing test pulse (P2) (under our experimental conditions, this amounted to about 30% slow inactivation in the absence of the drug) allowed us to determine the fraction of channels in the slow inactivated-like state. The dose-dependent effects of A803467 on the currents elicited by P1 and P2 were then compared to ascertain the amount of resting vs. slow inactivated channel block. As shown in Figure 3.4.1, hCav3.2 channels A803467-induced channel inhibition that resembled features of enhanced slow inactivation, as evident from a reduction in the IC<sub>50</sub> of P2 current inhibition. In contrast, the hCav3.1 and hCav3.3 channels did not show stabilization of the slow inactivated-like channel conformation. The combined effects of A8023467 on different kinetic states of hCav3.2 channels predicts substantial total/combined inhibition of Cav3.2 currents in the high nanomolar to the low micromolar range which is well within the therapeutic range of A803467.

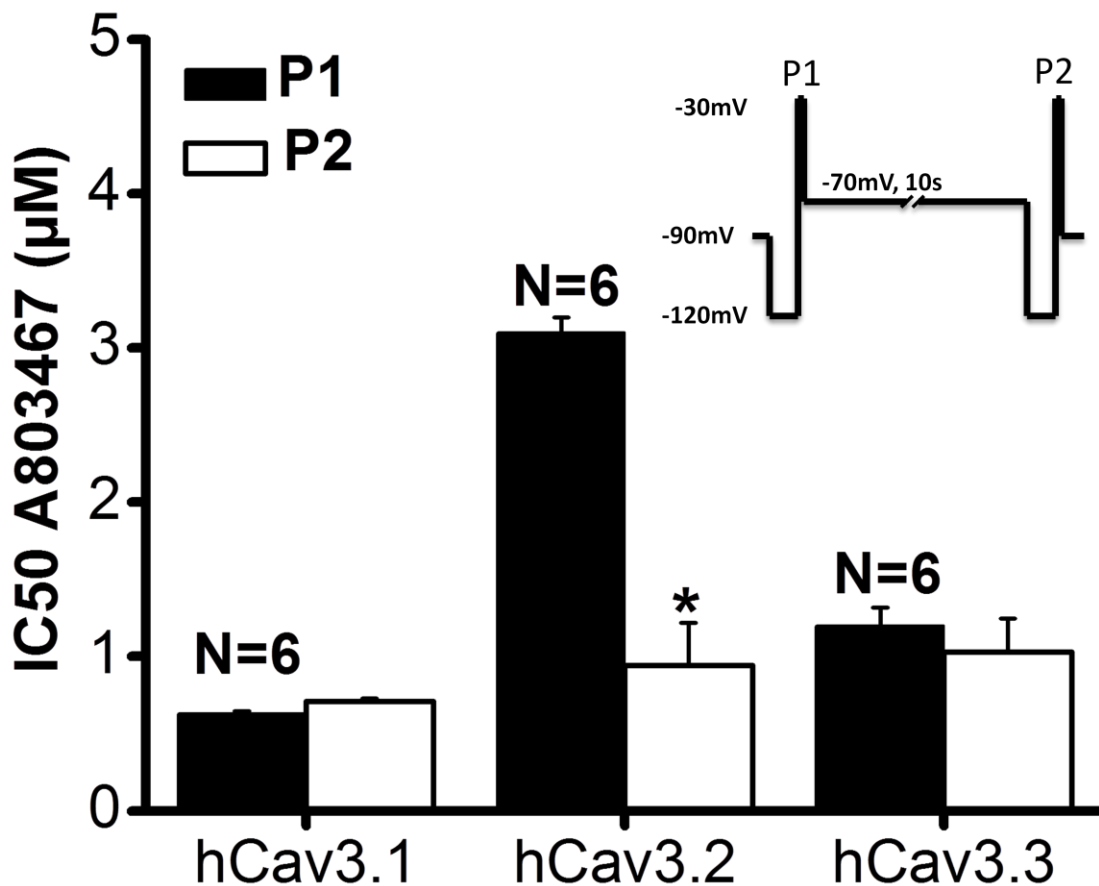


**Figure 3.4.1 A803467 block of Cav3 channel subtypes in a partial slow inactivated state.**<sup>(221)</sup>

Summary of IC<sub>50</sub>s for A803467 block of Cav3 channel subtypes in a partial slow inactivated state. The inset shows the whole cell voltage command protocol used to induce slow inactivation (i.e., a test pulse P1, followed by a 10 s conditioning pulse to -70 mV, a brief hyperpolarization to remove fast inactivation, and a second test pulse P2 to determine the fraction of slow inactivated channels). Note that only Cav3.2 channels display a decrease in IC<sub>50</sub> for A803467 inhibition during P2, indicating a selective increase of A803467 affinity for slow inactivated Cav3.2 channels (\*p < 0.05, Student's T-test).

### **3.5 A locus analogous to the Nav local anesthetic binding site controls A803467 block of Cav3.2.**

Given the structural similarity between T-type and Nav channels, we hypothesized that the drug binding site on these two types of channels may be conserved. Sodium channels possess multiple drug interaction sites, including a receptor site for binding of local anesthetics and anticonvulsive drugs<sup>(242)</sup>. A key locus for local anesthetic block of Nav channels was first identified by Ragsdale and colleagues<sup>(243)</sup>. The authors revealed that tyrosine (Tyr) 1771 and phenylalanine (Phe) 1764 in Nav1.2 were important determinants of local anesthetic block of Nav1.2 channels, and that mutagenesis of these two residues (especially residue 1764) resulted in a reduction in etidocaine blocking affinity for the channel. In hCav3.2 channels, the residue equivalent to these two residues are valine and glutamine (Figure 3.5.1) indicating that one key component of the local anesthetic binding site is absent in T-type calcium channels. However, Yarov-Yarovoy and colleagues<sup>(244, 245)</sup> identified several other amino acid residues in the IS6 and III S6 segments of the Nav1.2  $\alpha$  subunit that also affected drug interactions. These authors showed that in addition to residue Tyr 1771 and Phe 1764, mutagenesis of isoleucines (Ile) 409 and 1469 reduced local anesthetic interactions. ClustalW2 multiple sequence alignment of hNav1.8 vs hNav1.2 and hCav3.2 revealed that these regions were highly conserved in these channels (Figure 3.5.1). The corresponding loci of these residues in Cav3.2 are Ile 403 and Val 1551, indicating that Cav3.2 channels may possess some of the structures needed for local anesthetic interactions.

```

Nav1.8      YMIFFVLVIFLGSFYLVNLILAVVT 397
Nav1.2      YMIFFVLVIFLGSFYLINLILAVVA 425
Cav3.2      NFIYFILLIIVGSFFMINLCLVVIA 419
            :*:*:*:*:*::***:::* *.*:::

            :::*:*:*:*:*::*.*:*:*:*

NavAb       AWVFFIPFIFVVTFVMINLVVAIIVD-- 219
Nav1.8      MYLYFVIFIIFGGFFTLNLFVGVIIIDNF 1421
Nav1.2      MYLYFVIFIIFGSFTLNLFIGVIIIDNF 1476
Cav3.2      MLLYFISFLLIVSFVLNMFVGVVVENF 1558
            *  ***: *::: .**.**:*:***::**

Nav1.8      PAVGIIFFTTYIIISFLIMVNMYIAV 1720
Nav1.2      PSVGIFFFVSYIIISFLVVNMYIAV 1774
Cav3.2      PALSPVYFVTFVLVAQFVLVNVVAV 1858
            *::: .:*::: :::** :**

```

**Figure 3.5.1 Sequence alignment of the local anesthetic binding regions in Nav channels with the analogous regions in hCav3.2.<sup>(221)</sup>**

Residues involved in local anesthetic binding to Nav channels are indicated in bold. Note the overall degree of sequence similarity between T-type channels, sodium channels and the NavAb bacterial sodium channel whose crystal structure has recently been resolved.

To determine whether these residues may be involved in A803467 interactions with hCav3.2, we replaced Ile 403 and Val 1551 with alanines and then assessed A803467 block of these mutant channels. As shown in Figure 3.5.2, these amino acid substitutions resulted in a significant decrease in A803467 blocking affinity for hCav3.2 (by over one order of magnitude for the V1551A, I1556 substitution). This effect was not secondarily due to reduced slow inactivation, as the only gating parameter that was significantly altered was a shift in half-activation voltage of the I403A mutant (Table 3.2).

Next, we tested whether these mutations affected the ability of A803467 to enhance slow inactivation of hCav3.2. As shown in Figure 3.5.3, the A803467-induced stabilization of a slow inactivated like state of the wild-type channel was abolished in the two mutant channels.

Calcium Channel	$V_{0.5}^{act}$ (mV)	$E_{rev}$ (mV)	Gmax ( $\mu$ S)	Vh (mV)	IC50 Tonic ( $\mu$ M)
hCav3.2	$-44.3 \pm 1.4$ N=7	$27.3 \pm 0.7$ N=7	$-1.9 \pm 0.08$ N.S N=7	$-64.2 \pm 0.93$ N.S. N=5	$7.0 \pm 0.51$ N=6
hCav3.2 I403A	$-54.0 \pm 1.8^*$ N=11	$20.3 \pm 1.8^*$ N=11	$-1.7 \pm 0.09$ N.S N=11	$-63.8 \pm 0.87$ N.S. N=6	$20.0 \pm 1.5^{**}$ N=6
hCav3.2 V1551A	$-47.0 \pm 1.1$ N.S. N=13	$23.8 \pm 1.5$ N.S. N=13	$-1.9 \pm 0.06$ N.S N=13	$-67.0 \pm 0.98$ N.S. N=6	$40.0 \pm 3.1^{**}$ N=6
hCav3.2 V1855Y	$-29.64 \pm 2.1^*$ N=14	$14.64 \pm 2.1^*$ N=14	$-3.9 \pm 0.14^*$ N=14	$-58.4 \pm 0.56^*$ N=6	$1.8 \pm 0.41^*$ N=6

**Table 3.2. Biophysical parameters of wild-type and mutant hCav3.2 calcium channels<sup>(221)</sup>.**

Asterisks denote statistical significance relative to control (\*p<0.05, \*\*p<0.01, N.S. – not significant).

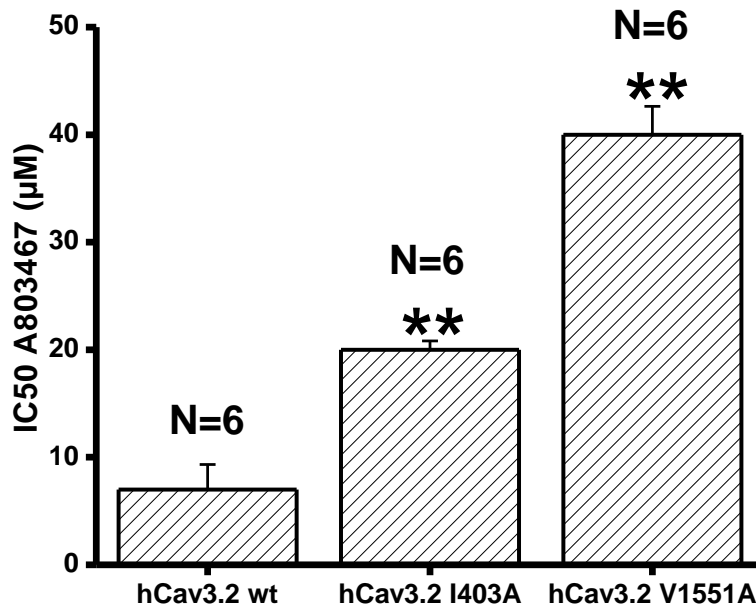


**Figure 3.5.2 Summary of IC<sub>50</sub>s for tonic A803467 block of wild-type (Wt) and mutant Cav3.2 channels<sup>(221)</sup>.**

Currents were elicited by stepping to a test potential of -30 mV from a holding potential of -110 mV. Significance was assessed using ANOVA (\*\*p < 0.01).

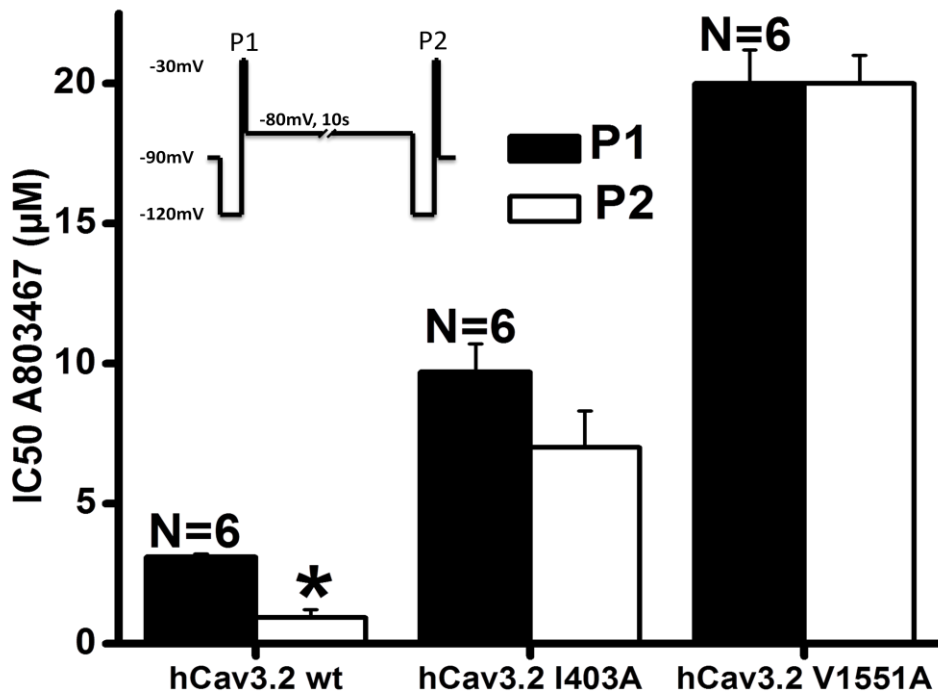


**Figure 3.5.3. IC<sub>50</sub> values for A803467 block of slow inactivated Cav3.2 channels<sup>(221)</sup>.**

The slow inactivation protocol was the same protocol as that described in Figure 3.4.1 except holding potential was stepped to -80 mV. Note that the mutant channels do not show an increase in blocking affinity for the slow inactivated state (\*p < 0.05, t-test).

To further support the hypothesis that a locus analogous to the sodium local anesthetic binding site controls A803467 block of Cav3.2, we introduced a tyrosine residue in position V1855 of Cav3.2 (corresponding to Tyr 1771 in hNav1.2) and determined the consequences on A803467 block of hCav3.2 (Figure 3.5.4). The introduction of Tyr 1855 significantly increased A803467 resting state blocking affinity by approximately four-fold (Figure 3.5.4A) and preserved the ability of the compound to stabilize the fast inactivated state (Figure 3.5.4B). Furthermore, we observed a significant increase in blocking activity in response to the slow inactivation pulse paradigm, as evident from a reduction in the IC<sub>50</sub> during P2 (Figure 3.5.4C). Unlike substitutions in positions 403 and 1551, tyrosine substitution of residue 1855 induced a ~10 mV depolarizing shift in the voltage dependences of activation (not shown) and inactivation (Figure 3.5.4B), indicating that this locus is important for channel gating.

Finally, we mutated the glutamine residue in position 1848 of hCav3.2 to the phenylalanine found in the corresponding position in Nav1.2 channels (see Figure 3.5.1)<sup>(243)</sup>. In addition we also substituted this residue with another hydrophobic residue leucine. When expressed in tsA-201 cells, both mutants yielded T-type currents, albeit with much reduced whole cell current amplitudes compared to those seen with wild-type channels, without any effects on half-activation potential (not shown). In fact, reliable current recordings required us to increase the ionic strength of the extracellular recording solution to 20 mM barium. Under these conditions, we were at least able to test the ability of A803467 to mediate tonic (resting) blocking affinity. As shown in Figure 3.5.5, the compound exhibited a twenty-fold increase in affinity for the phenylalanine mutant, and a ten-fold increase for the leucine mutant compared with wild-type channels bathed in the same barium solution. In both mutants, block was completely reversible upon washout (not shown).

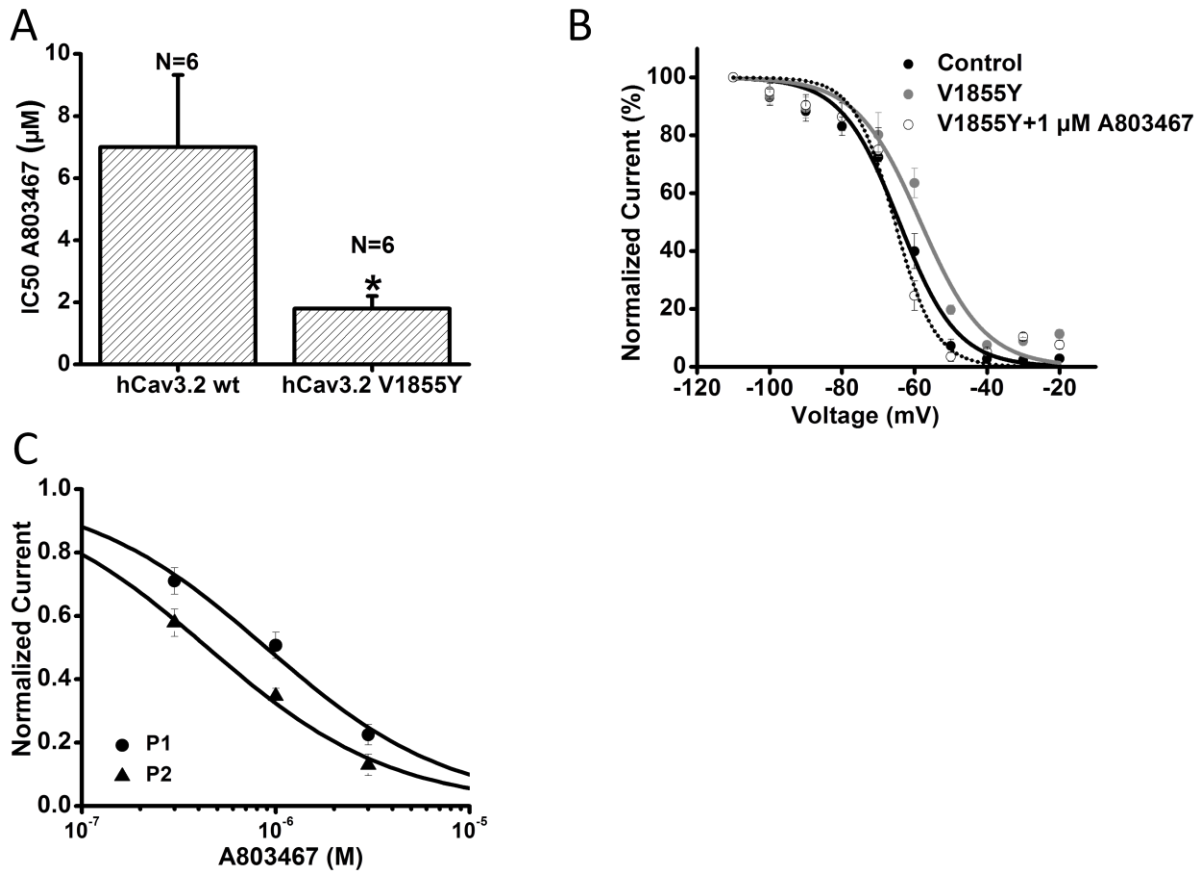


**Figure 3.5.4. Effect of a tyrosine substitution in position 1855 of hCav3.2<sup>(221)</sup>.**

A. IC<sub>50</sub> for tonic A803467 of Wt and mutant V1855Y (\*p < 0.05, t-test). B. Steady state inactivation curves recorded in the presence and the absence of 5 µM A803467. Note the hyperpolarizing shift from -58 mV to -64 mV. For comparison, the inactivation curve of the Wt (Control) channel is included. C. Dose dependence of slow inactivated channel block of mutant hCav3.2 V1855Y expressed as the fractional current at various drug concentrations.

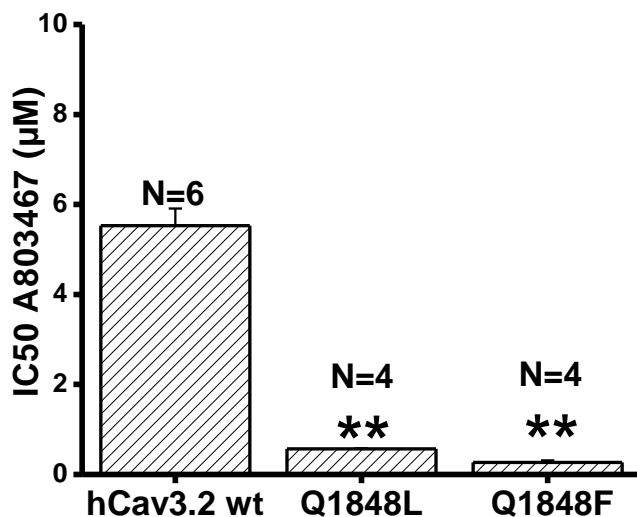


**Figure 3.5.5. Summary of IC<sub>50</sub>s for tonic A803467 block of wild-type (Wt) and mutant Q1848L and Q1848F hCav3.2 channels.**

Currents were elicited by stepping to a test potential of -20 mV from a holding potential of -110 mV. Asterisks denote statistical significance relative to control (\*\*p<0.01). All recordings in this figure were performed in 20 mM barium due to the small current amplitudes of the mutants. IC<sub>50</sub> values were obtained by fitting dose response curves with the Hill equation as described in Figure 1. Both substitutions in position 1848 produced submicromolar block by this compound.

Altogether, these data indicate that both tonic and slow inactivated-like channel block of Cav3.2 channels by A803467 is mediated by interactions of this compound with residues that are analogous to those comprising the local anesthetic receptor site in sodium channels.

### **3.6 Mixed Nav1.8/Cav3.2 inhibitors – a potential strategy to treat pain?**

A803467 was originally identified as a potent inhibitor of hNav1.8 channels with a mode of action that appears to involve at least in part a stabilization of the slow inactivated state<sup>(240)</sup>.

Furthermore, this compound was shown to reduce neuropathic and inflammatory pain in animal models<sup>(237)</sup>. Here, we demonstrate that A803467 also blocks T-type channels with high affinity, with IC50's that fall into the range of therapeutic concentrations and that block of the Cav3.2 channel subtype appears to stabilize slow inactivation. The similarities between Nav1.8 and Cav3.2 channel inhibition by this compound are striking and underscored by the observation that mutations in Cav3.2 in regions corresponding to the local anesthetic interaction site in sodium channels antagonize A803467 action. Altogether, our findings suggest that evolutionarily conserved regions between sodium and LVA calcium channels may give rise to similar drug interactions or binding sites, such as the ones described in this report.

Both hNav1.8 and T-type Cav3.2 channels are functionally expressed in nociceptive DRG and lamina I spinal cord neurons<sup>(127, 246)</sup> and are known to regulate their excitability. Increased excitability of both channel subtypes has been linked to the development of hyperalgesia and allodynia in various animal models of pain<sup>(122, 203, 246)</sup>. Conversely, knockout or inhibition of T-type or sodium channels mediates analgesia<sup>(94, 175)</sup>.

Given the potent blocking effects of A803467 on Cav3.2 channels, it is possible that the previously reported effects of this compound on AP firing in DRG neurons and the associated analgesia may be at least in part mediated by T-type channel inhibition. Given that Nav and Cav

channels work together to prolong subthreshold depolarizations within lamina I neurons<sup>(127, 246, 247)</sup>, a dual action of A803467 may promote a synergistic inhibition of pain signaling. Slow inactivation is significantly enhanced during prolonged depolarizations or during neuronal burst firing. Promotion of a slow inactivated like state of both channel subtypes may thus mediate frequency dependent inhibition of channel activity and therefore reducing overall neuronal excitability. Reduction in neuronal excitability may make compounds such as A803467 ideally suited towards treatment of neuronal hyperexcitability disorders including pain and may perhaps be extended to conditions such as epilepsy. The apparent conservation in the drug receptor site between Nav and Cav3.2 channels may provide an opportunity for the synthesis of more potent antagonists acting on both of these channel subtypes.

## CHAPTER FOUR: T-TYPE CALCIUM CHANNEL BLOCK BY PROTOXINS I AND II

### 4.1 Background:

One of the central themes to this thesis is that T-type calcium channels share many structural similarities with VGSCs. In the previous chapter, I determined that a compound (A803467) that mediated high affinity block of hNav1.8, also blocked T-type calcium channels with high affinity. I also determined that this compound functionally interacted with a region identified in VGSCs as the local anesthetic binding site and that a structurally similar site can be found in all T-type calcium channels.

Another class of molecules known to be effective blockers of voltage gated ion channels are polypeptide toxins. The effects of toxins on ion channels have been extensively documented<sup>(44, 120, 248-256)</sup> (for review see Catterall et al.,)<sup>(121)</sup> and one toxin isolated from scorpion venom (kurtoxin) is already known to be a potent blocker of T-type calcium channels<sup>(257)</sup>. However, this toxin has also been shown to block high-voltage activated calcium channels<sup>(258)</sup>.

Ion channel toxins can be loosely classified based on the mechanism by which they modulate channel activity. For instance in VGSCs, pore blockers occlude the conduction pathway (e.g. tetrodotoxin, saxitoxin,  $\mu$ conotoxin) and gating modifiers shift the voltage dependence of activation and inactivation (e.g.  $\beta$ -scorpion toxins enhance activation and  $\alpha$ -scorpion toxins slow inactivation)<sup>(121)</sup>.

Similarly, in VGCCs the smaller marine snail toxins (conotoxins) tend to block the pore of calcium channels, while the larger spider toxins often affect channel gating<sup>(44, 120, 121, 257, 259-261)</sup>. More recently, two peptide toxins (ProTx I and ProTx II), isolated from Peruvian Green Velvet Tarantula (*Thrixopelma pruriens*) venom, have been shown to be potent blockers and gating modifiers of both sodium and calcium channels<sup>(254, 262, 263)</sup>. Given the structural similarities

between these two classes of ion channels and the common mechanisms of toxin block, I hypothesized that sodium and T-type calcium channels may share similar structural determinants for toxin block.

ProTx I and II belong to the inhibitory cysteine knot (ICK) family of peptide toxins that are known to interact with voltage-gated ion channels<sup>(261, 263)</sup> and to be potent inhibitors of voltage-gated sodium channels<sup>(248, 254, 262, 263)</sup>. More recently, several studies demonstrated that ProTx I could also potentially block the human Cav3.1 calcium channel<sup>(263, 264)</sup>. One of these studies showed that ProTx I was selective for hCav3.1 over hCav3.2 and that this selectivity may be in part attributed to the S3-S4 linker in domain IV of hCav3.1<sup>(264)</sup>

In this chapter, I tested to what extent these two protoxins inhibited T-type calcium channels and attempted to identify the structural determinants of ProTx I block. It is important to note that although both protoxins come from the same tarantula species and are both thought to be ICK peptide toxins, their overall sequence identity is less than 30% and their structures are quite different<sup>(261)</sup>. Indeed results presented in this chapter and from a recently published paper<sup>(261)</sup> suggest that these two peptide toxins bind to different areas of voltage-gated ion channels and that ProTx I may block in a region analogous to the site for  $\alpha$ - $\delta$  Scorpion Toxins and ProTx II blocks in a region that more closely resembling that of  $\beta$  Scorpion Toxins (see figure 4.1.1). The results presented here further support the notion of different blocking sites in that ProTx II showed selective block of human Cav3.2 (hCav3.2), albeit with far less efficacy than previous reports suggested<sup>(263)</sup>, while ProTx I potently and preferentially blocked native and transiently expressed T-type channels in the sub- to low micromolar range. Given this potency and selectivity, I therefore focused on elucidating the key determinants of ProTx I binding affinity to

hCav3.1 by using hCav3.1-hCav3.3 chimeras, as well as sequence alignment between T-type and Nav channels and toxin interaction sites.

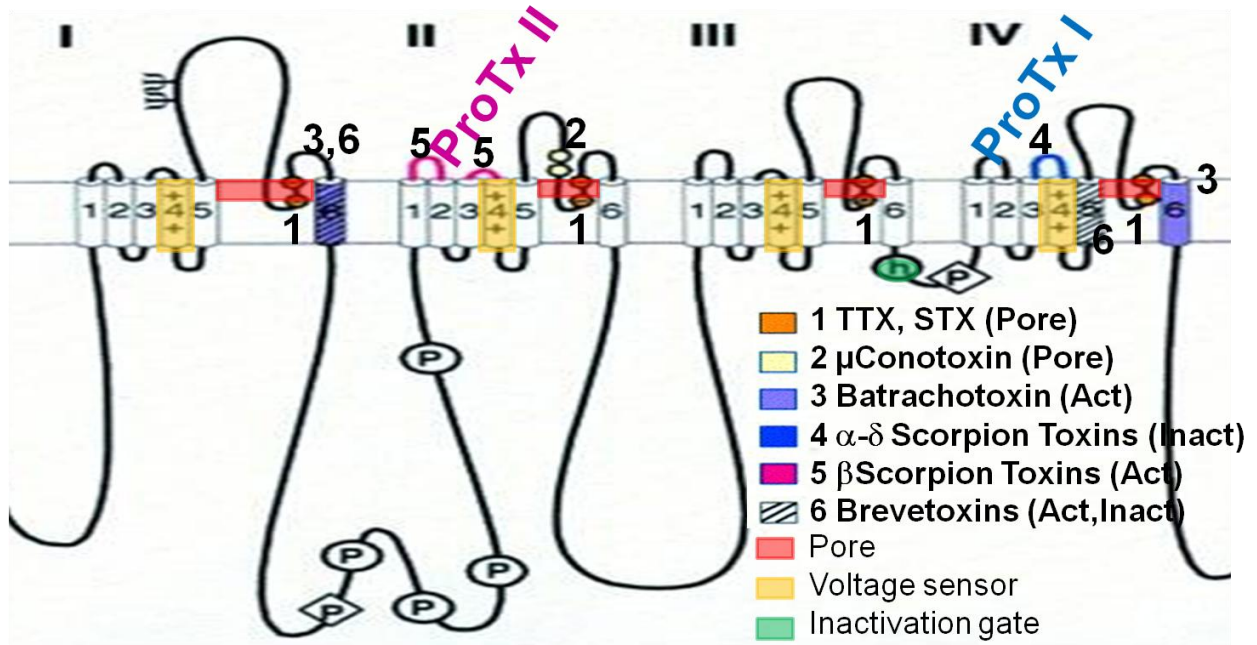


**Figure 4.1.1** Schematic showing various types of toxins and their sites of ion channel interaction (modified from Catterall et al., 2006)<sup>(121)</sup>.

## 4.2 Results

### 4.3 ProTx II is a preferential blocker of hCav3.2

ProTx II was originally identified as a potent inhibitor of sodium channels with fifteen to hundred- fold selectivity for hNav1.7 versus other sodium channels<sup>(254, 263)</sup>. It was also reported to be a potent inhibitor of L-type calcium channels and to mediate a greater degree of inhibition of rCav3.1 versus rCav3.2<sup>(263)</sup>. Our observations indicate that ProTx II in fact blocks hCav3.2 more potently than the other T-type calcium channels and when applied to endogenous Cav3.2 that are found in acutely isolated mouse DRG neurons<sup>(127)</sup>, a similar result was observed with a slightly higher degree of block (Figure 4.3.1). ProTx II also dramatically shifts the steady state inactivation curve of hCav3.2 towards more hyperpolarized potentials (Table 4.1) which produces additional inhibition at typical neuronal resting membrane potentials. Interestingly, although ProTx II only weakly blocked hCav3.1 and hCav3.3, there were significant negative shifts in the half activation potentials of these channels in the presence of 1  $\mu$ M of the toxin (Table 4.1). Together, these data indicate that ProTx II interacts with hCav3.2 channels in a way similar to  $\beta$ -scorpion toxin interactions with sodium channels<sup>(121)</sup>, and that it also modulates the gating behavior of hCav3.1 and hCav3.3 channels.

Clone	Current Block (%) ProTx II (1 $\mu$ M)	V <sub>0.5act</sub> (mV) Con	V <sub>0.5act</sub> (mV) ProTx II (1 $\mu$ M)	Vh ( mV) Con	Vh (mV) ProTx II (1 $\mu$ M)
hCav3.1	8.9 $\pm$ 1*	-51.6	-64.5**	-73.7	-76.5
hCav3.2	29 $\pm$ 0.4	-49.4	-52.1	-64.2	-76.5*
hCav3.3	8.9 $\pm$ 0.3*	-50.0	-60.7*	-79	-77

**Table 4.1 Summary of biophysical parameters of various T-type calcium channels in the absence or presence of 1  $\mu$ M ProTx II.**

Asterisks denote statistical significance relative to hCav3.2 for current block, or relative to control for all other parameters (\*p<0.05, \*\*p<0.01).

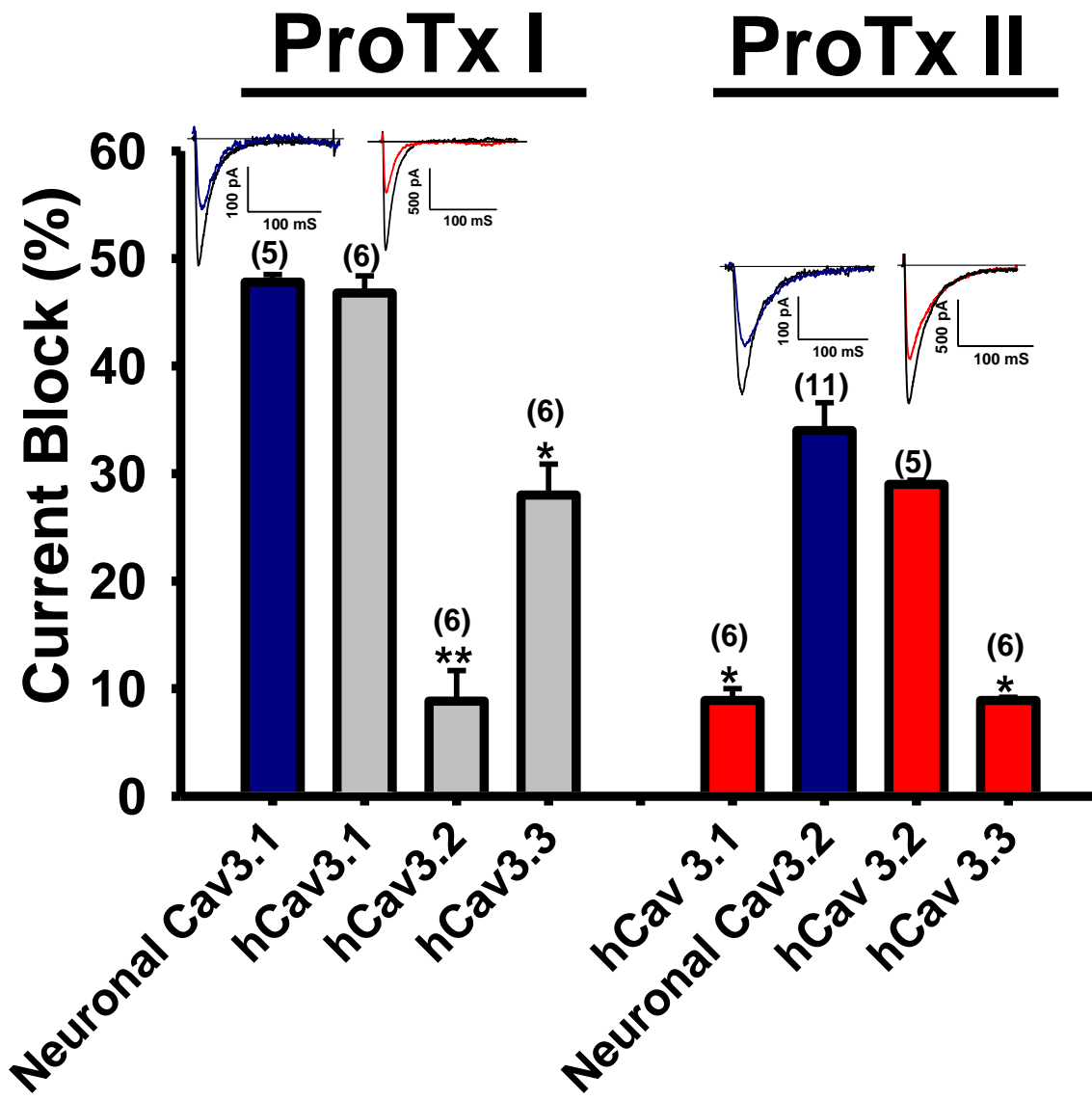


**Figure 4.3.1 Tonic block of mouse neuronal or recombinant human Cav3.X (T-type) calcium channels.**

Tonic block of T-type calcium channels was induced by either 1  $\mu\text{M}$  application of ProTx I or 1  $\mu\text{M}$  application of ProTx II. For recordings from native channels, ProTx I was tested on mouse thalamic neurons, ProTx II was tested on mouse DRG neurons, which respectively, expressed Cav3.1 and Cav3.2 channels. Shown are representative current traces from these experiments showing similar ProTx I block of native thalamic mouse T-type currents (first trace) and recombinant human Cav3.1 (second trace), and similar ProTx II block of mouse DRG T-type current (third trace) and recombinant human Cav3.2 (fourth trace) (control traces are depicted in black). Error bars reflect standard errors, asterisks denote statistical significance relative to either hCav3.1 (ProTx I) or hCav3.2 (ProTx II) (\* $p < 0.05$ , \*\* $p < 0.01$ ). Currents were elicited by stepping from a holding potential of  $-110$  mV to a test potential of  $-20$  mV.

#### **4.4 ProTx I is a potent and selective blocker of hCav3.1 versus other T-type channels.**

In our hands when applied to transiently expressed human T-type calcium channels, ProTx I preferentially inhibited hCav3.1, with less block of hCav3.3 and only very little inhibitory effect on hCav3.2. We tested 1  $\mu$ M ProTx I on endogenous Cav3.1 that are found in acutely isolated mouse thalamic neurons<sup>(265)</sup> and saw almost identical block to the transiently expressed hCav3.1 (Figure 4.4.1, Table 4.2). Contrary to previous findings, we did not observe any significant positive shifts in the half activation potential of hCav3.1 in the presence of 1  $\mu$ M ProTx I, in spite of its potent inhibitory effects, nor was the gating of hCav3.3 channels affected (Figure 4.4.1 A,C and Table 4.2). In contrast, hCav3.2 channels underwent shifts in both the half-activation and inactivation potentials in the presence of the toxin (Figure 4.4.1 B, Table 4.2).

Clone	Current Block (%) ProTx I (1 $\mu$ M)	V <sub>0.5act</sub> (mV) Con	V <sub>0.5act</sub> (mV) ProTx I (1 $\mu$ M)	Vh (mV) Con	Vh (mV) ProTx I (1 $\mu$ M)
hCav3.1 wt	50 $\pm$ 1.5	-52.3	-52.3	-74	-76
hCav3.2 wt	8 $\pm$ 2.8**	-52.6	-58.8*	-64	-75*
hCav3.3 wt	26 $\pm$ 2*	-50.1	-50.1	-79	-75

**Table 4.2 Summary of biophysical parameters of various T-type calcium channels in the absence or presence of 1  $\mu$ M ProTx I.**

Asterisks denote statistical significance relative to hCav3.1 for current block, or relative to control for all other parameters (\*p<0.05, \*\*p<0.01).

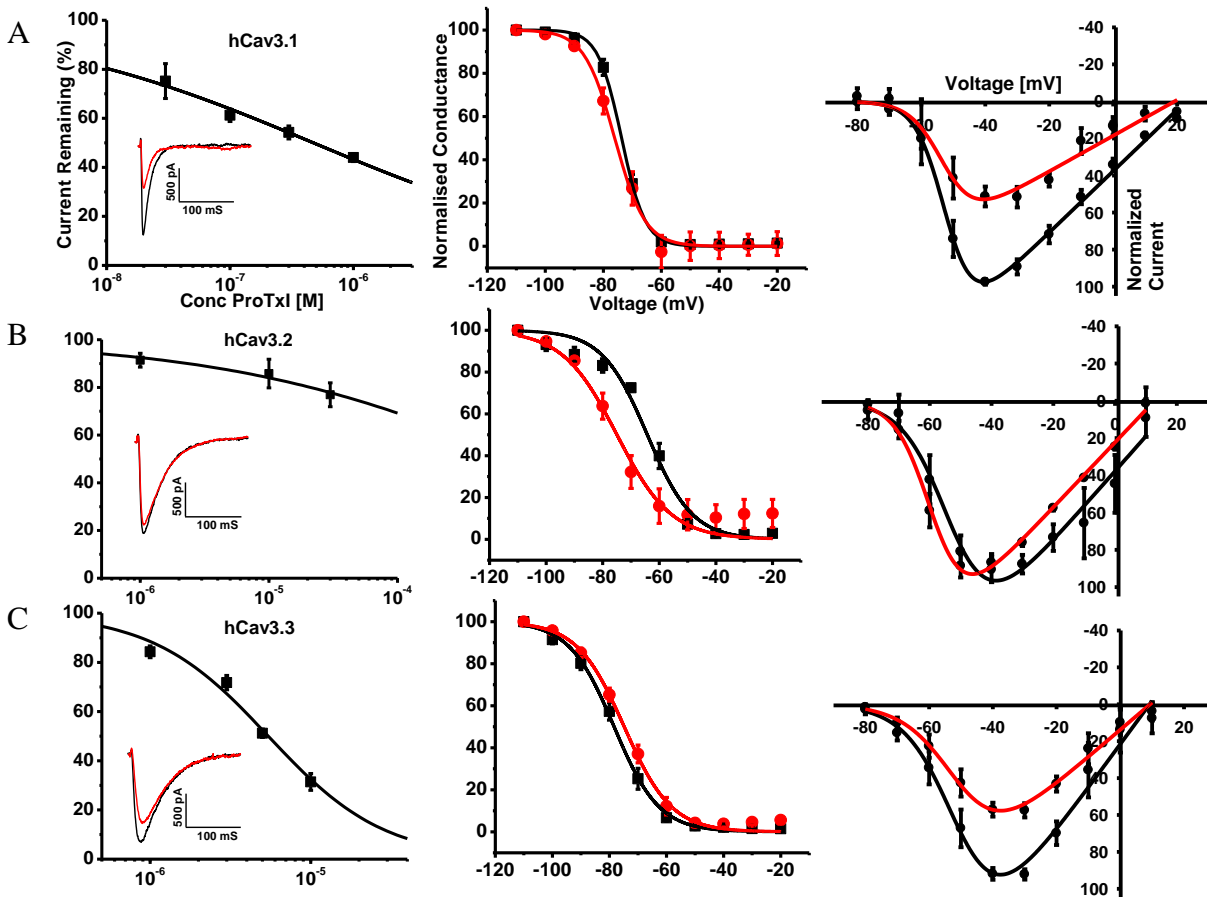


**Figure 4.4.1 A,B,C, ProTx I Dose response (left), steady state inactivation (middle) and current voltage relations (right) for hCav3.1, hCav3.2 and hCav3.3, respectively.**

Steady state inactivation and current voltage relations were recorded prior to and after application of 1  $\mu$ M ProTx I. Ensemble dose response curves for tonic channel inhibition by ProTx I were fitted via the Hill equation and IC<sub>50</sub>'s for hCav3.1, 3.2 and 3.3 were 0.64, 94.6 and 5.4  $\mu$ M respectively. Insets are representative current traces of each calcium channel before and after (red trace) application of 1  $\mu$ M ProTx I (Note that the trace for hCav3.1 is the same as in figure 1). All other data were fitted with the Boltzmann equation and are from multiple paired experiments (n = 5-6 per channel). Note the negative shift in both the half activation and steady state inactivation potential in the presence of 1  $\mu$ M ProTx I for hCav3.2 despite this concentration having minimal effect on tonic block.

#### **4.5 The domain IV region of hCav3.1 is important for ProTx I block and function of hCav3.1**

Our lab had previously constructed a series of chimeric channels in which we had swapped various membrane domains between Cav3.1 and Cav3.3<sup>(193)</sup>. We used a subset of these chimeras to ascertain which of the membrane domains were responsible for the differences in ProTx I blocking effects on these two channel subtypes. As shown in Figure 3, chimeras that contained the domain IV region of hCav3.1 exhibited a degree of block that was similar in magnitude to that of the wild-type channel, whereas constructs that contained Cav3.3 sequence in this domain behaved like the wild-type Cav3.3 channels (Figure 4.5.1). These data indicate that domain IV is a major determinant of ProTx I action on hCav3.1. In addition, replacing domain II in the chimeras with corresponding Cav3.3 sequence (GIGI) further weakened the blocking effect, while having only Cav3.1 domain II and domain IV (IGIG) produced block equivalent to wild-type. This suggests that domain II may also contribute to toxin action on hCav3.1. We also examined the effect of the toxin on the gating behavior of these sets of chimeras. Most of the chimeras did not undergo a toxin induced change in half-activation or inactivation potential as expected from our observation with wild-type channels, although two constructs exhibited a minor depolarizing shift in half activation potential when the toxin was applied (Table 4.3). We note that a previous study in which ProTx I was shown to induce a dramatic shift in half activation potential of Cav3.1 used a cDNA derived from rat<sup>(263)</sup>. We therefore tested ProTx I on rat Cav3.1 and although there was a slight positive shift in activation, it did not reach significance. We did, however, observe a small but significant negative shift in the steady state inactivation that was consistent with the previous findings<sup>(263)</sup> and which curiously contrasts with our observation with human Cav3.1 where no significant shift was observed (Table 4.3).

A more recent study also found that ProTx I impedes Nav1.2 and TRPA1 channel activation by binding to and stabilizing the voltage sensor in its closed conformation<sup>(261)</sup>. It remains to be seen whether a similar interaction occurs with T-type calcium channels.

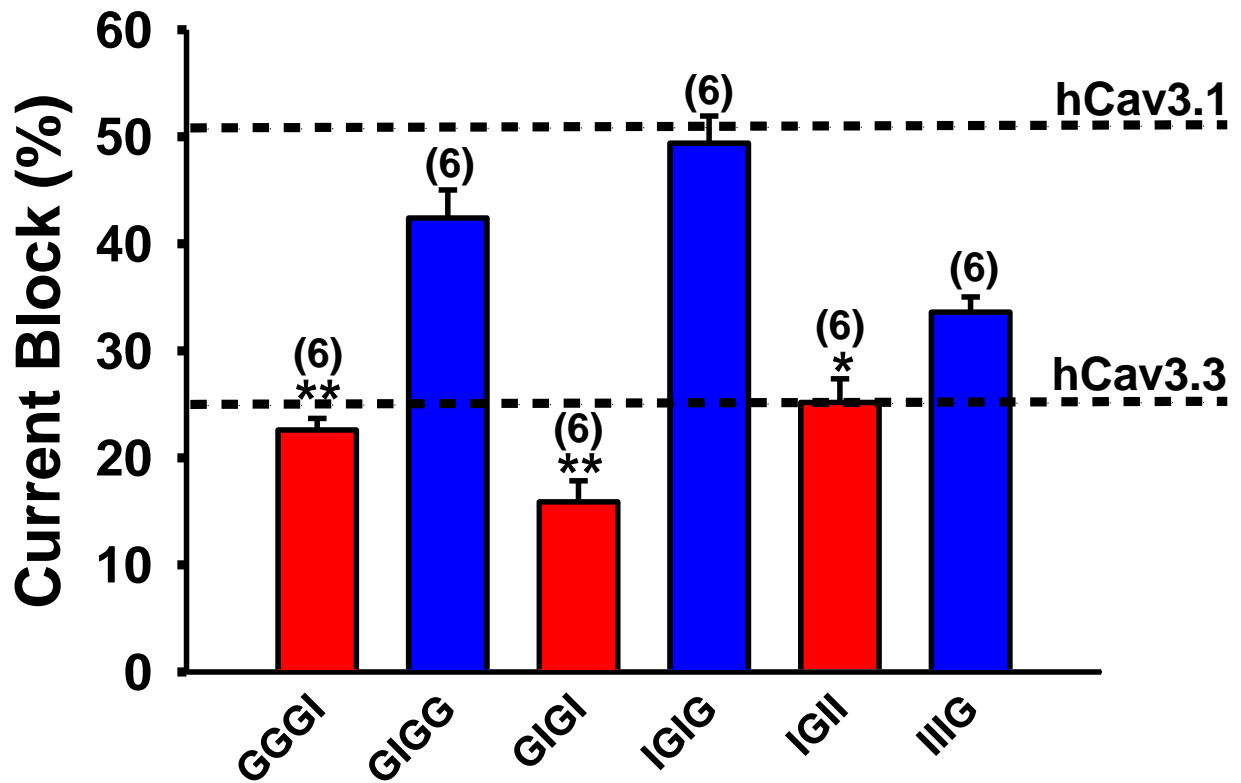


**Figure 4.5.1. Tonic block of hCav3.1-hCav3.3chimeras by 1  $\mu$ M application of ProTx I.**

Chimera nomenclature is as follows: hCav3.1 sequence in domains I-IV is denoted by “G”, hCav3.3 sequence is denoted by “I”. Note that block of hCav3.1 and Chimeras that contain domain IV of hCav3.1 are similar (see top dashed line). The bottom dashed line represents percent tonic block of 1  $\mu$ M ProTx I of wild-type hCav3.3. (n=5-6 per channel, at 1 $\mu$ M). Error bars reflect standard errors, asterisks denote statistical significance relative to hCav3.1 (\*p<0.05, \*\*p<0.01). Currents were elicited by stepping from a holding potential of -110 mV to a test potential of -20 mV.

Chimera	Current Block (%) ProTx I (1μM)	V <sub>0.5act</sub> (mV) Con	V <sub>0.5act</sub> (mV) ProTx I (1μM)	V <sub>h</sub> (mV) Con	V <sub>h</sub> (mV) ProTx I (1μM)
hCav3.1 wt	50 ± 1.5	-52.3	-52.3	-74	-76
GGGI	23 ± 1**	-43.5	-44.5	-75.3	-77.5
GIGG	43 ± 2.6	-56.9	-49.0 #	-76.1	-75.9
GIGI	16 ± 1.9**	-41.1	-33.5 #	-73.2	-73.2
IGIG	50 ± 2.5	-41.8	-34.6 #	-68.9	-69.3
IGII	25 ± 2.2*	-42.5	-41.0	-74.0	-73.7
IIIG	35 ± 1.4	-41.7	-38.8	-72.5	-73.7
rCav3.1 wt	60 ± 1.6	-57.6	-54.2	-75.1	-80.9 #

**Table 4.3 Summary of biophysical parameters of human Cav3.1, rat Cav3.1 and hCav3.1 hCav3.3 chimeras in the absence or presence of 1 μM ProTx I.**

Asterisks denote statistical significance relative to hCav3.1 for current block. The hash tag denotes significance relative to control (#, \*p<0.05, \*\*p<0.01).

#### **4.6 Substitution of individual amino acid residues in the putative toxin blocking sites does not affect ProTx I block of hCav3.1**

Given the high degree of conserved amino acid sequence between T-type calcium channels, we used ClustalW2 multiple sequence alignment of both the domain II and domain IV regions of these channels to determine if there were any sites that were unique to hCav3.1 that might be involved in toxin block, taking into consideration the loci of amino acid residues that are known to be involved in toxin block of voltage-gated sodium channels<sup>(249, 250, 253)</sup>. Our alignment (Figure 4.6.1 A) yielded nine candidate residues; two in domain II of hCav3.1 and seven in domain IV. To determine whether these residues may be involved in ProTx I block of hCav3.1, we replaced all nine residues with corresponding residues in Cav3.3, and then assessed ProTx I block of these mutant channels.

As shown in Figure 4.6.1B, three of the amino acid residues resulted in non-functional channels. Surface biotinylation experiments revealed that these mutant channels trafficked appropriately to the cell surface (data not shown), indicating that their inability to support whole cell currents was not due to an absence of expression. Instead, since these substitutions are in the region thought to be involved in voltage-dependent inactivation, it is possible that these substitutions disrupted this mechanism enough to prevent current passing through the channel. Of the remaining mutations, although none resulted in a significant decrease in ProTx I block, two of the mutations (V1618A and Q1631K), displayed a significant negative shift in their half inactivation potential compared to wild-type channels. In addition, the V1618A mutant also showed a significant positive shift in half activation potential compared to wild-type (Table 4.5) thus indicating, that although these individual amino acid residues could not account for the blocking effects of this toxin, they did alter the gating behavior of the channel.

Clone DOM IV mut	IC50 Tonic ProTx I ( $\mu\text{M}$ )	$V_{0.5\text{act}}$ (mV) Con	$V_{0.5\text{act}}$ (mV) ProTx I ( $1\mu\text{M}$ )	Vh(mV) Con	Vh (mV) ProTx I ( $1\mu\text{M}$ )
hCav3.1 wt	$0.64 \pm 1.5$	-52.3	-52.3	-74	-76
hCav3.1 V1618A	$0.66 \pm 2.2$	-51.5	-46.8*	-79*	-77
hCav3.1 Q1631K	$0.92 \pm 4.5$	-53.2	-54.3	-84*	-82
hCav3.1 S1659A	$1.29 \pm 4$	-53.1	-50.8	-77	-79
hCav3.1 M1696V	$1.27 \pm 4.8$	-51.5	-49.1	-74	-79
DOM II mut	Current Block (%) ProTx I ( $1\mu\text{M}$ )	$V_{0.5\text{act}}$ (mV) Con	$V_{0.5\text{act}}$ (mV) ProTx I ( $1\mu\text{M}$ )	Vh(mV) Con	Vh (mV) ProTx I ( $1\mu\text{M}$ )
Q826A	$40 \pm 1.5$	-53.6	-51.2	-75.2	-73.6
G827D	$38 \pm 2.2$	-52.4	-52.7	-77	-72
QG826-7AD	$40 \pm 2.5$	-51	-48.2	-74	-76.3

**Table 4.5 Summary of biophysical parameters of wildtype hCav3.1 and hCav3.1 domain IV and domain II mutants in the absence or presence of 1  $\mu\text{M}$  ProTx I.**

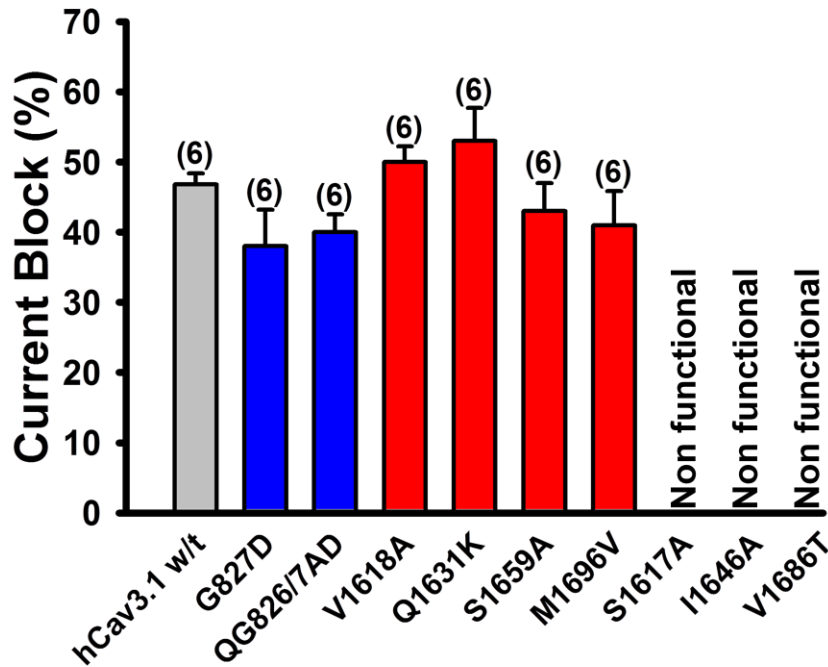
Asterisks denote statistical significance relative to wild-type hCav3.1 (\* $p < 0.05$ ).

**A Domain II**

hNav1.7 ELFLADVE<sup>Q</sup>LSVLR<sup>S</sup>FRL<sup>L</sup>RVFKL  
hCav3.1 EIVG<sup>Q</sup><sup>Q</sup><sup>G</sup>GLSVLRTFRLMRVLKL  
hCav3.2 EIVG<sup>Q</sup>AD<sup>G</sup>GLSVLRTFRL<sup>L</sup>RVLKL  
hCav3.3 EIVG<sup>Q</sup>AD<sup>G</sup>GLSVLRTFRL<sup>L</sup>RVLKL

**Domain IV**

hNav1.7 FTGECV<sup>L</sup>LK<sup>L</sup>ISLRH-YYFTVGWNI<sup>F</sup>DFV<sup>V</sup>VI<sup>S</sup>I<sup>V</sup>GMFLADLI--ETYFV<sup>S</sup>PTLFRVIRLARI<sup>G</sup>RILRLVKGAKGIR<sup>T</sup>LLFAL<sup>M</sup>MSL  
hCav3.1 FVLE<sup>S</sup>V<sup>L</sup>LK<sup>L</sup>VAFG<sup>F</sup>RR<sup>F</sup><sup>Q</sup>DRWNQ<sup>L</sup>DLAIV<sup>L</sup>LS<sup>I</sup>MGITL<sup>E</sup>EIEVNA<sup>S</sup>LPINPTIIRIMRVLRIARV<sup>L</sup>KLLKMA<sup>V</sup>GMRALLDTV<sup>M</sup>QAL  
hCav3.2 FVFEAALK<sup>L</sup>VAFG<sup>F</sup>RR<sup>F</sup><sup>Q</sup>KDRWNQ<sup>L</sup>DLAIV<sup>L</sup>LS<sup>M</sup>MGITL<sup>E</sup>EIE<sup>S</sup>AALPINPTIIRIMRVLRIARV<sup>L</sup>KLLKMATGMRALLDTV<sup>V</sup>QAL  
hCav3.3 FVLEAALK<sup>L</sup>VAFGLRR<sup>F</sup><sup>F</sup><sup>Q</sup>KDRWNQ<sup>L</sup>DLAIV<sup>L</sup>LSAMGITL<sup>E</sup>EIEINAALPINPTIIRIMRVLRIARV<sup>L</sup>KLLKMATGMRALLDTV<sup>V</sup>QAL

**B**

**Figure 4.6.1 Sequence alignment and tonic block of human Cav3.1 and Cav3.1 mutants induced by 1  $\mu$ M application of ProTx I.**

**A.** Sequence alignment of human sodium channel 1.7 (hNav1.7) versus the three T-type calcium channels (Mutations highlighted in red) and **B.** Tonic block of human Cav3.1 and Cav3.1 mutants induced by 1  $\mu$ M application of ProTx I. Domain II mutations are denoted in blue, domain IV mutations are shown in red (n=5-6 per channel, at 1  $\mu$ M). Note that the last three mutations in graph (all domain IV), produced a non-functional channel despite trafficking to the membrane. Since this region has been shown to be involved in the inactivation gating of the channel, it is possible that these mutations disrupted this mechanism enough to prevent current passing through the channel. Error bars reflect standard errors. Currents were elicited by stepping from a holding potential of -110 mV to a test potential of -20 mV.

#### 4.7 Discussion:

Previous studies have shown that the tarantula venom peptides ProTx I and ProTx II inhibit voltage-gated sodium channels by shifting their voltage dependence of activation to more positive potentials<sup>(262, 263)</sup>. In our studies, we used these two toxins to try to inhibit low voltage activated T-type calcium channels. Our results showed that ProTx I preferentially blocked hCav3.1 at sub-micromolar concentrations, but we did not observe any shift in half activation potential. Contrary to previous findings<sup>(263)</sup>, ProTx II appeared to preferentially block hCav3.2. This toxin caused a significant negative shift in half inactivation voltage of hCav3.2 but no significant change in half activation potential. We failed to see significant block of hCav3.1 or hCav3.3 in the presence of 1  $\mu$ M of the toxin, however we observed significant negative shifts in the half activation potentials at these low concentrations.

The apparent differences between some of our results and those of previous studies may be in part be due to the different expression systems, recording methods and clones used. In the previous studies, HEK cells and *Xenopus* oocytes were used to express rat clones of the T-type channels and toxin effect and channel kinetics were measured on tail currents as an indicator of potency. We attempted to address this discrepancy by using ProTx I on a rat Cav3.1 clone available to us and although our results showed a similar positive shift in activation (Table 4.3), it did not reach significance. We did, however, observe the negative shift in the steady state inactivation that was consistent with the previous finding (Table 4.3). As mentioned previously, another study found that ProTx I impedes Nav1.2 and TRPA1 channel activation by binding to and stabilizing the voltage sensor in its closed conformation and that ProTx I preferential binds to the insect isoform of these channels<sup>(261)</sup>. Unfortunately, this paper was published well after the experiments in this chapter were conducted and therefore further experiments will need to be

conducted to determine whether this is also the case with the human T-type calcium channels. It would also be prudent to determine how toxin actions are affected by different experimental conditions so that the precise biophysical interactions of these and other toxins with T-type calcium channels can be determined.

Finally, my initial results show that ProTx II is selective for Cav3.2 vs the other T-types but because of the lower affinity, I did not pursue this channel-toxin interaction further. However, three dimensional modeling from Bill Catterall's group describes how  $\beta$ -scorpion toxin might bind to Nav1.2 and how two crucial glutamic acids may form a docking system for the toxin<sup>(121, 256)</sup>. These two glutamic acids are not only conserved in T-types, but are also equi-distant (58 amino acids) apart, suggesting the overall structure of the binding site may again be similar. Again, further investigation of the Domain 2 region of the T-types will need to be carried out to see if this is indeed the case.

#### **4.8 Conclusions:**

We showed that ProTx I and ProTx II potently and preferentially block hCav3.1 and hCav3.2 respectively. These two toxins block and modify T-type calcium channels using mechanisms similar to their interaction with sodium channels<sup>(262, 263)</sup>. However, the shift in the voltage dependence of inactivation to more negative potentials more closely resembles  $\beta$ -scorpion toxin interactions with sodium channels<sup>(121)</sup>. We failed to see a shift of voltage dependence of activation to more positive potentials that were seen in previous studies<sup>(252, 263, 266)</sup>, but this may be due to different cDNA constructs that were used previously.

Several residues in a highly conserved region between T-type and sodium channels corresponded to potential toxin binding sites. However, mutagenesis of several of these residues on an individual basis did not alter the blocking effects of Protoxin I. Despite this result, the data in this

chapter provides further insights into the structural similarities between sodium and T-type calcium channels and the apparent conservation in toxin binding sites.

Overall, our data suggest that both ProTx I and ProTx II interact with Cav3.1 and Cav3.2 respectively, in a way that is similar to  $\beta$ -scorpion gating-modifier toxins interact with sodium channels and therefore they may be useful towards exploring the gating mechanisms of T-type calcium channels. Finally, the apparent similarities in the toxin binding sites between Nav and Cav channels may provide insights into the development and synthesis of more potent and/or selective antagonists that act on either or both of these channel subtypes.

**CHAPTER FIVE: SYNTHESIS AND EVALUATION OF 1,4-DIHYDROPYRIDINE  
DERIVATIVES WITH T-TYPE CALCIUM CHANNEL BLOCKING ACTIVITY THAT  
ATTENUATE INFLAMMATORY AND NEUROPATHIC PAIN**

**5.1 Background:**

In the previous two chapters, I investigated the structural similarities between sodium and T-type calcium channels to determine whether known drug and toxin binding sites in VGSCs were also present in LVA calcium channels. I then examined whether compounds previously identified as selective VGSC blockers could also block T-type calcium channels. The aim of this work was primarily to find potent blockers of LVA channels and to try and better understand drug-LVA calcium channel interactions.

For this chapter, I examined a class of drugs, 1,4-DHPs, that have also been extensively studied and are best known for their potent block of HVA calcium channels, the close relative of LVA T-type calcium channels. DHPs are an important class of calcium channel blockers that are used to treat conditions such as hypertension and angina<sup>(38, 216, 267)</sup>. Their primary target in the cardiovascular system is the Cav1.2 L-type calcium channel isoform. However, some articles suggest that DHPs used to treat these diseases, such as Isradipine and Benidipine, may also exert their therapeutic effect via T-type calcium channels<sup>(39, 268)</sup>. They suggest that the mixed L/T-type block of these drugs adds to their therapeutic efficacy, possibly via aldosterone secretion lowering blood pressure (T-type calcium channels have previously been identified in regulating aldosterone secretion)<sup>(39, 105, 269-271)</sup>.

Therefore, using similar logic to that outlined in the previous chapters, I examined whether DHPs could not only block HVA calcium channels as previously reported<sup>(11, 39, 214)</sup>, but also whether they could be modified to be more potent and selective for T-type calcium channels.

The first indication that this may indeed be possible lies in the similarities in sequence of Cav1.2 and Cav3.2 in the region thought to be involved in DHP-binding. Previous studies using site-directed mutagenesis and predictive modeling of channel structure show that the DHP binding site in Cav1.2 may be at the interface of domains III and IV of the channel<sup>(40, 218, 272)</sup>. Several other reports predict up to nine, mostly hydrophobic amino acid residues, come together to form a crevice that allows DHPs to dock and produce their inhibitory effect<sup>(40)</sup>. Although this area is relatively close to the pore of the channel, it is commonly thought that this effect of DHPs is via modulation of the gating of the channel, rather than acting via pore block<sup>(40, 217, 272)</sup>.

Furthermore, sequence alignment reveals that many of these hydrophobic residues involved in DHP binding to Cav1.2 are conserved within the T-type channels, suggesting that there may be a similar “crevice” within domains III and IV and that DHPs may also bind to this site in T-type channels. Conversely, comprehensive mutagenesis studies by Peterson et al.,<sup>(40, 217, 273)</sup> show that substitution of the critical tyrosine 1152, to phenylalanine (Y1152F), produced a *K<sub>d</sub>* value 12.4-fold higher in Cav1.2. Interestingly, the corresponding amino acid in all T-types is also a phenylalanine, perhaps explaining why most DHPs block L-type more potently than T-type channels.

In the first part of this chapter, we describe the synthesis of a series of novel DHP derivatives that have a condensed 1,4-DHP ring system (hexahydroquinoline) and report on their abilities to block both L-type and T-type calcium channels. Previous studies showed that the preferred substituent at the C-4 position of DHPs is a phenyl ring because of animal toxicity observed with heteroaromatic rings<sup>(40, 274)</sup>. In addition, ester groups at the C-3 and C-5 positions have also been shown to be important for modulating activity and tissue selectivity<sup>(37, 275-277)</sup>. Finally, a study by Goldmann and Stoltefuss<sup>(277)</sup> indicated that at least one ester group must be *cis* to the double

bond of DHPs to allow for hydrogen bonding to the drug receptor site. Here, we describe how the ten novel DHP derivatives in which substituted cyclohexane rings are fused to the DHP ring and how different ester groups attached to this backbone affect L- and T-type calcium channel block.

In the second part of this chapter, using the results and structural information obtained from the first series of compounds that identified the ester moiety as crucial for T-type channel block, we examined a second series of similar compounds that had different substituents on the ester moiety to determine if any of the compounds would produce a further increase in blocking activity while remaining selective for T-type channels. Two lead compounds termed N10 and N12, were identified and then characterized in detail for functional effects on transiently expressed Cav3.2 channels and examined for analgesic properties in mouse models of inflammatory and neuropathic pain.

## **5.2 Results from novel DHP compounds.**

DHPs are a class of drugs widely used in the treatment of cardiac and vascular diseases such as hypertension, angina and atherosclerosis<sup>(5, 37, 278)</sup>. Their principal target is thought to be the L-type calcium channel Cav1.2<sup>(40, 127, 217, 267, 279)</sup>. However several recent reports have noted that some DHPs also block the T-type calcium channel isoforms, Cav3.1 and Cav3.2<sup>(11, 39, 214)</sup>. Since these channels are both expressed in vascular smooth muscle and are involved in cardiac pacemaking and aldosterone secretion, some reports suggest that the beneficial effects of DHP treatment may be in part due to their additional block of T-type calcium channels<sup>(39, 105, 269)</sup>. Here, we compare the effects of our new DHP series on L-type and T-type channels expressed transiently on tsA-201 cells to attempt to identify both mixed and selective calcium channel blockers.

Using the whole cell patch clamp technique, we recorded current from tsA- 201 cells transiently transfected with either rat Cav1.2 and ancillary calcium channel subunit cDNA (L-type), or human Cav3.1. We then conducted an initial screening by applying 10 $\mu$ M of each of our compounds to test for tonic (i.e., resting state) block.

### **5.2.1. Tonic block of L and T-type calcium channels by novel DHP-based compounds.**

Results in Figure 5.2.1A show robust peak current inhibition (greater than 75%) for compounds M2, M3 and M4, while the remainder of the compounds showed less than 50% block of the L-type current. In Figure 5.2.1B, a similar set of experiments were carried out except that cells were now transfected with the Cav3.1  $\alpha$ 1 subunit. These results show that compounds M2, M3 and M4 were again effective at blocking peak current, with compound M4 producing almost complete block of the T-type current. Interestingly, compound M12 also showed effective block of the Cav3.1 current.

Together, these results show that compounds M2, M3 and M4 were effective blockers of both L and T-type calcium channels, whereas compound M12, was selective for the Cav3.1 calcium channel over Cav1.2. Given that the differences between these compounds are their ester groups, this suggests that ester moiety plays a key role in the ability of these compounds to block T-type calcium current.

Compounds M6 through M10 all failed to significantly (<50%) block L and T-type current at our screening concentration of 10 $\mu$ M. This may be due to the introduction of a benzoyloxy substituent on the phenyl ring of these compounds. This addition of a second ester moiety dramatically increases their size, which may well have a detrimental effect on the ability of these compounds to dock to either channel.

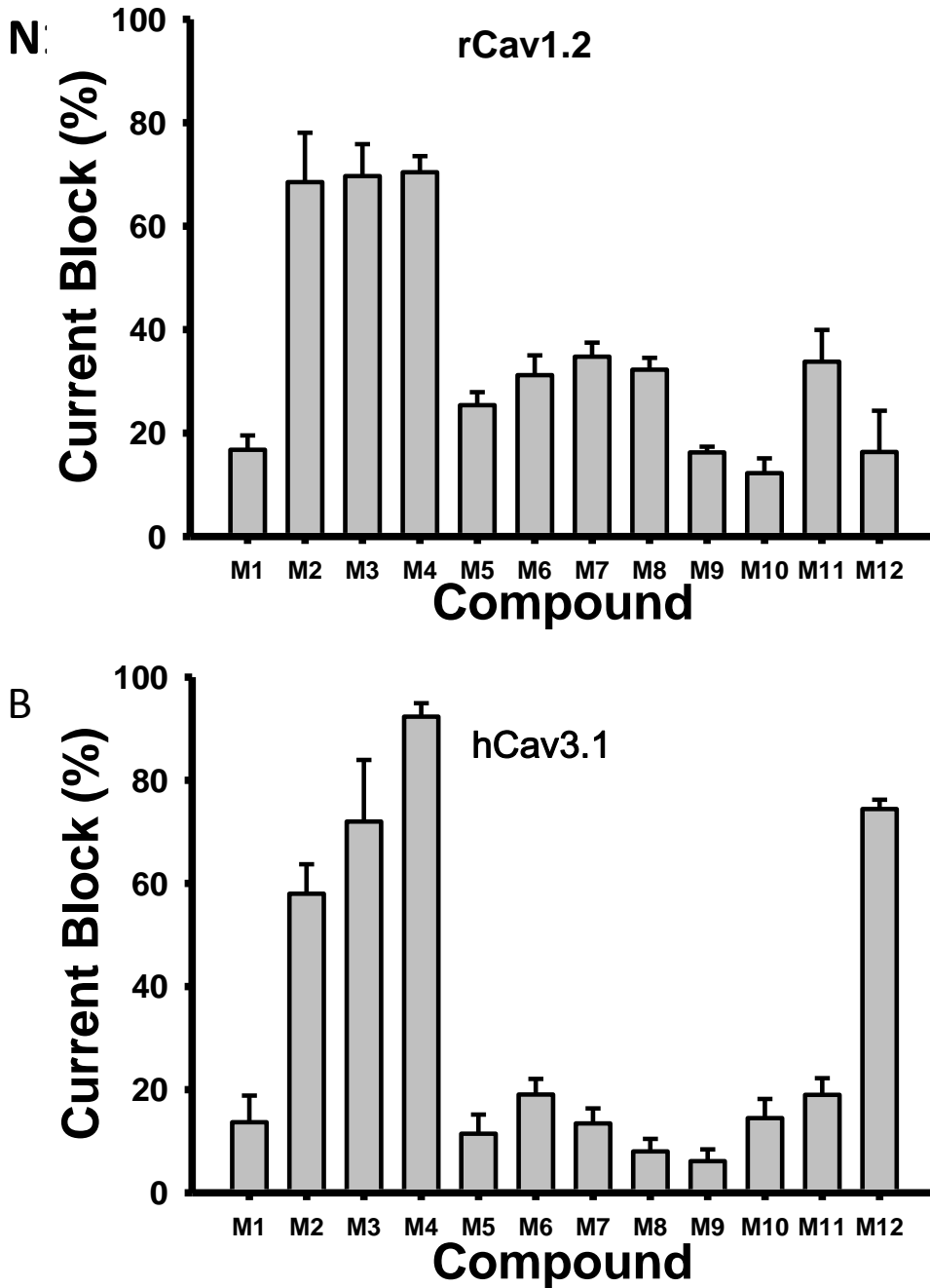


**Figure 5.2.1 Tonic block of L and T-type calcium channels by novel DHP-based compounds.**

**A.** Tonic block of rat Cav1.2 (L-type) induced by 10  $\mu$ M of application of DHP-based compounds (n=4-5 per channel). Note the dramatic block of compounds M2, M3, and M4. **B.** Tonic block of human Cav3.1 (T-type) with the same compounds (n=4-5 per channel, at 10 $\mu$ M). Note in addition to M2, M3, and M4 block, M12 produces significant block of hCav3.1. Error bars reflect standard errors.

Compounds M11 and M12, which were developed and published previously<sup>(227)</sup>, have a very similar DHP scaffold to compounds M1-M10 except that their ester group is modified with 3-pyridylmethyl. Neither one of these two compounds effectively blocked Cav1.2 current; however M12 had potent inhibitory effects on Cav3.1 current (~80% block). This result was somewhat surprising given the similarities between the two compounds, however M12 does have a different substituent on the phenyl ring and two additional methyl groups at 6-position of the hexahydroquinoline ring. The second modification at the 6-position of the hexahydroquinoline ring is present in all of our ten novel compounds (which do not block Cav3.1) and therefore is unlikely to be the factor determining sub-type selectivity. This suggests that the substituent on the phenyl ring is the critical component for the preferential block of Cav3.1 T-type channels over Cav1.2. M12 also blocked the Cav3.2 and Cav3.3 channel subtypes with similar potency as Cav3.1 (data not shown).

### **5.2.2 Comparison of dihydropyridine block of L- and T-type calcium channels.**

The blocking action of compounds M4 and M12 on L-type and T-type channels were then subjected to a more detailed analysis, including dose-dependence and effects on steady state activation and inactivation properties of the channels. As shown in Figure 5.2.2.1A, M4 blocks Cav1.2 with an IC<sub>50</sub> of 4 μM and mediates a hyperpolarizing shift in the half-inactivation potential ( $V_h$ ) of the channel by 15 mV. Time course of M4 block shows a gradual, dose-dependent onset of channel inhibition, followed by a slow, partial recovery of the current upon washout to approximately 50% of original peak amplitude. Figure 5.2.2.1B and C show that M4 blocks T-type currents with a similar IC<sub>50</sub> and time course. Unlike Cav1.2, there was no significant shift in  $V_h$  of these channels. However, there was a significant hyperpolarizing shift in the half-activation potential ( $V_{0.5 \text{ act}}$ ) of both T-type channels (see Table 5.2.1).

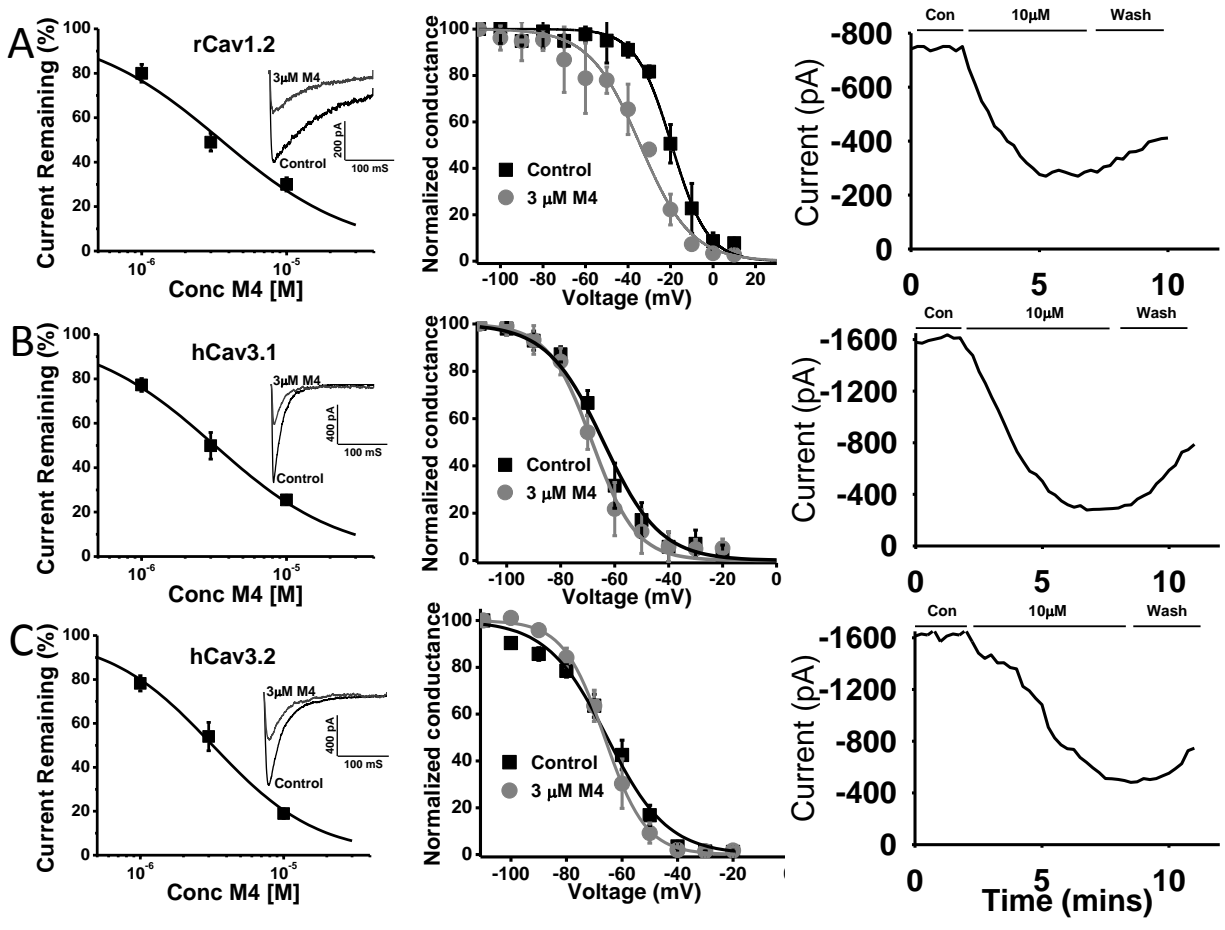


**Figure 5.2.2.1** Characterization of novel M4 DHP based compound with L and T-type calcium channels.

**A. B. C.** M4 Dose response curves, steady state inactivation curves and time course of drug block for rCav1.2, hCav3.1 and hCav3.2 respectively. Insets are representative current traces of each calcium channel before and after application of 3 $\mu$ M M4. Steady state inactivation curves were recorded prior to and after application of 3 $\mu$ M M4. Ensemble dose response curves for tonic channel inhibition by M4 compound were fitted via the Hill equation. All other data were fitted with the Boltzmann equation and are from multiple paired experiments. Note the negative shift in the half inactivation potential in the presence of M4 for rCav1.2.

	<b>IC50 M4 (<math>\mu</math>M)</b>	<b>IC50 M12 (<math>\mu</math>M)</b>	<b>Control <math>V_{0.5}^{act}</math> (mV)</b>	<b>M4 (3<math>\mu</math>M) <math>V_{0.5}^{act}</math> (mV)</b>	<b>M12 (3<math>\mu</math>M) <math>V_{0.5}^{act}</math> (mV)</b>	<b>Control <math>V_h</math> (mV)</b>	<b>M4 (3<math>\mu</math>M) <math>V_h</math> (mV)</b>	<b>M12 (3<math>\mu</math>M) <math>V_h</math> (mV)</b>
<b>rCav1.2</b>	<b>4</b>	<b>&gt;30</b>	<b>-7.5</b>	<b>-6.3</b>	<b>N.A.</b>	<b>-19.5</b>	<b>-34.3**</b>	<b>N.A.</b>
<b>hCav3.1</b>	<b>2.4</b>	<b>3.2</b>	<b>-31</b>	<b>-46**</b>	<b>-31</b>	<b>-64</b>	<b>-68</b>	<b>-63</b>
<b>hCav3.2</b>	<b>3.2</b>	<b>1.5</b>	<b>-36</b>	<b>-47**</b>	<b>-24**</b>	<b>-65</b>	<b>-66</b>	<b>-61</b>

**Table 5.2.1 Summary of biophysical parameters of various calcium channels in the absence and the presence of M4 and M12 compounds.**

Note, since rat Cav1.2 had no significant block at 10  $\mu$ M and 30  $\mu$ M (data not shown) for M12, the effects of this compound were not tested further on this channel. Asterisk denotes statistical significance relative to control (\*\* $p < 0.001$ ).

The effects of M12 on the biophysical characteristics of Cav3.1 and Cav3.2 are shown in Figures 5.2.2.2A and B, and Table 5.2.1. The IC<sub>50</sub>s of the compound determined from dose response curves are 3.2 and 1.5  $\mu$ M, respectively, for Cav3.1 and Cav3.2. M12 does not appear to affect  $V_h$  of either channel, but it mediates a depolarizing shift of the  $V_{0.5}$  act of Cav3.2 (+12 mV). The time course of M12 block reveals a rapid onset of inhibition, followed by a fast and almost complete recovery of both T-type channel currents which are both desirable features in drug molecules<sup>(280)</sup>. We applied M12 at a concentration of 30  $\mu$ M to Cav1.2 channels, but did not detect any additional block compared to our initial test concentration of 10 $\mu$ M (16.3 $\pm$  3%, n=3 data not shown). Altogether, this indicates that M12 is at least 30-fold selective for Cav3.2 over Cav1.2.

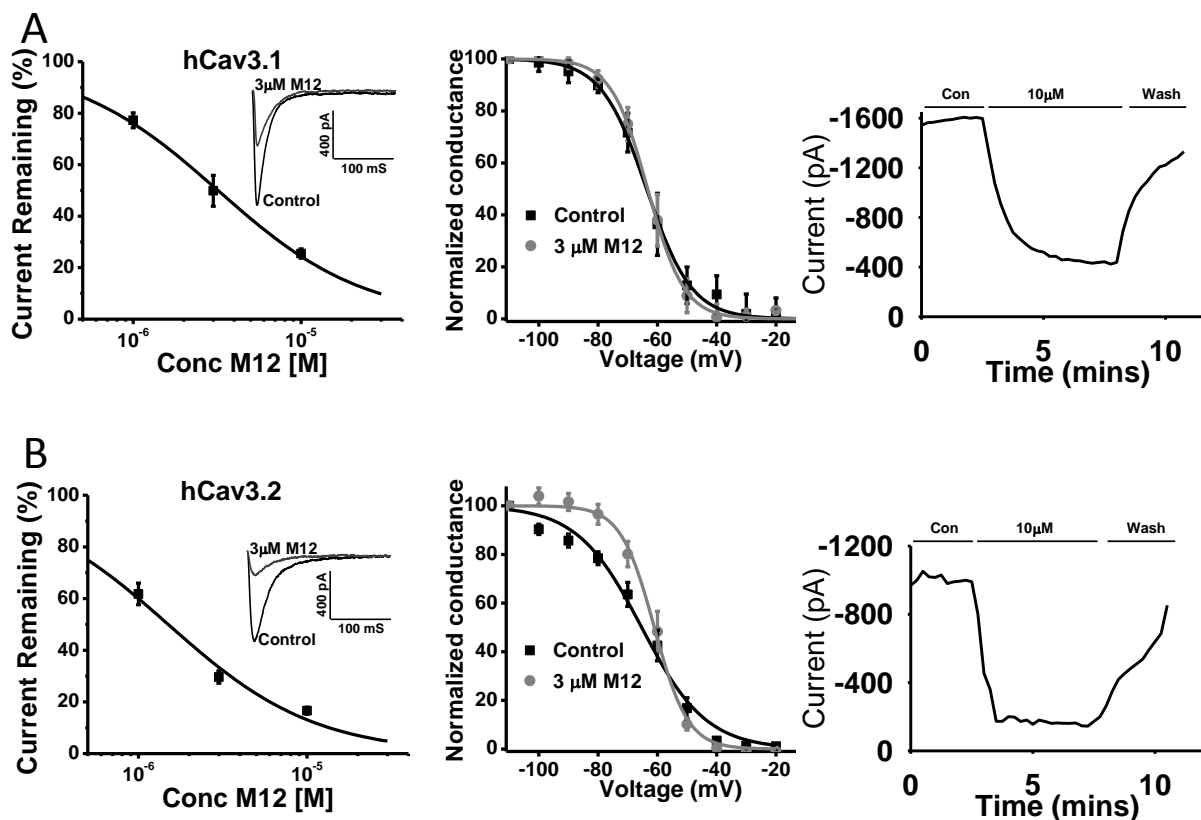


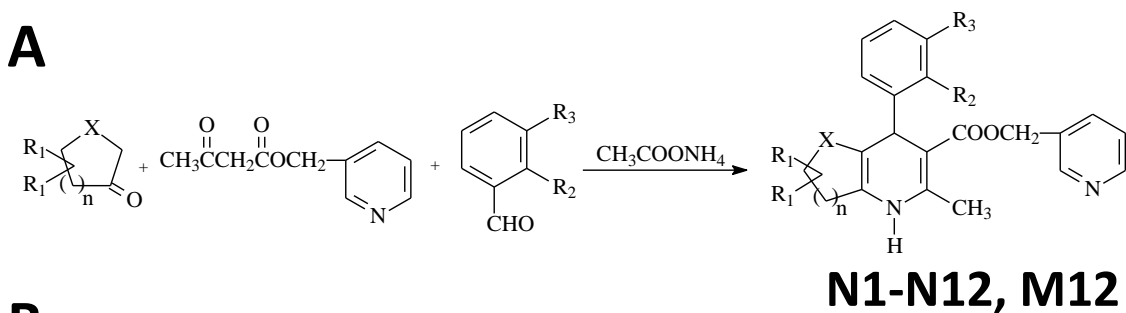
**Figure 5.2.2.2 Characterization of novel M12 DHP-based compound on T-type calcium channels.**

**A. B.** M12 Dose response curves, steady state inactivation curves and time course of drug block for hCav3.1 and hCav3.2 respectively. Insets are representative current traces of each T-type calcium channel before and after application of 3  $\mu$ M M12. Data were fitted as per previous figure. Note the rapid washout of M12 in the two T-type calcium channels compared to the previous M4 compound. Since there was very little block of M12 on rCav1.2 even at concentrations as high as 30  $\mu$ M (<20%), dose response and steady state inactivation curves were not performed.

## **5.4 Potent and selective DHP blockers of T-type calcium channels attenuate inflammatory and neuropathic pain.**

### **5.4.1 Effects of DHP derivatives on transiently expressed L- and T-type calcium channels**

In the first series of novel synthesized compounds, we identified a new DHP scaffold that could be exploited to produce a potent T-type channel selective inhibitor (M12)<sup>(116)</sup>. These findings had suggested that changing the substituents on the phenyl ring and adding two additional methyl groups at 6-position of the hexahydroquinoline ring of the new DHP scaffold leads to potent and selective DHP-based T-type channel block<sup>(116)</sup>. Based on this information, we screened a second series of related DHP-based compounds with structures similar to M12. This series of compounds had minor modifications made to either the positioning of the methyl groups on the hexahydroquinoline ring and/or small changes to the substituents on the phenyl ring, or they contained different rings fused to the DHP structure (tetrahydrothiophene) (Figure 5.4.1A, B).



**B**

Compound	X	n	R <sub>1</sub>	R <sub>2</sub>	R <sub>3</sub>	Melting Point (°C)	Molecular Weight
N1	SO <sub>2</sub>	1	H	Cl	Cl	203	464
N2	SO <sub>2</sub>	1	H	F	Cl	184	448
N3	SO <sub>2</sub>	1	H	F	F	233	432
N4	CO	2	H	Cl	Cl	205	442
N5	CO	2	H	Cl	CF <sub>3</sub>	196	476
N6	CO	2	6,6- diCH <sub>3</sub>	Cl	Cl	221	470
N7	CO	2	6,6- diCH <sub>3</sub>	F	Cl	204	454
N8	CO	2	6,6- diCH <sub>3</sub>	F	F	211	438
N9	CO	2	6,6- diCH <sub>3</sub>	F	CF <sub>3</sub>	185	488
N10	CO	2	7,7- diCH <sub>3</sub>	Cl	Cl	230	470
N11	CO	2	7,7- diCH <sub>3</sub>	F	F	200	438
N12	CO	2	7,7- diCH <sub>3</sub>	Cl	CF <sub>3</sub>	191	504
M12	CO	2	6,6- diCH <sub>3</sub>	Cl	CF <sub>3</sub>	192	504

**Figure 5.4.1 Schematic and table showing series 2 DHP-based compounds**

**A.** The synthetic route for the preparation of DHP-based compounds examined in this study. **B.** Specific substituents at the R<sub>1</sub> through R<sub>3</sub> positions depicted in panel A.

Using the whole cell patch clamp technique, we screened these compounds for potency and selectivity of calcium channel block. An initial screen using 10  $\mu$ M of each of the compound series revealed various degrees of Cav3.2 channel block (Figure 5.4.2). Among the series, compounds N10 and N12 were identified as particularly potent hCav3.2 peak current blockers, whereas these compounds mediated much less inhibition of the rat Cav1.2 L-type calcium channels (Figure 5.4.2). We therefore characterized the effects of N10 and N12 on the biophysical properties and activities of transiently transfected hCa<sub>v</sub>3.2.

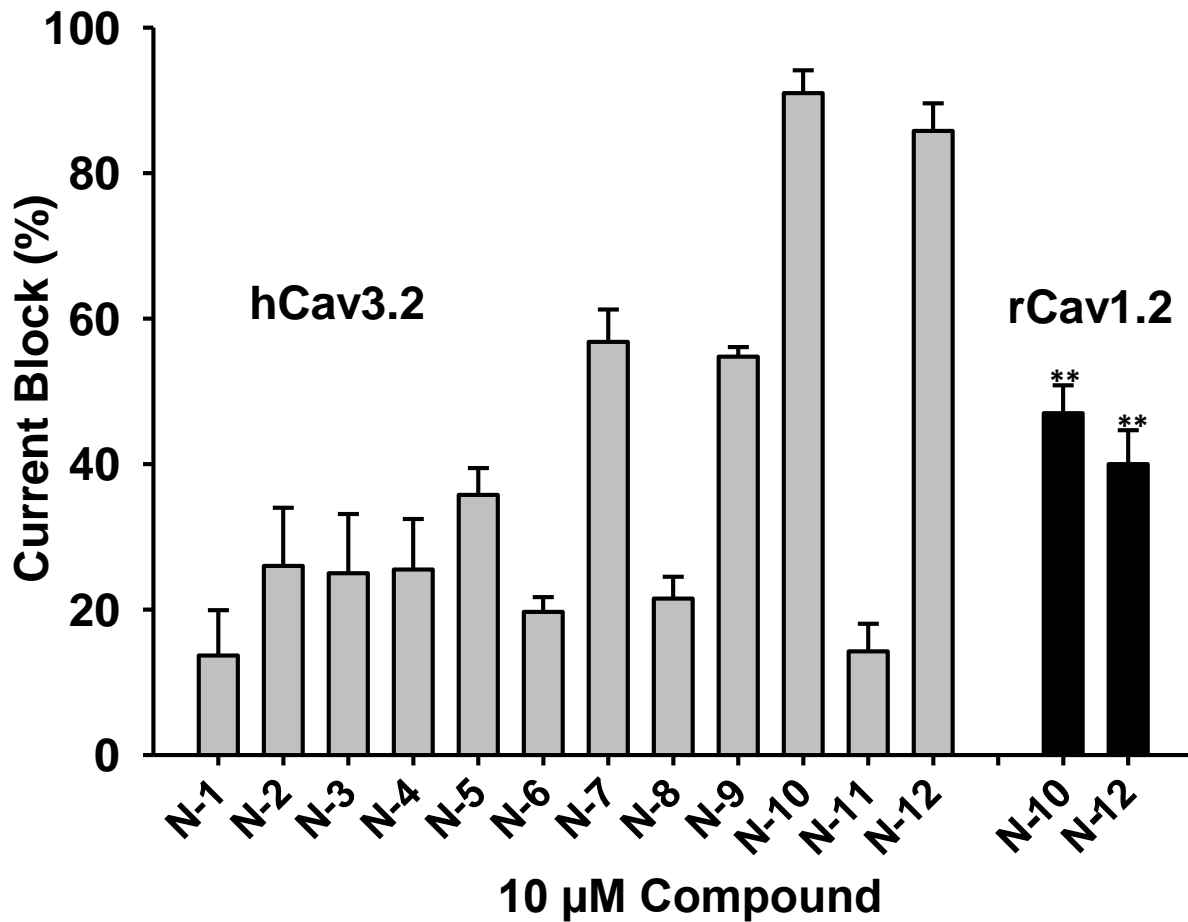


**Figure 5.4.2. Tonic block of L and T-type calcium channels by second series of DHP-based compounds.**

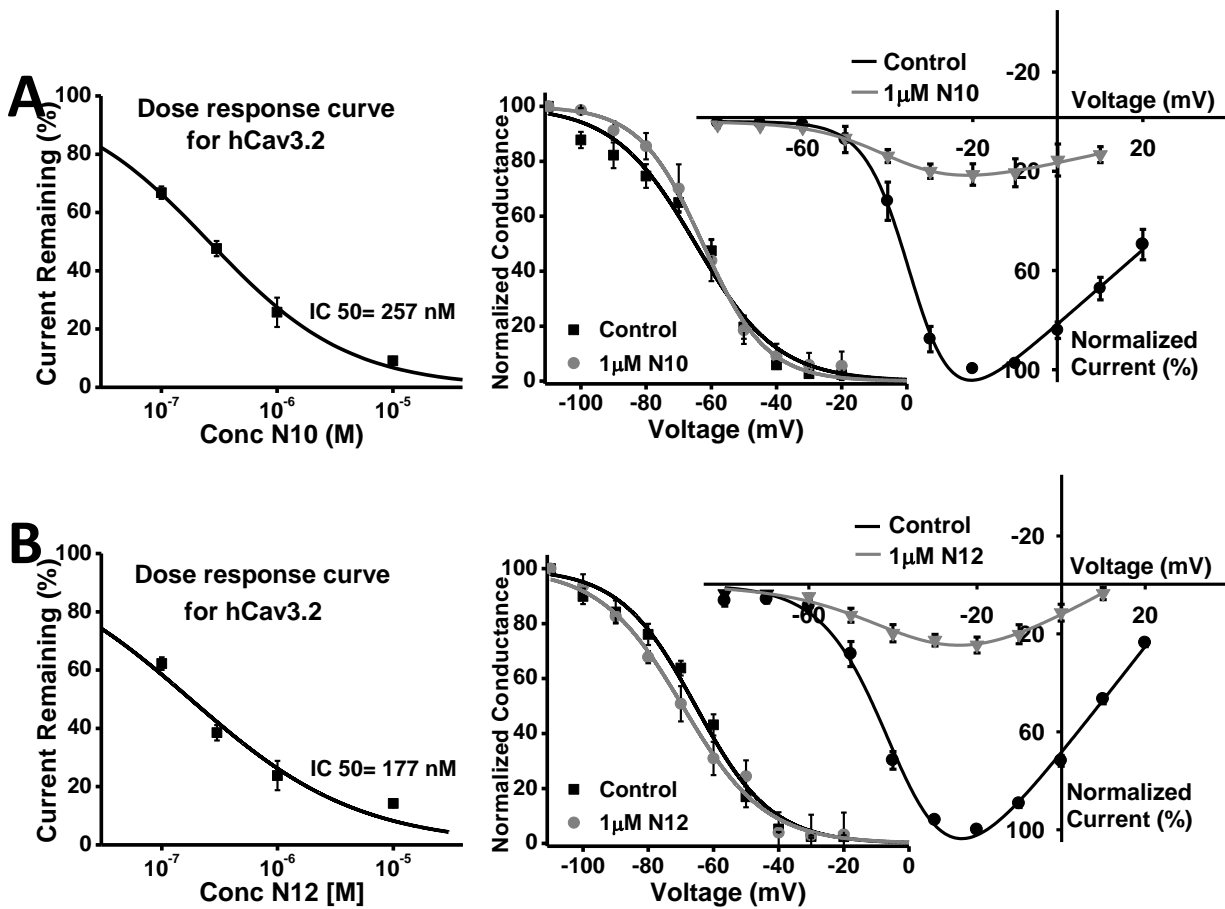
Percentage of whole cell current inhibition of human Cav3.2 (T-type) and rat Cav1.2 (L-type) channels in response to 10  $\mu$ M application of the compound series (n=6 per compound). Note the potent and preferential block of Cav3.2 channels by compounds N10 and N12 versus rCav1.2 channels. Asterisks denote significance for Cav1.2 channel block relative to block of hCav3.2 (\*\*P < 0.01). Error bars reflect standard errors. For hCav3.2 channels, the holding and test potentials were respectively -110 and -20mV, for rCav1.2 channels the holding and test potentials were -110 and 0 mV.

Figure 5.4.3A shows that N10 potently blocks hCav3.2 with an IC50 of 257 nM, but has minimal effect on the activation and inactivation properties of the channel (Table 5.4.1). Similarly, as shown in Figure 5.4.3B, N12 blocks Ca<sub>v</sub>3.2 with an IC50 of 177 nM without affecting the voltage dependences of activation and inactivation. There was also no significant effect on the kinetics of activation and inactivation (data not shown). These results are in contrast with our previous findings with M12 which shifted the half activation voltage of Ca<sub>v</sub>3.2 by +12 mV and which blocked the channels with an IC50 of 1.5 μM<sup>(116)</sup>.

<b>IC50 N10</b> <b>(<math>\mu</math>M)</b>	<b>IC50 N12</b> <b>(<math>\mu</math>M)</b>	<b>Wild- type</b> <b><math>V_{0.5act}</math></b> <b>(mV)</b>	<b>N 10</b> <b>(1<math>\mu</math>M)</b> <b><math>V_{0.5act}</math></b> <b>(mV)</b>	<b>N12</b> <b>(1 <math>\mu</math>M)</b> <b><math>V_{0.5act}</math></b> <b>(mV)</b>	<b>Wild- type</b> <b><math>V_h</math> (mV)</b>	<b>N 10</b> <b>(1<math>\mu</math>M)</b> <b><math>V_h</math> (mV)</b>	<b>N12</b> <b>(1 <math>\mu</math>M)</b> <b><math>V_h</math> (mV)</b>
<b>0.26</b>	<b>0.17</b>	<b>-36.0</b>	<b>-37.4</b>	<b>-33.6</b>	<b>-65</b>	<b>-62.6</b>	<b>-69.5</b>

**Table 5.4.1. Summary of biophysical parameters of hCav3.2 calcium channel in the absence and the presence of compounds N10 and N12.**

Note that there was no statistical significance in the gating behavior of the channel in the absence and the presence of the compounds (n=6).



**Figure 5.4.3 Characterization of novel N10 and N12 DHP-based compounds with hCav3.2.**

**A. Left panel:** Dose response relations for N10 block of Cav3.2 channels. The IC<sub>50</sub> from the fit with the Hill equation was 257 nM (n=6) **Middle panel:** Effect of 1 μM N10 on the steady state inactivation curve for Cav3.2 channels. **Right panel:** Effect of 1 μM N10 on the current voltage relation for Cav3.2 channels. The data in the middle and right panels were fitted with the Boltzmann equation and data were obtained from 6 paired experiments **B.** Same as in panel A, but with compounds N12 rather than N10. The IC<sub>50</sub> for N12 block was determined to be 177 nM (n=6).

These results are intriguing given that M12 and N12 are nearly identical except for the positioning of the dimethyl groups on the hexahydroquinoline scaffold (Figure 5.4.4A). Along these lines, compound N11, which has a very similar structure to N10 and N12, produced minimal block when applied at a concentration of 10  $\mu$ M (Figure 5.4.2). The only difference between these compounds is that N10 and N12 have at least one chlorine atom on the phenyl ring (Figure 5.4.4B) indicating that this substituent interacts with key residues within the drug interaction site of Cav3.2.

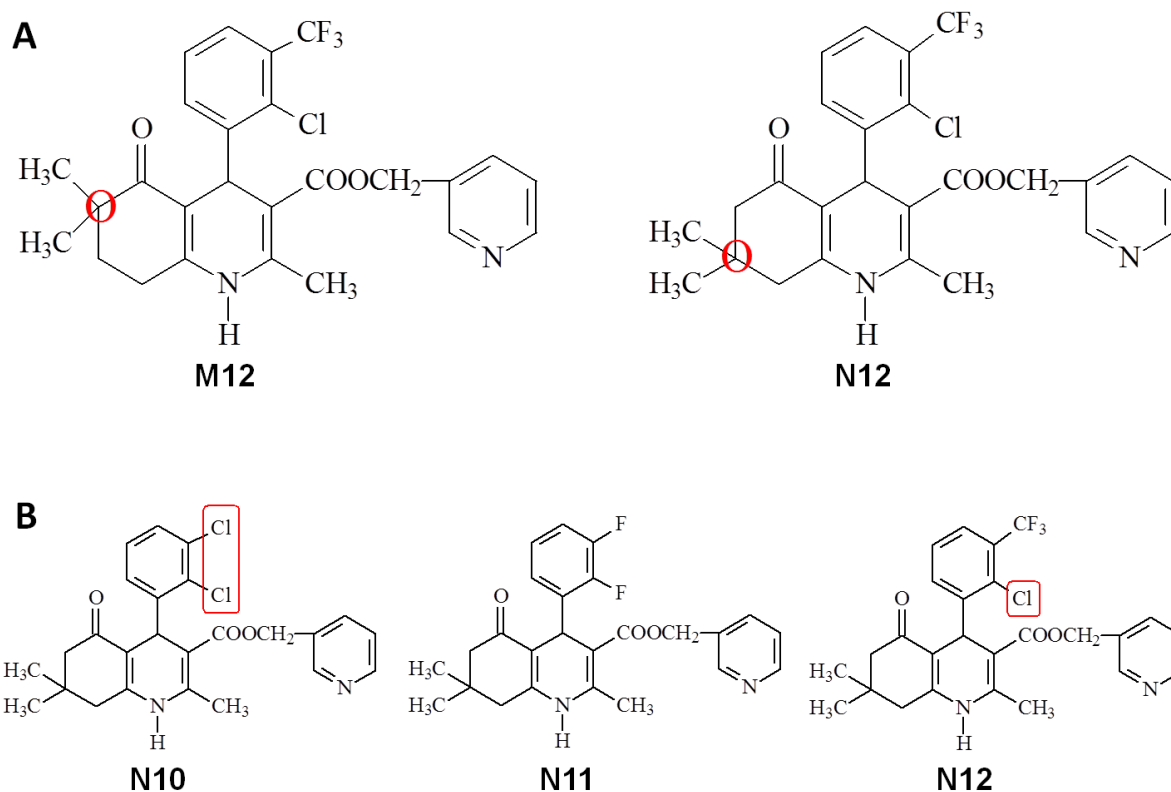


**Figure 5.4.4 Schematic highlighting structural differences between M12 and N10-12 compounds**

**A.** Schematic diagram highlighting (red circle) the different position of the dimethyl groups on the hexahydroquinoline scaffold of M12 and N12. Note that this slight modification results in an almost ten-fold increase in  $IC_{50}$  for N12 versus M12 in hCav3.2 (177 nM vs 1.5  $\mu$ M). **B.** Schematic diagram highlighting (red box) the different (chlorine) substituents at position 2 and 3 of the phenyl ring of compounds' N10 and N12. Note: N11 produces very little hCav3.2 channel block compared to compounds N10 and N12 that potently and selectively block hCav3.2.

## **5.5 Results of potent and selective DHP blockers on animal models of pain.**

### **5.5.1 Effects of M12, N10 and N12 on inflammatory pain**

To determine if the compound series could be effective *in vivo*, we first evaluated their effects on the acute nociceptive (phase 1) and inflammatory pain (phase 2) phases in a standard formalin test<sup>(130)</sup>. Figure 5.5.1.1 shows that i.t. treatment of mice with M12 (20 minutes before the formalin test) significantly reduced paw licking/biting time in a dose dependent manner in the first phase of the formalin test ( $65 \pm 5\%$ ) (Figure 5.5.1.1A) and significantly reduced paw licking/biting time at  $3\mu\text{g}$  in the second phase ( $33 \pm 7\%$ ) (Figure 5.5.1.1B). I.p. treatment of mice 30 minutes before formalin injection also resulted in a significant decrease in paw licking/biting time in both the first and second phases (Figures 5.5.1.1C and D), although maximum efficacy was achieved at a concentration of  $3\text{ mg/kg}$  ( $42 \pm 5\%$  and  $30 \pm 7\%$  inhibition, respectively). We note that the effects of M12 abated when delivered at  $10\text{ mg/kg}$  (see Figure 5.5.1.1D). This may perhaps be due to the activation of other (pronociceptive) targets at these higher doses.

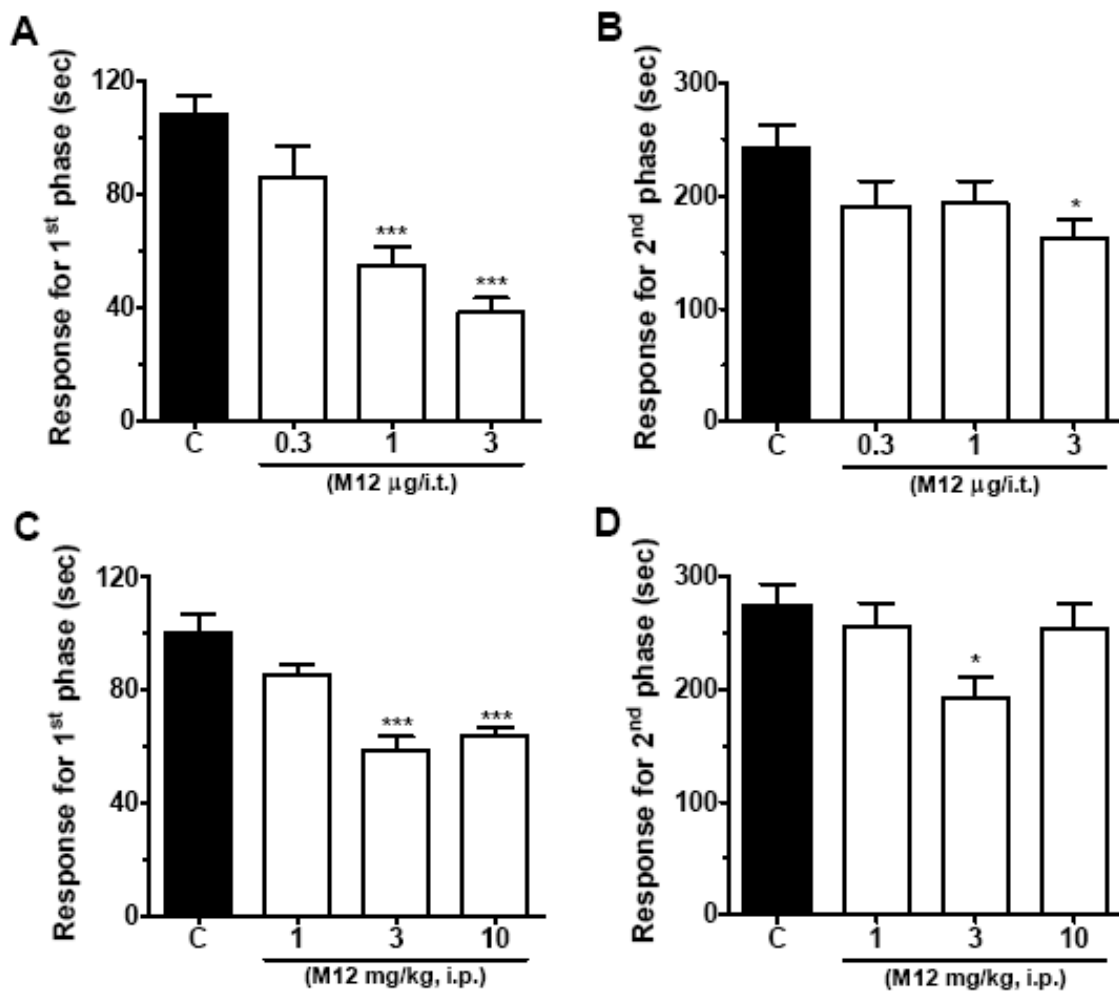


**Figure 5.5.1.1 Effects of M12 on inflammatory pain**

**A. B.** Effect of increasing doses of intrathecal M12 on the first and second phases of formalin-induced pain, expressed as the time spent licking and biting the paw (termed “response”). We used 7 mice per randomized group in 2 experimental runs. **C. D.** Effect of increasing doses of i.p. M12 on the first and second phases of formalin-induced pain. Data are from 6-8 mice per randomized group in 2 experimental runs. Asterisks denote the significance relative to the control group (\*P < 0.05, \*\*P < 0.01, \*\*\*P < 0.001, one-way ANOVA followed by Dunnett’s test).

Figures 5.5.1.2 and 5.5.1.3 illustrate the effects on compounds N10 and N12 on formalin induced pain responses. Although N10 significantly reduced paw licking/biting times in both the first and second phases of the formalin test, it required a ten times higher dose compared with M12 (compare Figures 5.5.1.1 and 5.5.1.2, but note that the doses for the three compounds differ in Figures 5.5.1.1, 5.5.1.2, and 5.5.1.3). N12 on the other hand produced potent analgesic effects (Figure 5.5.1.3).

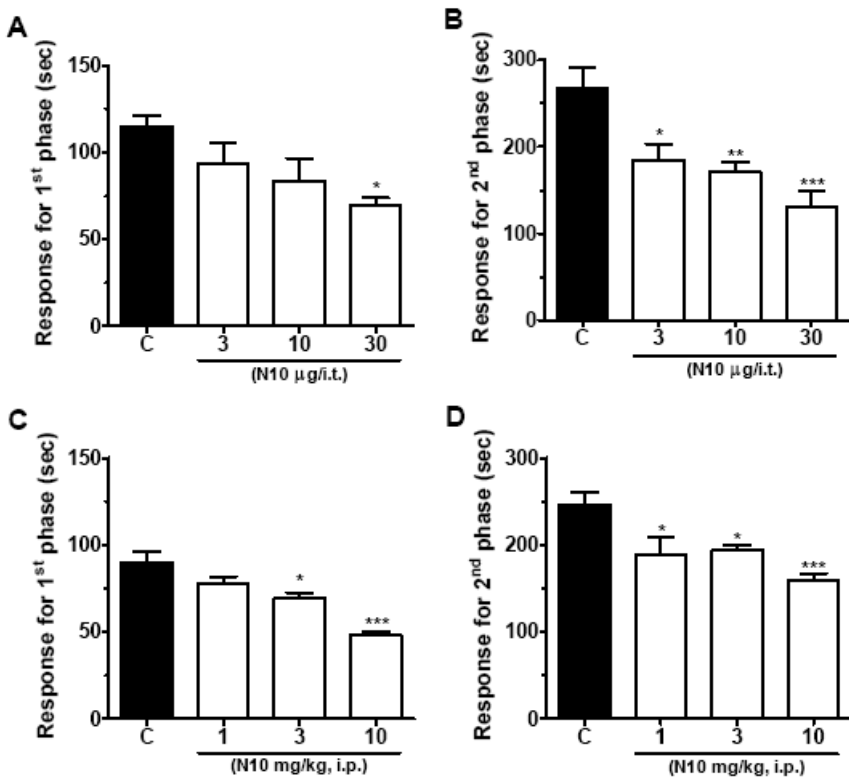


**Figure 5.5.1.2 Effects of N10 on inflammatory pain**

**A. B.** Effect of increasing doses of intrathecal N10 on the first and second phases of formalin-induced pain, expressed as the time spent licking and biting the paw (termed “response”). Data are from 7 mice per randomized group in 2 experimental runs. **C. D.** Effect of increasing doses of i.p. N10 (co-administered with formalin) on the first and second phases of formalin-induced pain. Data are from 6-8 mice per randomized group in 2 experimental runs. (\* $P < 0.05$ , \*\* $P < 0.01$ , \*\*\* $P < 0.001$ , one-way ANOVA followed by Dunnett’s test).

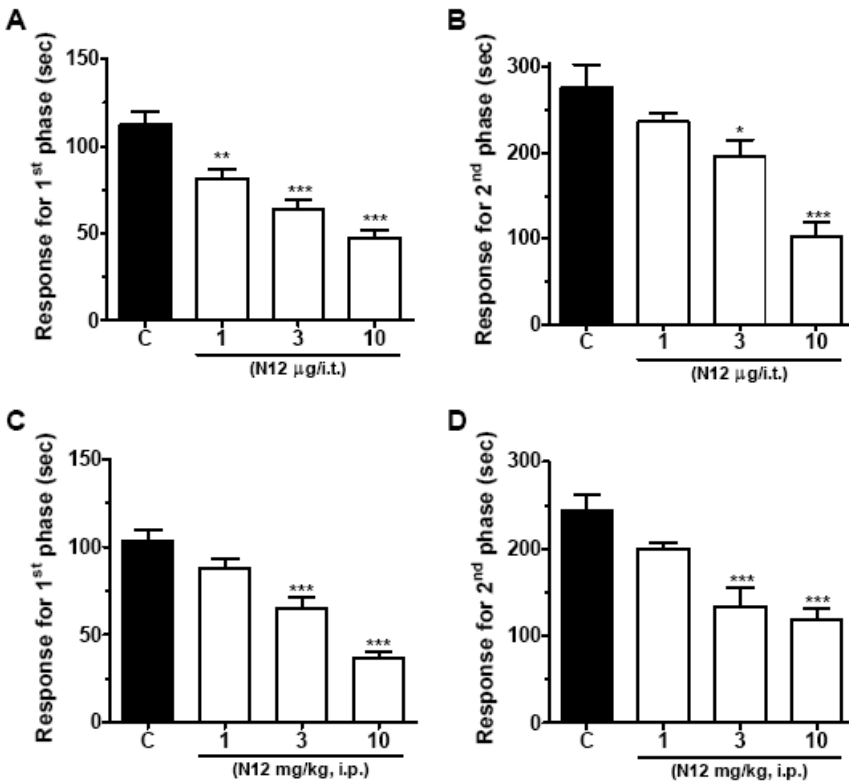


### Figure 5.5.1.3 Effects of N12 on inflammatory pain

**A. B.** Effect of increasing doses of intrathecal N12 on the first and second phases of formalin-induced pain, expressed as the time spent licking and biting the paw (termed “response”). Data are from 6-7 mice per randomized group in 2 experimental runs. **C. D.** Effect of increasing doses of i.p. N12 on the first and second phases of formalin-induced pain. Data were obtained from 7 mice per randomized group in 2 experimental runs. (\*P < 0.05, \*\*P < 0.01, \*\*\*P < 0.001, one-way ANOVA followed by Dunnett’s test).

### **5.5.2. Analgesic effects of M12 and N12 are mediated via Cav3.2 calcium channels**

To determine whether the analgesic effects observed with these compounds was in fact mediated via Cav3.2 channels, we repeated the formalin test in wild-type and Cav3.2 null mice. For this purpose, we focused on compounds M12 and N12. Mice were injected i.p. with either vehicle (control) or concentration of drug that had shown maximum analgesic effects in previous experiments (M12 at 3mg/kg, N12 at 10mg/kg). As shown clearly in Figures 5.5.2A and B, M12 no longer showed efficacy in Cav3.2 null mice in either phase. Similarly, the effects of N12 were precluded in the absence of Cav3.2 channels (Figures 5.5.2D and E), altogether indicating that both M12 and N12 mediate their anti-nociceptive/analgesic effects via this channel type rather than another molecular target.

Finally, it was important to test whether M12 or N12 had any negative side effects on locomotor activity. This was assessed by open field tests on animals that were treated i.p. with either 3mg/kg M12 or 10mg/kg N12. As seen in Figures 5.5.2C and F, no significant impairment was observed suggesting that the reduced response times in the formalin test seen with wild-type animals was not due to altered motor behavior.

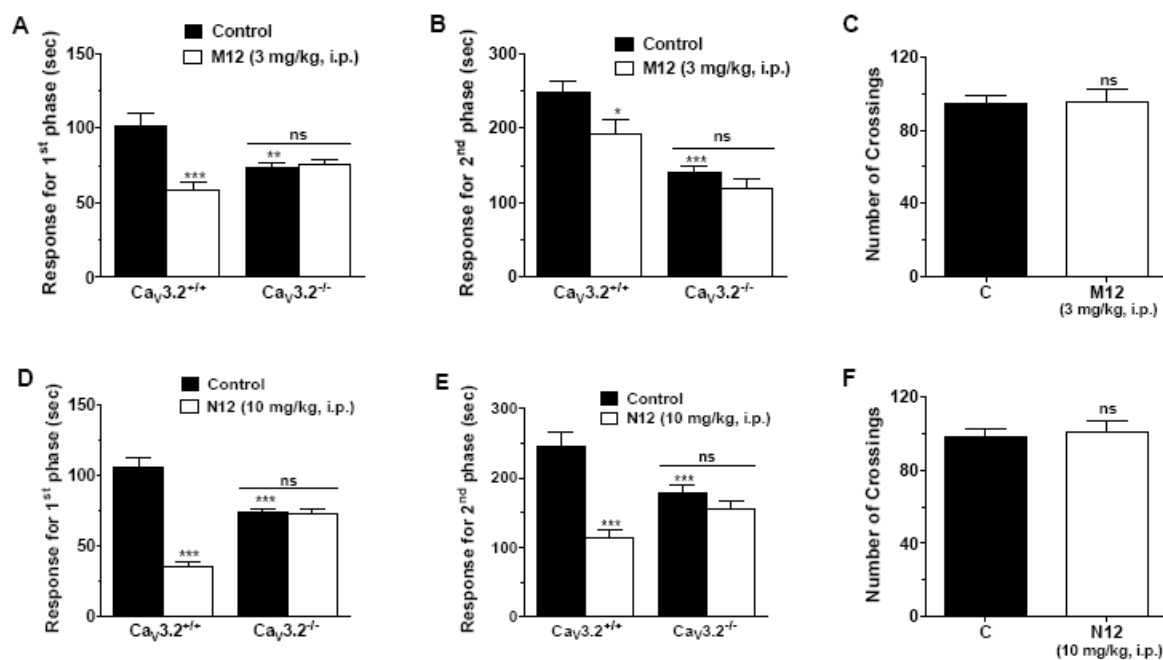


**Figure 5.5.2. Data showing M12 and N12 analgesic effects are mediated via Cav3.2 calcium channels and have no side-effects on locomotor activity.**

**A. B.** Comparison of the effect of 3 mg/kg i.p. M12 on the first and second phases of formalin-induced pain (expressed as the time spent licking and biting the paw - termed “response”) in wild-type and Cav3.2 knockout mice respectively. **D. E.** Comparison of effect of 3 mg/kg i.p. N12 on the first and second phases of formalin-induced pain in wild-type and Cav3.2 knockout mice respectively. \*P < 0.05, \*\*P < 0.01, \*\*\*P < 0.001 when comparing treatment; and ##P < 0.01, ###P < 0.001 for comparison between genotypes (two-way ANOVA followed by Tukey’s test). Note that control mice were of the same genetic background as the Cav3.2 null mice. Data in panels A, B, D and E are from 6 mice per randomized group in 2 experimental runs. **C. F.** Effect of 3 mg/kg i.p. M12 and N12 on locomotor activity of wild-type mice in the open field respectively. Each bar represents the mean responses from 6-7 animals and the error bars indicate the S.E.M. Control values (indicated by “C”) are from animals injected with 5% of DMSO and the asterisks denote the significance relative to the control group.

### **5.5.3. Effect of compound N12 on neuropathic pain**

To determine if N12 also produces analgesia in neuropathic pain states, we examined its therapeutic action (14 days after nerve injury) in chronic sciatic nerve injured (PNI)-mice. Sciatic nerve injury triggered mechanical hyperalgesia as verified by a significant decrease of mechanical withdrawal thresholds when compared to pre-PNI baseline levels of control group ( $P < 0.001$ ). Treatment of mice with N12 delivered i.p. (10 mg/kg) almost completely reversed mechanical hyperalgesia 1 hour after treatment (Figure 5.5.3). This effect lasted for several hours and remained statistically significant 3 hours after treatment, although the effects appear to slowly decrease after peaking at 1 hour. Although we do not know the metabolic stability of N12 *in vivo*, these data show that N12 is remarkably effective in reversing mechanical hyperalgesia in response to nerve injury.

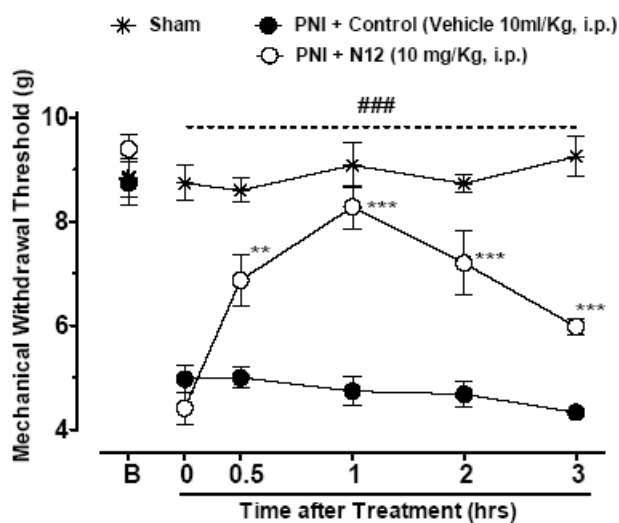


**Figure 5.5.3 Effect of compound N12 on neuropathic pain.**

Blind analyses of the time course of sciatic nerve injury induced mechanical hyperalgesia in mice treated with vehicle or N12. Each circle represents the mean  $\pm$  S.E.M. ( $n=7$ ), and is representative of 3 independent experiments. (\*\* $P < 0.01$ , \*\*\* $P < 0.001$ , two-way ANOVA followed by Tukey's test). The dashed line and hashtag indicate the range of data points where injured animals differed from the sham treated group ( $P < 0.001$ ).

## 5.6 Discussion

Since their introduction in the 1960s, DHPs have been widely used for the treatment of cardiovascular diseases such as hypertension and angina<sup>(35, 38, 39, 216, 267, 279)</sup>. Both their structure-activity relationships and their docking sites on the Cav1.2 channel sequence have been extensively investigated<sup>(40, 41, 217, 272)</sup> and as a result much is known about the drug structural determinants that are involved in docking to the DHP receptor site. Their continued development centers on their ability to block the L-type calcium channel Cav1.2 with high affinity, with modifications designed primarily to improve cardio selectivity and stability<sup>(218, 279)</sup>. Some DHPs however, are also known to be effective at blocking T-type calcium channels at clinically relevant concentrations<sup>(11, 214)</sup>. So, in this chapter, we focused on using a condensed dihydropyridine-based scaffold to try and produce more and possibly better examples of T-type channel block with DHPs and then tested them in animal models of a disease known to be associated with T-type channels, pain.

What we discovered in the first part of this study, was that the ability to inhibit T-type calcium channels is dependent on the specific DHP scaffold and that it can be exquisitely sensitive to the side chain substituents. Indeed, the results from the first part of this chapter demonstrate that small modifications of the ester group on a condensed 1,4-DHP ring system

(hexahydroquinoline) resulted in 30-fold selectivity for Cav3.2 channels over Cav1.2<sup>(116)</sup>.

The initial results also suggested that adding a bulky ring structure to the core phenyl ring was detrimental to their ability to block L- and T-type calcium channels and this could not be improved upon by increasing the chain length of the ester on the pyridine ring. In contrast, in the M1-5 series, increasing the side group chain length from a methyl to an ethyl group, or

introducing a ring structure (compound M3) at this locus mediated a significant increase in blocking affinity.

The sensitivity of the blocking affinity to substitution at this site is further underscored by the reduced blocking effects in compounds M1 and M5. Interestingly, the Cav3.1 channel was similarly sensitive to the modifications at both positions, with compounds M6-M10 being poorly effective, and compounds M2-M4 being the most potent. The most notable exception to these commonalities between L-type and T-type channel blocking determinants was compound M12 in which the ester group was modified with 3-pyridylmethyl<sup>(227)</sup>. Surprisingly, neither M11 nor M12 compound blocked Cav1.2, despite the fact that both compounds showed myorelaxant activity<sup>(227)</sup>. However, when we tested these two compounds on T-type calcium channels, we found M12 to be an effective inhibitor that blocked all three T-types with IC<sub>50</sub>s in the low μM range. The onset of current block was rapid, followed by a quick, almost complete recovery of peak current during the drug washout phase, which is a desirable property in a drug molecule<sup>(280)</sup>. Furthermore, this compound blocked T-type channels with at least 30-fold selectivity over Cav1.2. To our knowledge the only other DHP to selectively block T-type channels without appreciable inhibition of L-types is the R(-)-isomer of efonidipine, whose selectivity and voltage dependent block would be considerably less using our voltage clamp protocols<sup>(212)</sup>.

Why then is M12 selective for T-types over L-types? It has been previously shown that L-type channel inhibition is sensitive to substitution at the 6-position of the hexahydroquinoline ring<sup>(276)</sup>. The addition of a large aromatic ring structure may thus not be accommodated by the L-type calcium channel DHP site. It is possible that the three dimensional arrangement of the DHP binding site on T-type channels is more tolerant to this substitution. Interestingly, M11 did not mediate any significant degree of T-type channel inhibition, despite their being only relatively

small differences between compounds M11 and M12 (Figure 5.3.1). Further experiments will be required to identify the chemical structures that render M11 ineffective at blocking T-type channels.

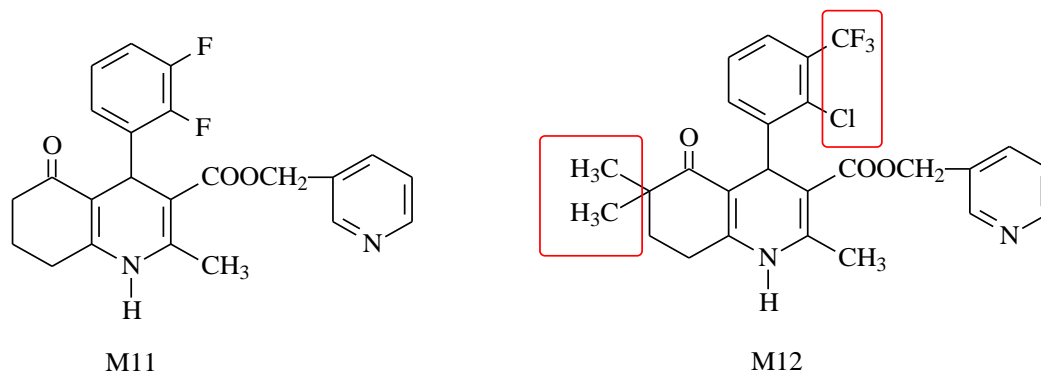


**Figure 5.6.1 Schematic diagram comparing compound M11 versus M12.**

The substituents on the phenyl ring and two additional methyl groups at 6-position of the hexahydroquinoline ring on M12 are highlighted with red boxes.

Among the second set of derivatives, it is interesting to note that the most effective compound N12, also had the highest affinity for Ca<sub>v</sub>3.2 channels among the compounds examined. However, the increased affinity for Cav3.2 was also paralleled by an increase in the blocking effects of N12 for Cav1.2 (40% inhibition at 10 μM compared to 20% for M12 at the same concentration), indicating that the same structural modifications on the DHP scaffold affect both L-type and T-type channel block. In contrast, despite having a similar affinity for Cav3.2 compared to N12, N10 was much less effective *in vivo*. This may be due to factors such as bio-availability or metabolic stability<sup>(216, 276, 277, 280)</sup>.

It is important to reiterate that by simply moving the dimethyl groups on the hexahydroquinoline scaffold, blocking affinity of N12 versus M12 increased by ten-fold (0.17 μM versus 1.5 μM). Conversely, removal of the chlorine atoms on the phenyl ring (N11) dramatically reduced the extent of Cav3.2 block. These findings indicate that the interactions between Cav3.2 channels and the new DHP scaffold are exquisitely sensitive to modifications at these positions and may thus guide further efforts in improving blocking activity and/or selectivity over Cav1.2 channels. It is also interesting to note that the small structural modifications on N12 abolished the effects of this compound on activation/inactivation gating. This observation fits well with the data collected from compounds M4 and M12<sup>(116)</sup>, which have the same hexahydroquinoline backbone and also did not alter steady state inactivation. In contrast, M4 potently shifted the half-inactivation potential of Cav1.2 L-type calcium channels towards more hyperpolarized voltages<sup>(116)</sup>. Hence, the DHP interaction site in Cav3.2 channels does not appear to couple to the inactivation machinery in the same manner as that in L-type channels which are known to undergo a drug induced inactivated channel conformation<sup>(101)</sup>. With that being said, it has been previously reported that a series of dialkyl 1,4-dihydro-4-(2'alkoxy-6'-pentadecylphenyl)-2,6-

dimethyl-3,5 pyridine dicarboxylate compounds mediated pronounced hyperpolarizing shifts in Cav3.1 channels<sup>(214)</sup>, indicating that coupling between DHP binding and the inactivation gate in T-type channel can be achieved with the appropriate DHP backbone.

There are considerable efforts in the pharmaceutical sector to identify and develop high affinity, selective blockers for T-type calcium channels. These channels are important regulators of cellular excitability and can contribute to low threshold exocytosis including the release of aldosterone<sup>(11, 39, 269, 271)</sup>. In addition, alteration of T-type channel activity has been associated with a number of pathophysiological conditions including epilepsy and cardiac hypertrophy<sup>(90, 93, 94, 122, 133, 174-176, 234, 281, 282)</sup>. It is also becoming increasingly clear that Cav3.2 T-type channels are key players in the transmission and processing of nociceptive information<sup>(124, 127, 156, 171, 173, 282)</sup>.

Despite the growing interest in T-type calcium channels and the growing evidence for their involvement in the pain signaling pathway, finding effective and selective blockers of these channels has remained a challenge.

Our aim here was to design and improve DHP-based selective T-type calcium channel blockers and demonstrate that these types of compounds could be effective in various animal models of pain. Our results reveal that our DHP-based compounds were effective at reducing pain responses in mice subjected to peripheral inflammation or nerve injury. Altogether, these findings fit with previous studies showing that T-type calcium channel inhibition or knockdown is efficacious in these conditions<sup>(124, 175, 176)</sup>. Although not tested here, one may expect a similar protection from colonic hypersensitivity as reported recently for compounds such as mibefradil. However, whether DHP-based selective T-type calcium channel blockers have the negative side effect of Rho Kinase inhibition that mibefradil does, is yet to be elucidated<sup>(97, 124)</sup>.

Finally, it is also well established that excessive secretion of aldosterone leads to hypertension, a disorder that is presently treated with DHPs that are selective L-type blockers<sup>(269, 271)</sup>. Recent research suggests that using a mixed L and T-type calcium channel blocker such as the DHPs Efonidipine or Benedipine, may be far more effective at treating hypertension by reducing aldosterone secretion through inhibition of T-type channels<sup>(39, 269)</sup>. In this context, the mixed L- and T-type blockers M2-M4 may provide scaffolds for the development of novel antihypertensives. Although there are several emerging T-type channel blockers, including some that are now in phase 1 clinical trials, relatively few compounds remain that are preferentially targeting T-type channels. Our findings that M12 is a potent T-type channel inhibitor with minimal L-type calcium channel blocking activity and that N12 reduces inflammatory and neuropathic pain hypersensitivity via potent T-type channel inhibition, provides an opportunity to increase this arsenal of T-type channel inhibitors. Moreover, this new class of DHPs represents a novel pharmacophore around which it may be possible to perform comprehensive molecular modeling that would further advance the design of drugs aimed at developing higher affinity and perhaps even T-type channel subtype selective inhibitors.

## CHAPTER SIX: CHARACTERIZATION OF NOVEL CANNABINOID BASED T-TYPE CALCIUM CHANNEL BLOCKERS WITH ANALGESIC EFFECTS.

### 6.1 Background:

The final research chapter of this thesis examines a series of novel cannabinoid-based molecules that use a carbazole scaffold similar in structure to endogenous molecules known to be involved in T-type calcium channel regulation. Many of the known organic compounds that have been shown to modulate T-type calcium channels have structures similar to endogenous anandamide-related molecules named lipoamino acids<sup>(113, 114, 130)</sup>. Lipoamino acids are closely related to endocannabinoids<sup>(113, 130-132)</sup>, therefore, it is not surprising that these endogenous molecules interact and block both CB receptors and T-type calcium channels<sup>(113, 130-132)</sup>.

Lipoamino acids are involved in neuronal excitability and therefore affect conditions such as sleep, pain and inflammation, epilepsy, as well as cardiovascular modulation<sup>(114, 131, 283)</sup>. These are all conditions that T-type calcium channels are known to be involved in<sup>(54, 79, 92, 104, 178, 234)</sup> and although it's easy to speculate that lipoamino acids might exert their regulatory effects via T-type calcium channel pathways<sup>(114, 131)</sup>, their exact mechanism of action remains largely unresolved, because of their promiscuous interactions with other targets, such as G-protein-coupled receptors and other ion channels, including TRPV1<sup>(283-287)</sup>.

Previous work has also shown that mixed T-type/cannabinoid block has beneficial effects in inducing analgesia in animal models of inflammatory pain<sup>(113, 130)</sup>. However, interactions with CB receptors, particularly CB<sub>1</sub> receptors, can also have side effects that may affect mood and memory, in addition to their known psychoactive effects<sup>(219, 220)</sup>. A goal of this study therefore is to try and produce a cannabinoid-like compound with the beneficiary analgesic effects without the interaction with CB receptors.

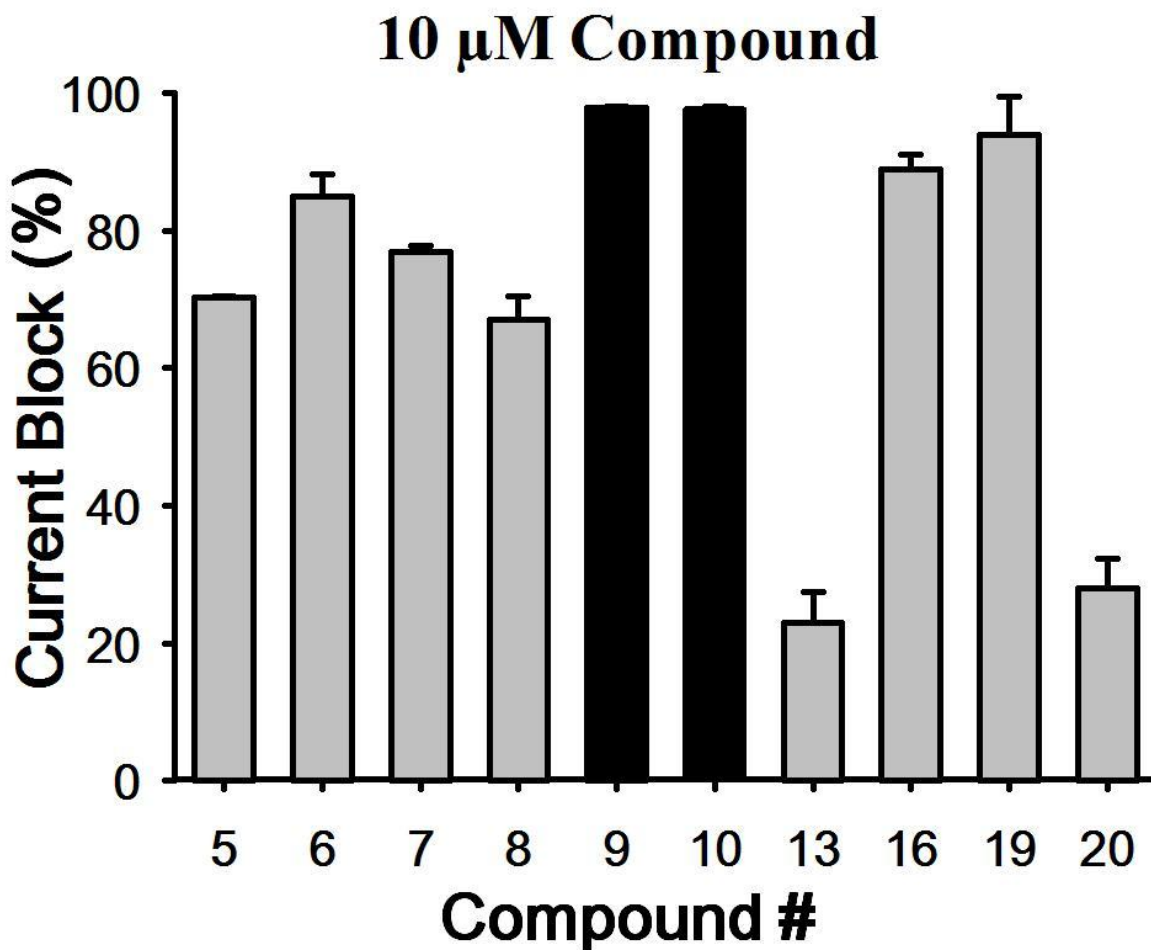
To this end, the work presented here aims to build on previous studies of a novel series of cannabinoid ligands with the primary structure bearing a carbazole scaffold that were synthesized and characterized in this laboratory<sup>(113, 130)</sup>. These compounds produced mixed cannabinoid receptor/T-type channel blockers that were found to be efficacious in animal models of inflammatory and neuropathic pain. Interestingly, from structure-activity relationships (SAR), it was determined that tertiary amines were important for Cav3.2 block<sup>(113, 114, 130)</sup> and that the length of the linker attaching the tertiary amine to the carbazole scaffold affected binding to CB<sub>1</sub> and CB<sub>2</sub> receptors.<sup>(288)</sup> In addition, some of these compounds also appeared to preferentially and potently inhibit T-type channels *in-vitro*.

In this study, we characterize and optimize Cav3.2 calcium channel selectivity in a new novel series of carbazole derivatives using the aforementioned compounds as a starting point.

## **6.2 Results:**

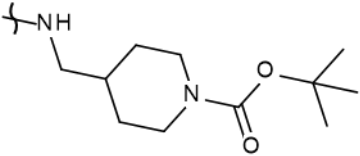
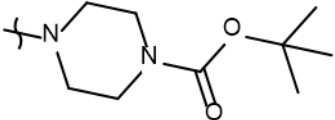
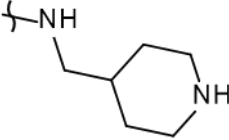
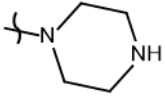
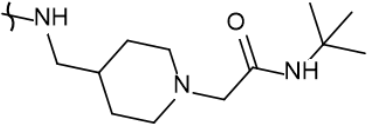
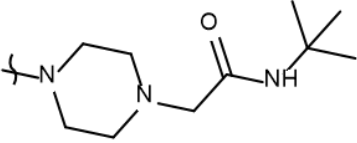
### **6.2.1 In-vitro characterization of the novel cannabinoid-based compounds**

We developed our new series of compounds based on a carbazole scaffold with an added heterocyclic bearing a tertiary amine. We also modified the chain length attached to the nitrogen of the carbazole, the length of the linker between the amide bond and the heterocycle ring. We then introduced a lipophilic moiety attached to the heterocycle. The entire first set of 10 compounds was screened using whole-cell voltage clamp techniques for their ability to mediate tonic block of transiently expressed hCav3.2 channels (Figure 6.2.1.1). Next, we used radioligand binding assays to assess the affinities of these compounds for both CB<sub>1</sub> and CB<sub>2</sub> receptors (Table 6.2.1.1).



**Figure 6.2.1.1** Percentage of whole cell current inhibition of human Cav3.2 (T-type) in response to 10  $\mu$ M application of the compound series (n=6 per compound).

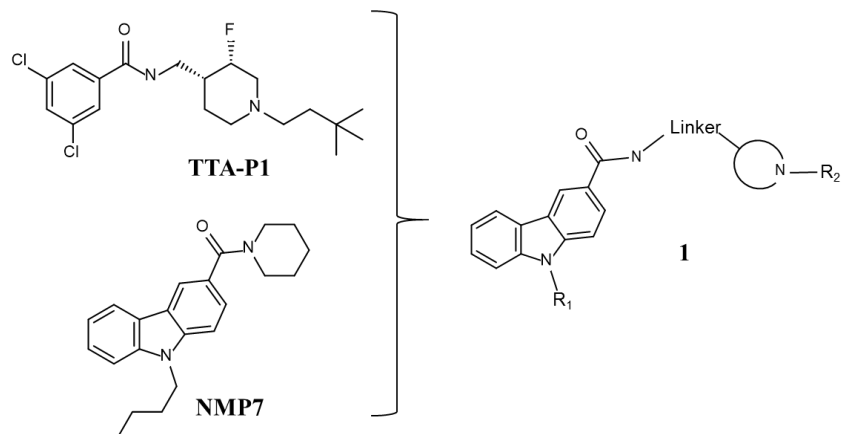
Note the potent and preferential block of Cav3.2 channels by compounds **9** and **10**. Error bars reflect standard errors. For Cav3.2 channels, the holding and test potentials were -110 and -20mV respectively.

No.	R1	R2	<i>r</i> CB1 $K_i^b$ (nM)	<i>h</i> CB2 $K_i^b$ (nM)
5			n.b.	n.b.
6			>5,000	2,957 ± 1,362
7			n.b.	n.b.
8			283 ± 65	2,833 ± 1305
9			>5,000	>5,000
10			15.0±6.9	1,968±906

**Table 6.2.1.1. Radioligand competitive binding assays (mean ± SEM) for carbazole-based analogues.**

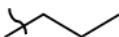
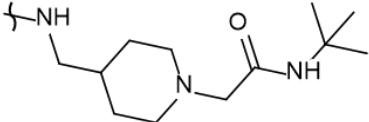
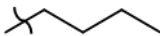
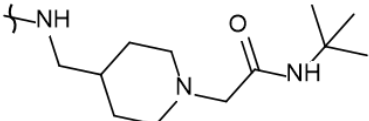
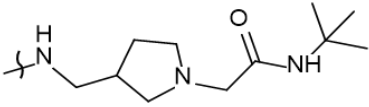
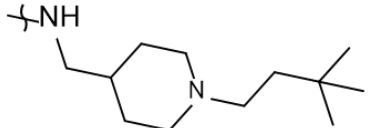
**5-10:** systematic variation in the linker length. Values are means of three experiments run in triplicate with standard deviation; n.b. no binding.

In the course of our initial exploratory work on the structure–activity relationship for this novel series of T-type channel blockers, we decided to determine the optimal linker length attached to the carbazole’s carbonyl (Figure 6.2.1.2).



**Figure 6.2.1.2 Piperidine containing T-type Ca<sup>2+</sup> inhibitors TTA-P1, dual T-type channel blocker/cannabinoid agonist NMP7 and chemical optimization plan 1 to decrease cannabinoid receptor affinities.**

We observed various degrees of inhibition of these channels, with compounds **9** and **10** being the most potent blockers of expressed hCav3.2. These two compounds mediated near complete inhibition at our standard test concentration of 10  $\mu$ M (Figure 6.2.1.1). Interestingly, both of these compounds are very similar in structure, with both having a cyclic tertiary amine attached to the carbazole scaffold (Table 6.2.1.1). Previous work has indicated that this modification helps confer T-type channel blocking activity onto various organic molecules<sup>(113, 127, 130, 213)</sup>, in agreement with our data presented here. As shown in Table 6.2.1.1, compound **10** showed high affinity binding to CB<sub>1</sub> receptors (15 nM), whereas its affinity for the CB<sub>2</sub> receptor was approximately 100-fold lower (2  $\mu$ M). Compound **9** however, did not bind to the two receptors with an affinity less than 5  $\mu$ M for CB<sub>1</sub> and CB<sub>2</sub> respectively. The only difference between compounds **9** and **10** is the elongated chain attached to the nitrogen of the carbazole in **9** (Table 6.2.1.1). This type of modification has been shown to alter cannabinoid receptor binding<sup>(113, 130, 288)</sup>, but it has not been demonstrated whether this modification affects the interactions of these compounds with Cav3.2. Among the first series of compounds **5** to **10**, replacement of a piperazine moiety by a methylpiperidine moiety appeared to be the most optimal for decreasing cannabinoid receptor affinity without impacting Cav3.2 calcium channel block. This striking difference in affinity for cannabinoid receptors between compounds bearing a piperazine moiety compared to a methylpiperidine moiety underscores the importance of chain length when developing compounds that preferentially target Cav3.2 calcium channels over cannabinoid receptors. Next, we determined the optimal chain length attached to the carbazole's endocyclic nitrogen (Table 6.2.1.2, compounds **13**, **16**, **19** and **20**).

No.	R1	R2
13		
16		
19		
20		

**Table 6.2.1.2. Analogues of compound 9: systematic variation in N-alkyl chain length and in the region occupied by the heterocycle.**

Among the linear N-1 alkyl chains, a pentyl chain seemed to be the most optimal for occupying its interaction site Cav3.2 channels, because systematically decreasing the length from n-pentyl in compound **9** negatively impacted the respective Cav3.2 blocking activities. Replacement of the piperidine ring by a pyrrolidine moiety<sup>(113)</sup> had a slight negative effect on Cav3.2 block, probably due to the lack of optimal ligand-receptor van der Waals contacts. Replacing the amide chain on the piperidine ring by an alkyl chain<sup>(130)</sup> dramatically decreased the Cav3.2 block. As is clearly seen in the traces in Figure 6.2.1.3A, the slight structural modification in compounds **9** compared to **10** does indeed impact hCav3.2 channel inhibition. The affinity of compound **9** versus **10** increased more than two-fold with the IC<sub>50</sub> of **9** and **10** being 1.48 μM and 3.68 μM respectively (Figure 6.2.1.3B and Table 6.2.1.3). In addition, compound **10** shifted the half activation potential of hCav3.2 by -12 mV (Figure 6.2.1.3C and Table 6.2.1.3). There was no significant effect on half-inactivation potential (P=0.143) (Figure 6.2.1.3D and Table 6.2.1.3). We then tested the Cav3 channel subtype selectivity of compound **9** using a single concentration of 3 μM. This concentration blocked hCav3.2 by 69.3± 4% (n=8), which was significantly (P<0.05) greater than that of either hCav3.1 (44.5± 7%; n=5) or hCav3.3 (42.5±5%; n=5). Compound **9** was thus chosen for further testing in animal models of pain.

	$V_{0.5act}$ (mV) 3 $\mu$ M	$V_h$ (mV) 3 $\mu$ M	IC50 Tonic ( $\mu$ M)
Wt hCav3.2	-30.0	-53.1 $\pm$ 1.67	
Compound 9	-29.7	-58.2 $\pm$ 1.43	1.48 $\pm$ 0.2
Compound 10	-42.0*	-58.3 $\pm$ 1.31	3.68 $\pm$ 0.5

**Table 6.2.1.3. Summary of biophysical parameters of hCav3.2 calcium channel in the absence and the presence of compound 9 and 10.**

Note that 3  $\mu$ M of compound **10** produces a significant 12 mV negative shift in the half activation potential of hCav3.2 and although there is a trend for both compounds to shift the half inactivation potential of the channel, it did not reach statistical significance.

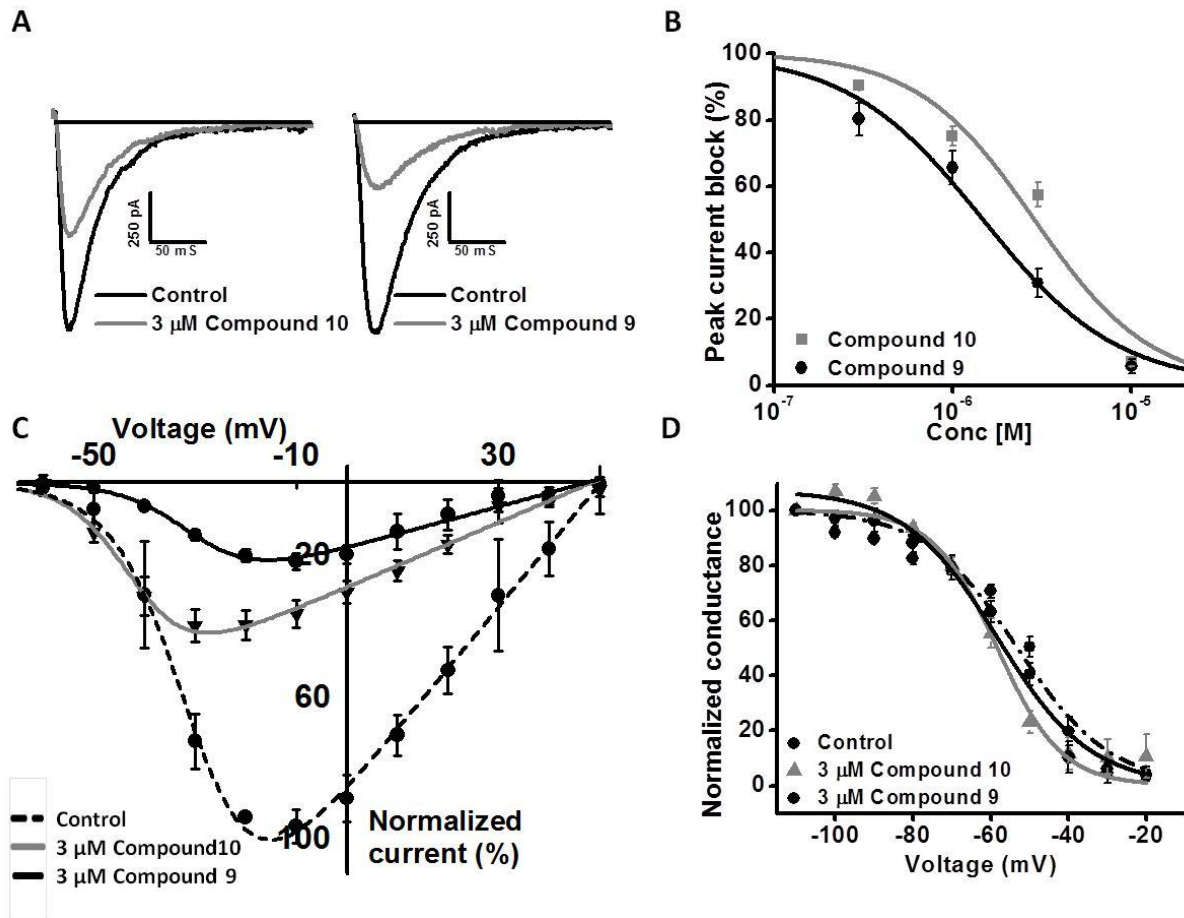


**Figure 6.2.1.3 Biophysical parameters of hCav3.2 before and after application of compounds 9 and 10.**

**A.** Representative traces of hCav3.2 before and after application of 3  $\mu$ M compounds **10** and **9** respectively. **B.** Dose response relations for compound **9** and **10** block of hCav3.2 channels. The IC<sub>50</sub> from the fit with the Hill equation was 1.48 and 3.68  $\mu$ M respectively (n=6). **C.** Effect of 3  $\mu$ M compound **9** and **10** on the steady state inactivation curve for hCav3.2 channels. **D.** Effect of 3  $\mu$ M compound **9** and **10** on the current voltage relation for hCav3.2 channels. Note: The data in panels **B** and **C** were fitted with the Boltzmann equation and data were obtained from 6 paired experiments.

### **6.2.2 Effects of Compound 9 in-vivo on acute pain, locomotor activity and Cav3.2 KO mice.**

Given the Cav3.2 channel blocking property of compound 9, we hypothesized that this compound may affect pain transmission in animal models. Compound 9 was delivered by either i.t. or i.p. routes and its effects on both the acute nociceptive and the slower inflammatory pain phases of the formalin test were evaluated. One-way ANOVA revealed that i.t. treatment of mice with compound 9 (1-10  $\mu\text{g}/\text{i.t.}$ , 20 minutes before) significantly decreased pain response time in both first (Figure 6.2.2.1A) and second (Figure 6.2.2.1B) phases ( $61 \pm 8\%$  and  $76 \pm 10\%$  inhibition, respectively). I.p. treatment of mice with compound 9 (10-100 mg/kg, i.p., 30 minutes prior) also resulted in significantly (one-way ANOVA) reduced pain response time in both the first (Figure 6.2.2.1C) and second (Figure 6.2.2.1D) phases ( $47 \pm 2\%$  and  $66 \pm 48\%$  inhibition, respectively).

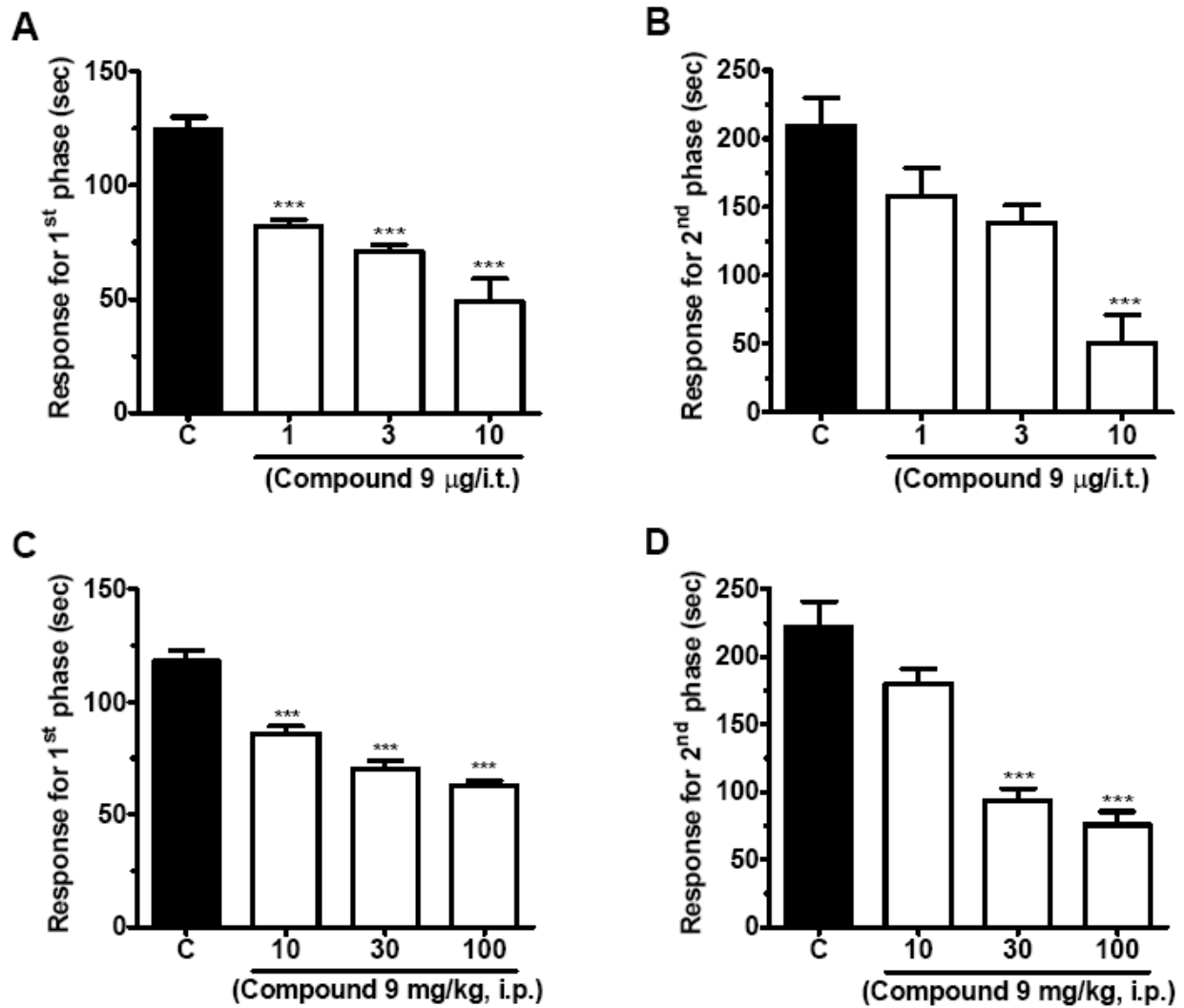


**Figure 6.2.2.1 Effects of Compound 9 in-vivo on acute pain**

**A. B.** Effect of increasing doses of intrathecal compound **9** on the first and second phases of formalin-induced pain. **C. D.** Effect of increasing doses of i.p. compound **9** (on the first and second phases of formalin-induced pain. Each bar represents the mean  $\pm$  S.E.M. ( $n=6-8$ ), and is representative of 2 independent experiments. Asterisks denote the significance relative to the control group (\*\*\*)  $P < 0.001$ , one-way ANOVA followed by Dunnett's test).

Importantly, systemic (*via* i.p.) treatment with compound **9** (30 mg/kg, i.p.) did not affect locomotor activity of mice assessed *via* an open-field test (Figure 6.2.2.2A), suggesting that the reduced response times observed in the previous formalin tests were not due to altered motor behavior. In order to investigate if the effects observed for compound **9** were specifically mediated *via* T-type channels, we performed a formalin test in Cav3.2 null mice that were treated either with vehicle or with compound **9** (10 µg/i.t.). The Cav3.2 null mice exhibited a lower mean response time when compared to wild-type mice, which is in agreement with previous data<sup>(94, 113)</sup>. As indicated in Figures 6.2.2.2B and C, they appear to be completely insensitive to i.t. treatment with compound **9** (10 µg i.t.) as revealed by two-way ANOVA, indicating that compound **9** mediates its analgesic effects specifically *via* Cav3.2 channels.

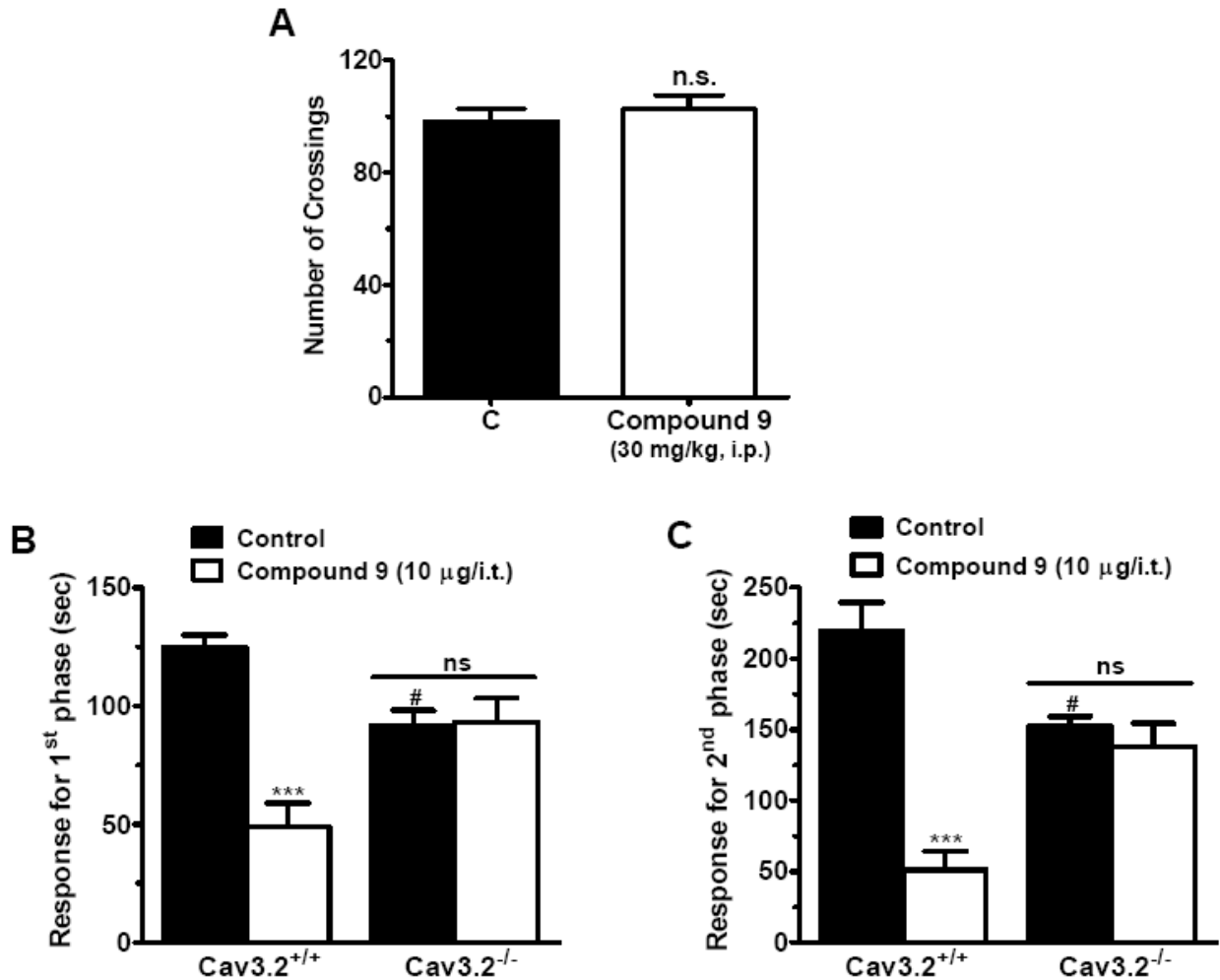


**Figure 6.2.2.2 Effects of Compound 9 in-vivo on locomotor activity and Cav3.2 KO mice.**

**A.** Effect of 30 mg/kg i.p. compound 9 on locomotor activity of wild-type mice in the open field test. **B. C.** Comparison of effect of 10 µg/i.t. intrathecal compound 9 on the first and second phases of formalin-induced pain in wild-type and Cav3.2 knockout mice respectively. Each bar represents the mean ± S.E.M. (n=6-7) and is representative of 2 independent experiments. Asterisks denote the significance relative to the control group \*\*\*P < 0.001 when comparing treatment; and #P < 0.05, for comparison between genotypes (two-way ANOVA followed by Tukey's test). Note that control mice were of the same genetic background as the Cav3.2 null mice.

### **6.2.3 Effect of Compound 9 on chronic neuropathic pain**

To verify whether compound 9 modulates pain transmission under neuropathic conditions, we analysed mechanical withdrawal thresholds of mice with a partial sciatic nerve injury (PNI) and treated with compound 9 (30mg/kg, i.p.) 14 days after nerve injury. As shown in Figure 6.2.3, sciatic nerve injury triggers mechanical hyperalgesia as confirmed by significant decrease of mechanical withdrawal thresholds when compared to baselines levels (Pre-PNI,  $P < 0.001$ ). Two-way ANOVA revealed that systemic (i.p.) treatment of mice with compound 9 (30 mg/kg, i.p.) significantly attenuated the mechanical hyperalgesia induced by sciatic nerve injury when compared with the PNI + Control group for longer than 3 hours after treatment. These data indicate that compound 9 treatment modulates pain transmission and mediates analgesia in this animal model of chronic neuropathic pain.

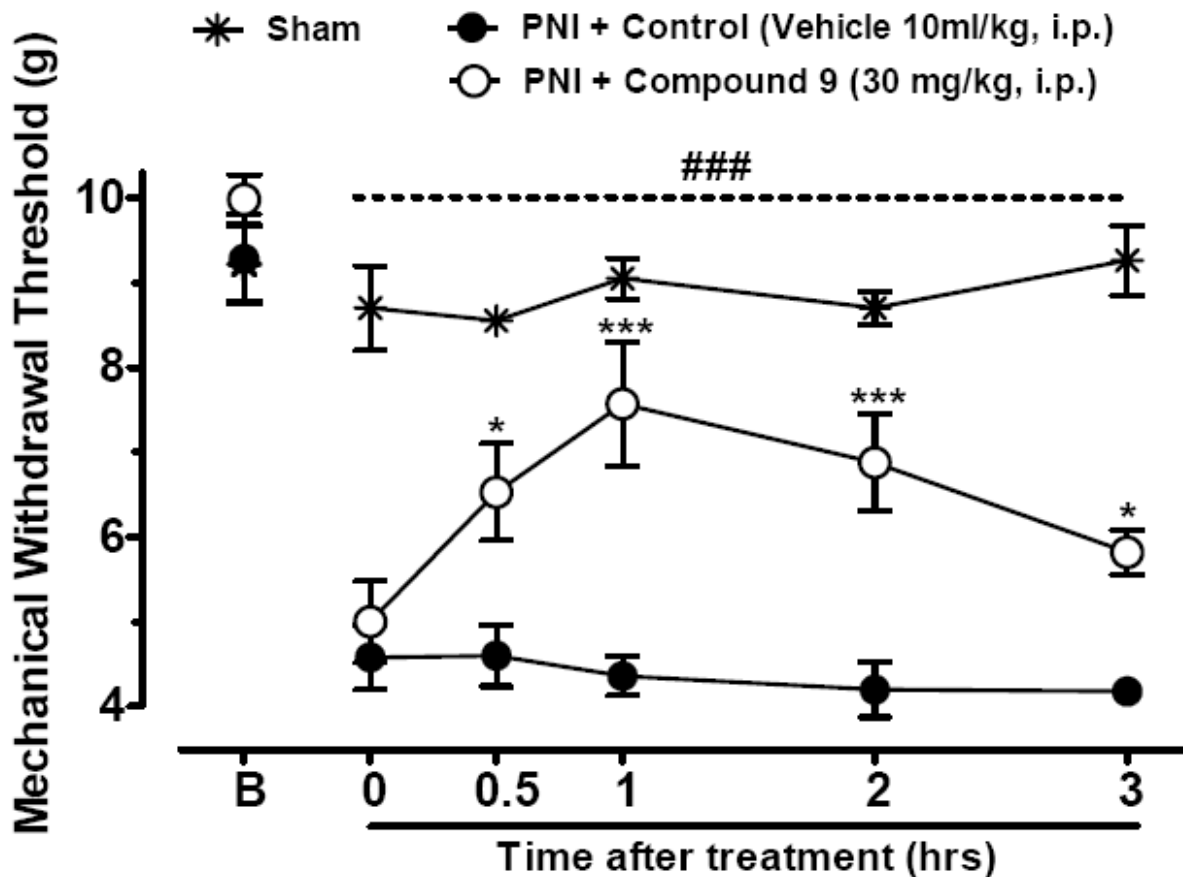


**Figure 6.2.3 Effect of Compound 9 on chronic neuropathic pain**

Blind analyses of the time course of treatment of neuropathic mice with vehicle or compound 9. Each circle represents the mean  $\pm$  S.E.M. (n=6), and is representative of 2 independent experiments. (\*P < 0.05, \*\*\*P < 0.001, two-way ANOVA followed by Tukey's test). The dashed line and hashtag signs indicate the range of data points where injured animals significantly differed from the sham treated group (P<0.001).

### 6.3 Discussion:

In this final study, we developed novel compounds with structures similar to that of endogenous compounds that are known to interact with members of the T-type channel family<sup>(113, 114, 130-132)</sup> and then modified them to reduce their affinity for cannabinoid receptors while attempting to increase their affinity for Cav3.2 channels.

Our synthesized compounds were based on a previous series of endogenous cannabinoid ligands that targeted both CB receptors and T-type calcium channels<sup>(113, 130)</sup>. Thus using data obtained from these experiments, we designed additional compounds with an extra substituted tertiary amine attached to the carbazole scaffold. We then extended the chain length attached to the carbazole to one of the compounds (compound **9**) to improve its selectivity for Cav3.2 channels over CB receptors<sup>(113, 130)</sup>. These data show that the length of the linker between the carbazole scaffold and the heterocyclic moiety is a key drug structural determinant that can be exploited to produce better and more selective Cav3.2 channel inhibitors. This compound blocked Cav3.2 channels with approximately 2-fold higher affinity than Cav3.1 and Cav3.3 channels. At this point we do not know if compound **9** affects other molecular targets such as high voltage activated channels or sodium channels. Nonetheless, the observation that their analgesic actions were abolished upon removal of Cav3.2 channels indicates that the primary biological target for compound **9** in the context of pain signaling is Cav3.2. The potent effects of compound **9** on pain response in injured wild-type animals fits with the notion that Cav3.2 channels play an important role in the afferent pain pathway<sup>(96, 118, 124, 154, 156, 171, 173, 174)</sup> and also with a number of previous studies showing that Cav3.2 channel blockers are efficacious in various pain models<sup>(122, 173, 176, 213)</sup>. Compound **9** blocked Cav3.2 channels in a concentration range that was similar to that previously reported for compounds such as **NMP-7**<sup>(130)</sup> and **NMP-181**<sup>(113)</sup>. These two

molecules, although structurally related to compound **9** did not discriminate among the three Cav3 family members, and mediated leftward shifts in the midpoint of the steady state inactivation curve. In contrast, compound **9** did not significantly affect voltage-dependent inactivation properties of Cav3.2 channels, suggesting that this compound does not interact strongly with inactivated channels. At this point it is not clear which structural differences among these compounds are responsible for these differential effects on channel gating. While other types of T-type calcium channel blockers such as **TTA-2**<sup>(289)</sup> or **Z123212**<sup>(127)</sup> that are efficacious in various pain models are also known to promote voltage-dependent inactivation of Cav3.2 channels, our data showing efficacy of compound **9** in neuropathic and inflammatory pain indicate that such state-dependent inhibition is not a prerequisite for antihyperalgesic effects *in vivo*.

Altogether our data suggest that using a carbazole scaffold is an effective strategy for developing potent Cav3.2 calcium channel blockers for treatment of inflammatory and neuropathic pain hypersensitivity. In addition, since T-type channels are associated with other disorders, including epilepsy and cardiac hypertrophy<sup>(10, 39, 54, 69, 70, 90, 124, 197, 281, 290, 291)</sup>, the novel pharmacophores identified here may also have the potential to treat these disorders.

## CHAPTER SEVEN: GENERAL DISCUSSION AND FUTURE DIRECTIONS

The aim of this thesis was to attempt to identify new blockers and modulators of T-type calcium channels. My goal was to not only expand the limited number of drugs known to interact with T-type channels, but to also understand their structure, physiology and function with an emphasis on their role in the pain pathway.

From an evolutionary standpoint, ion channels are thought to share a common ancestry and comparative genome analysis shows that most human ion channels originate from early metazoans<sup>(292)</sup>. Therefore, in the first part of my thesis, my strategy was to identify and use evolutionarily conserved regions to help identify possible drug interaction sites and, by extension, drugs that may interact with T-type calcium channels.

Evolutionarily conserved regions can be seen in even more primitive bacterial ion channels. In 1998, Roderick MacKinnon's group were the first to determine the three-dimensional (3-D) structure of a bacterial potassium channel (Kcsa) and because of the many evolutionary conserved regions, Kcsa became the defacto template for molecular modeling of ion channel physiology<sup>(293)</sup>.

More recently in 2011, Bill Catterall's group determined the three-dimensional structure of a bacterial VGSC, which contained enough sequence conservation versus mammalian VGSCs such that detailed modeling of sodium channel-drug interactions could be determined<sup>(294)</sup>. Indeed in chapter three of this thesis, Figure 3.5.1 shows the conserved amino acid sequence between the Nav bacterial channel and human Nav and Cav3.2 channels in a region that corresponds to the local anesthetic (LA) binding site. The 3-D structure of this bacterial channel further revealed fenestrations (windows) which the authors postulated could provide a hydrophobic pathway to the central pore cavity, where it would be possible for small molecules like local anesthetics to

interact. Whether these fenestrations also occur in T-type calcium channels is yet to be elucidated, but our results did show that some of the amino acids critical for LA binding are indeed found in Cav3.2 and conversely, by adding some critical amino acids that were otherwise not present in Cav3.2, we could dramatically increase LA blocking affinity for Cav3.2. This finding helped drive the principal hypothesis of this thesis that because of their evolutionarily conserved regions, studying drug-ion channel interactions in one voltage-gated ion channel member would help elucidate key structures and mechanisms of drug interactions with T-type calcium channels.

Using this hypothesis, I discovered that many of the known drug interaction sites of sodium channels shared a high degree of sequence identity in the same regions as the T-type calcium channels. Furthermore, in more recent articles, drugs that had been previously classified as “selective” sodium channel blockers were now shown to also block T-type calcium channels<sup>(261, 266, 295)</sup>. Indeed, because of the evolutionarily conserved critical domains of voltage gated ion channels, finding drugs that can be termed selective blockers within the sets and subsets of the “super family” of voltage-gated ion channels has proven to be difficult.

However, the idea of a drug that may bind to one or more ion channels (i.e. mixed blockers) may have some merit in the functional realm of providing treatment and therapy, especially if those ion channels are co-localised and/or appear to have similar function. In the case of Nav1.8 and Cav3.2 in DRG neurons, from a therapeutic point of view, reducing hyper-excitability by targeting/affecting both channels would seem to be advantageous. It is yet to be determined whether these channels act synergistically to regulate excitability as they do in prolonging sub-threshold depolarization in lamina I neurons<sup>(127)</sup>, or whether they act independently, but further

research may help to determine in this particular case whether mixed blockers would indeed be the best strategy.

There are also obvious advantages to finding selective blockers as targeting only one protein or ion channel may effectively reduce the chances of a drug having adverse side-effects. To this end, I examined molecules known to have exquisite selectivity for ion channels, peptide toxins. From early work that used TTX and  $\alpha$ -scorpion toxins to selectively block sodium channels and helped define mechanisms of synaptic transmission<sup>(296, 297)</sup>, to work by Olivera et al using  $\omega$ -conotoxins and  $\omega$ -agatoxins on calcium channels to help determine mechanisms of neurotransmitter release<sup>(47, 298)</sup>, toxins have been extensively used because of their unique ion channel selectivity.

Until recently however, toxins had not garnered much interest from the pharmaceutical industry as treatments because of their inherent traits of poor stability, low solubility, inability to translocate across the blood brain barrier (BBB) and the potential high cost of manufacturing (Most venomous animals produce minimal amounts of venom for only defensive or predatory purposes)<sup>(299)</sup>. Still, there are toxins that are nonetheless used as therapies and research in the field appears to be gaining momentum.

Some of the most promising “candidate” toxins for future therapeutic use may be the spider-venom peptides that contain the three-disulfide ICK motif, which produces a very stable molecule. These peptides have been shown to be orally active in invertebrates and more importantly, have been shown to cross the BBB in insects in order to access molecular targets in the CNS<sup>(292)</sup>.

More importantly, recent publications showed that two Protoxins with this ICK motif, found in the venom of the Peruvian green velvet tarantula, were both potent and selective for Nav and

Cav channels involved in pain signalling<sup>(266, 300)</sup>. Using toxins as pain therapy is not without precedent, Ziconatide (Prialt) is a synthetic form of  $\omega$ -conotoxin that was originally derived from cone snails but is now being used as an analgesic for severe forms of chronic pain<sup>(301, 302)</sup>.

Using my hypothesis to further explore whether there were any commonalities in toxin block between and within the sodium/calcium channel family, I was able to demonstrate that protoxins I and II were indeed selective for hCav3.1 and hCav3.2 respectively. However, when I tried using the reverse of my hypothesis and examine the slight differences in amino acid composition of known toxin binding sites within the subsets of the T-type calcium channels, I was unable to determine the precise cause for this selectivity. Furthermore, I did not observe the shifts in gating kinetics that other reports had indicated in the toxins' interactions with sodium and calcium channels. I postulated that this may be due to the different cDNA used in these experiments (rat vs human) and given that nature has spent over hundred million years on its own drug discovery program to find selective blockers, it's likely that not only speciation, but also the inherent differences between the gating components of Nav and Cav channels were also a factor.

Nonetheless, evolutionarily conserved regions of toxin binding do exist amongst voltage-gated ion channels and may provide key insights into developing or finding future T-type calcium channel blockers. A good example of this is the modeling of  $\beta$ -scorpion toxin binding to Nav1.2 from Bill Catterall's group<sup>(121, 256)</sup>. This research identified glutamic acids that are critical in forming a docking site for the binding of this toxin. When I analysed the sequence of hCav3.2, I determined that these amino acids are not only conserved, but also equi-distant (58 amino acids) apart, suggesting the overall structure of the binding site may again be similar. Future experiments will undoubtedly determine whether this toxin does indeed bind to a site analogous

to sodium channels, and/or whether nature has already produced a molecule that is exquisitely selective for T-type calcium channels.

In the second half of my thesis, I switched from examining the structures of ion channels and identifying where they interacted with drugs, to looking at the structure of drugs and seeing how they could be modified to be a better fit for ion channels. In order to do this, I first looked at a class of drugs that have been extensively researched and developed on high voltage activated calcium channels, 1,4-DHPs. DHPs are currently used to treat conditions such as hypertension and angina and development continues today on trying to make them more selective for their primarily target, the Cav1.2 L-type calcium channel<sup>(37, 218, 278)</sup>. However, a number of DHPs have also been shown to block low voltage activated T-type calcium channels<sup>(39, 212, 214)</sup> and from this concept, we came up with a series of novel DHP-based compounds, with one drug in particular that could selectively and potently inhibit T-type calcium channels in comparison to L-type calcium channels. Furthermore, from this first series of novel compounds, we were able to determine some of the key structures that were involved in the observed potency and selectivity. We then further refined the DHP structure to create a more potent lead compound that could mediate analgesia in animal models of pain. More importantly, we repeated our experiments using Cav3.2 null mice and all analgesic effects were lost and thus we were able to determine that the inhibition of the sensation of pain by our lead compound was likely via a T-type channel pathway.

This last observation is important to note since we have discussed in depth how drugs designed to target one ion channel family, often effectively block another. In the first part of this thesis, I demonstrated that drugs designed to block sodium channels more often than not, block T-type channels, so the converse would also apply. Given that sodium channels are also involved in pain

signaling and located within the peripheral nervous system<sup>(145, 199, 205, 303)</sup>, without the Cav3.2 null mice experiments, one could easily argue that our lead compound may well have mediated its effect via sodium channel block. However as mentioned, DHPs were originally designed to block cardiac L-type calcium channels and to have little interaction with sodium channels because of the critical role sodium channels such as Nav1.5 have in the heart. Therefore, using other HVA calcium channel selective drugs as templates would appear to be another effective strategy for developing selective LVA channel blockers.

Finally, the human body has developed numerous endogenous compounds that are activated upon injury or the sensation of pain. Some of these compounds, such as the cytokine Monocyte Chemoattractant Protein-1 (MCP-1)<sup>(215)</sup> and Anandamide<sup>(114, 131, 132)</sup>, are also known to potentially block T-type calcium channels. Whether their ability to block these channels has any inherent physiological role to play in the pain pathway is still not yet clear, however using an endogenous T-type channel blocker as the starting template for designing a pain therapy has some obvious advantages. Indeed, it has been proposed that both MCP-1 and Anandamide have the potential to be efficacious in pain therapy by being mixed blockers of both the Cav3.2 isoform and of the chemokine receptor 2 (CCR2)<sup>(215)</sup> and CB<sup>(113, 130)</sup> receptors respectively. This also opens up the possibility that like our discovery that sodium and T-type calcium channels may possess similar binding sites, both CCR2 and CB receptors may possess binding sites with common attributes to Cav3.2. However, as discussed previously, while a mixed blocker may increase the efficacy of a compound, it also increases the potential for unwanted side-effects.

Therefore as a final strategy for developing a T-type channel blocker as a potential therapy for pain, we decided to design a compound based on an endocannabinoid-related scaffold that could potentially block T-type calcium channels, but have minimal interaction with CB receptors. As

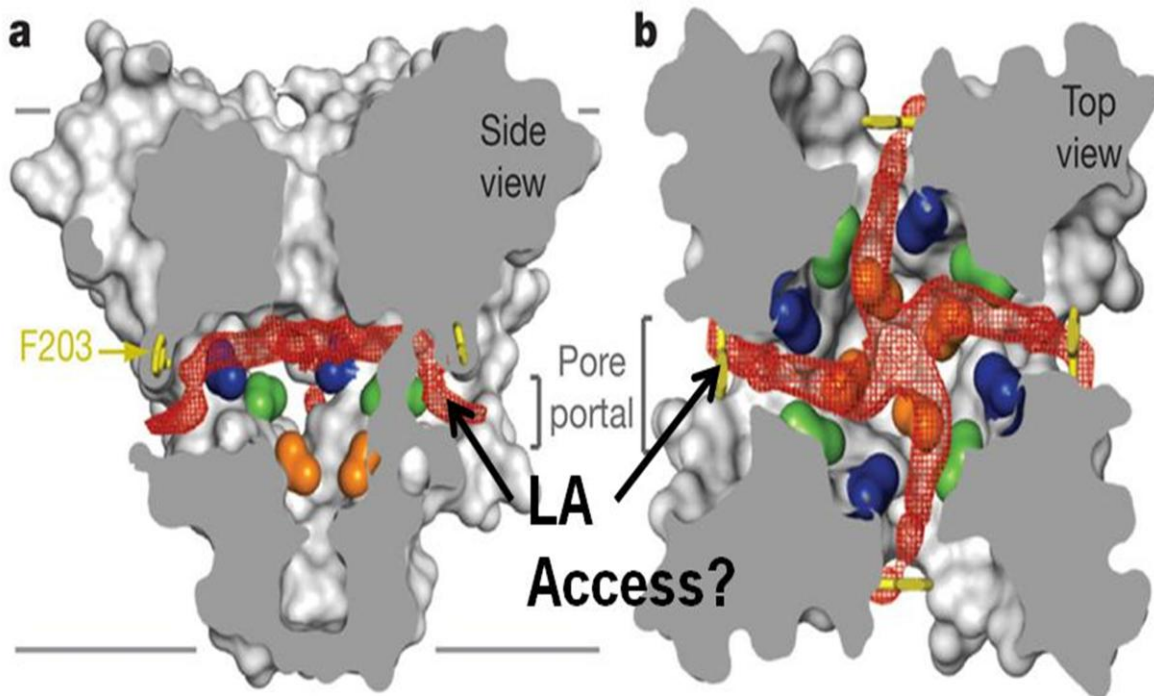
with our DHP-based compounds, we determined critical structures that were important for Cav3.2 block, important structures that determined selectivity and minimised compound binding to CB1 and CB2 receptors and finally using the same behavioural experiments as before identify a potent analgesic drug whose effect was likely due to its T-type calcium channel blocking ability.

This thesis demonstrated just a few of the many ways one could tackle the problem of developing a therapeutic drug to target a specific ion channel. This broad subject means that there are numerous directions that I did not explore that I could pursue in the future. For instance, I focused on the role of T-type calcium channels in the pain pathway and more specifically within the peripheral nervous system. However, T-type channels are also known to be involved in other hyperexcitability disorders such as arrhythmia<sup>(11, 70, 197)</sup> and epilepsy<sup>(54, 90)</sup>, the latter having well established animal models that some of the drugs described in this thesis, could easily be tested on<sup>(80, 281)</sup>. Indeed, current anti-convulsant drugs have many similar attributes to local anesthetics and although their mechanism of action is the regulation of sodium channels, the possibility that these drugs are also regulating T-type calcium channels, is only just beginning to be explored<sup>(103, 125, 177)</sup>.

While investigating models of local anesthetic binding, I noticed that some of the key determinants of anti-convulsant binding are also conserved in T-type calcium channels. One such model suggested a pivotal apparatus (possible hinged lid) for ion permeation, activation-inactivation coupling, and drug binding<sup>(304)</sup>. This model proposed that the tryptophan and phenylalanine of domain 4 (which are conserved in all T-types), would interact to form a recess, allowing anti-convulsants, (many of which have a diphenyl motif) to bind via dipole interactions among the phenyl groups of these 2 amino acids. Similarly, small hydrophobic drug molecules

could possibly go through the S6 recess through the postulated fenestrations and along the proposed “hydrophobic” pathway of local anaesthetic interaction with sodium channels (Figure 7.1)<sup>(294)</sup>. It would be important and fascinating to determine whether these drugs interacted with T-type channels in the same way and with the high degree of conserved sequence between Sodium and T-type channels within this region, it should be theoretically possible to model T-type calcium channel interaction with local anesthetic-like compounds such as A803467 in the near future.

Finally, understanding drug/T-type calcium channel interactions is still in its infancy compared to our knowledge of drug interactions with other ion channels. However, I believe that the results and findings presented in this thesis are an important contribution in pointing the way towards finding and developing better therapeutic compounds for T-type calcium channel related diseases.



Payandeh et al., Nature 2011

**Figure 7.1. 3-dimensional structure of NavAB as determined by the lab of W.A. Catterall.**

Side and side-down view through the pore model illustrating fenestrations (portals) and hydrophobic access to central cavity. phenylalanine 203 is the equivalent to Phenylalanine 1764 in the mammalian channel. These portals lead directly to proposed drug-binding sites within the central cavity and could potentially provide another access for small organic molecules like local anesthetics to reach their binding sites. Note the close proximity to residues important for local anesthetic drug binding.

## References

1. Catterall, W. A., Perez-Reyes, E., Snutch, T. P., and Striessnig, J. (2005) International Union of Pharmacology. XLVIII. Nomenclature and structure-function relationships of voltage-gated calcium channels, *Pharmacological reviews* 57, 411-425.
2. Clapham, D. E. (2007) Calcium signaling, *Cell* 131, 1047-1058.
3. Tsien, R. W., and Tsien, R. Y. (1990) Calcium channels, stores, and oscillations, *Annual review of cell biology* 6, 715-760.
4. Wadel, K., Neher, E., and Sakaba, T. (2007) The coupling between synaptic vesicles and Ca<sup>2+</sup> channels determines fast neurotransmitter release, *Neuron* 53, 563-575.
5. Carafoli, E. (2004) Calcium signaling: a historical account, *Biological research* 37, 497-505.
6. Cain, S. M., and Snutch, T. P. (2010) Contributions of T-type calcium channel isoforms to neuronal firing, *Channels* 4, 475-482.
7. Tsien, R. W., Ellinor, P. T., and Horne, W. A. (1991) Molecular diversity of voltage-dependent Ca<sup>2+</sup> channels, *Trends in pharmacological sciences* 12, 349-354.
8. Simms, B. A., and Zamponi, G. W. (2012) Trafficking and stability of voltage-gated calcium channels, *Cellular and molecular life sciences : CMLS* 69, 843-856.
9. Cain, S. M., and Snutch, T. P. (2011) Voltage-gated calcium channels and disease, *BioFactors* 37, 197-205.
10. Simms, Brett A., and Zamponi, Gerald W. (2014) Neuronal Voltage-Gated Calcium Channels: Structure, Function, and Dysfunction, *Neuron* 82, 24-45.
11. Perez-Reyes, E., Van Deusen, A. L., and Vitko, I. (2009) Molecular pharmacology of human Cav3.2 T-type Ca<sup>2+</sup> channels: block by antihypertensives, antiarrhythmics, and their analogs, *The Journal of pharmacology and experimental therapeutics* 328, 621-627.
12. Catterall, W. A. (2010) Ion channel voltage sensors: structure, function, and pathophysiology, *Neuron* 67, 915-928.
13. Bourinet, E., Zamponi, G. W., Stea, A., Soong, T. W., Lewis, B. A., Jones, L. P., Yue, D. T., and Snutch, T. P. (1996) The alpha 1E calcium channel exhibits permeation properties similar to low-voltage-activated calcium channels, *The Journal of neuroscience : the official journal of the Society for Neuroscience* 16, 4983-4993.
14. Tang, L., Gamal El-Din, T. M., Payandeh, J., Martinez, G. Q., Heard, T. M., Scheuer, T., Zheng, N., and Catterall, W. A. (2014) Structural basis for Ca<sup>2+</sup> selectivity of a voltage-gated calcium channel, *Nature* 505, 56-61.
15. Yang, J., Ellinor, P. T., Sather, W. A., Zhang, J. F., and Tsien, R. W. (1993) Molecular determinants of Ca<sup>2+</sup> selectivity and ion permeation in L-type Ca<sup>2+</sup> channels, *Nature* 366, 158-161.
16. Wheeler, D. G., Barrett, C. F., Groth, R. D., Safa, P., and Tsien, R. W. (2008) CaMKII locally encodes L-type channel activity to signal to nuclear CREB in excitation-transcription coupling, *The Journal of cell biology* 183, 849-863.
17. Wheeler, D. G., Barrett, C. F., and Tsien, R. W. (2006) L-type calcium channel ligands block nicotine-induced signaling to CREB by inhibiting nicotinic receptors, *Neuropharmacology* 51, 27-36.
18. Wheeler, D. G., Groth, R. D., Ma, H., Barrett, C. F., Owen, S. F., Safa, P., and Tsien, R. W. (2012) Ca(V)1 and Ca(V)2 channels engage distinct modes of Ca(2+) signaling to control CREB-dependent gene expression, *Cell* 149, 1112-1124.

19. Belardetti, F., and Zamponi, G. W. (2012) Calcium channels as therapeutic targets, *Wiley Interdisciplinary Reviews: Membrane Transport and Signaling* 1, 433-451.
20. Giusti-Rodriguez, P., and Sullivan, P. F. (2013) The genomics of schizophrenia: update and implications, *The Journal of clinical investigation* 123, 4557-4563.
21. Splawski, I., Timothy, K. W., Decher, N., Kumar, P., Sachse, F. B., Beggs, A. H., Sanguinetti, M. C., and Keating, M. T. (2005) Severe arrhythmia disorder caused by cardiac L-type calcium channel mutations, *Proceedings of the National Academy of Sciences of the United States of America* 102, 8089-8096; discussion 8086-8088.
22. Splawski, I., Timothy, K. W., Sharpe, L. M., Decher, N., Kumar, P., Bloise, R., Napolitano, C., Schwartz, P. J., Joseph, R. M., Condouris, K., Tager-Flusberg, H., Priori, S. G., Sanguinetti, M. C., and Keating, M. T. (2004) Ca(V)<sub>1.2</sub> calcium channel dysfunction causes a multisystem disorder including arrhythmia and autism, *Cell* 119, 19-31.
23. Krey, J. F., Pasca, S. P., Shcheglovitov, A., Yazawa, M., Schwemberger, R., Rasmusson, R., and Dolmetsch, R. E. (2013) Timothy syndrome is associated with activity-dependent dendritic retraction in rodent and human neurons, *Nature neuroscience* 16, 201-209.
24. Brini, M., and Carafoli, E. (2011) Calcium signaling and disease: preface, *BioFactors* 37, 131.
25. Catterall, W. A. (2011) Voltage-gated calcium channels, *Cold Spring Harbor perspectives in biology* 3, a003947.
26. Wheeler, D. B., Randall, A., and Tsien, R. W. (1994) Roles of N-type and Q-type Ca<sup>2+</sup> channels in supporting hippocampal synaptic transmission, *Science* 264, 107-111.
27. Hernandez-Ochoa, E. O., Contreras, M., Cseresnyes, Z., and Schneider, M. F. (2007) Ca<sup>2+</sup> signal summation and NFATc1 nuclear translocation in sympathetic ganglion neurons during repetitive action potentials, *Cell calcium* 41, 559-571.
28. Yasuda, T., Chen, L., Barr, W., McRory, J. E., Lewis, R. J., Adams, D. J., and Zamponi, G. W. (2004) Auxiliary subunit regulation of high-voltage activated calcium channels expressed in mammalian cells, *The European journal of neuroscience* 20, 1-13.
29. Arikkath, J., and Campbell, K. P. (2003) Auxiliary subunits: essential components of the voltage-gated calcium channel complex, *Current opinion in neurobiology* 13, 298-307.
30. Bech-Hansen, N. T., Naylor, M. J., Maybaum, T. A., Pearce, W. G., Koop, B., Fishman, G. A., Mets, M., Musarella, M. A., and Boycott, K. M. (1998) Loss-of-function mutations in a calcium-channel alpha1-subunit gene in Xp11.23 cause incomplete X-linked congenital stationary night blindness, *Nature genetics* 19, 264-267.
31. Mikami, A., Imoto, K., Tanabe, T., Niidome, T., Mori, Y., Takeshima, H., Narumiya, S., and Numa, S. (1989) Primary structure and functional expression of the cardiac dihydropyridine-sensitive calcium channel, *Nature* 340, 230-233.
32. Tanabe, T., Takeshima, H., Mikami, A., Flockerzi, V., Takahashi, H., Kangawa, K., Kojima, M., Matsuo, H., Hirose, T., and Numa, S. (1987) Primary structure of the receptor for calcium channel blockers from skeletal muscle, *Nature* 328, 313-318.
33. Williams, M. E., Feldman, D. H., McCue, A. F., Brenner, R., Velicelebi, G., Ellis, S. B., and Harpold, M. M. (1992) Structure and functional expression of alpha 1, alpha 2, and beta subunits of a novel human neuronal calcium channel subtype, *Neuron* 8, 71-84.
34. Lipscombe, D., Helton, T. D., and Xu, W. (2004) L-type calcium channels: the low down, *Journal of neurophysiology* 92, 2633-2641.

35. Zheng, W., Stoltefuss, J., Goldmann, S., and Triggle, D. J. (1992) Pharmacologic and radioligand binding studies of 1,4-dihydropyridines in rat cardiac and vascular preparations: stereoselectivity and voltage dependence of antagonist and activator interactions, *Molecular pharmacology* 41, 535-541.
36. Randall, A., and Tsien, R. W. (1995) Pharmacological dissection of multiple types of Ca<sup>2+</sup> channel currents in rat cerebellar granule neurons, *The Journal of neuroscience : the official journal of the Society for Neuroscience* 15, 2995-3012.
37. Ioan, P., Carosati, E., Micucci, M., Cruciani, G., Broccatelli, F., Zhorov, B. S., Chiarini, A., and Budriesi, R. (2011) 1,4-Dihydropyridine scaffold in medicinal chemistry, the story so far and perspectives (part 1): action in ion channels and GPCRs, *Current medicinal chemistry* 18, 4901-4922.
38. Katz, A. M., and Leach, N. M. (1987) Differential effects of 1,4-dihydropyridine calcium channel blockers: therapeutic implications, *Journal of clinical pharmacology* 27, 825-834.
39. Yamamoto, E., Kataoka, K., Dong, Y. F., Nakamura, T., Fukuda, M., Nako, H., Ogawa, H., and Kim-Mitsuyama, S. (2010) Benidipine, a dihydropyridine L-type/T-type calcium channel blocker, affords additive benefits for prevention of cardiorenal injury in hypertensive rats, *Journal of hypertension* 28, 1321-1329.
40. Hockerman, G. H., Peterson, B. Z., Sharp, E., Tanada, T. N., Scheuer, T., and Catterall, W. A. (1997) Construction of a high-affinity receptor site for dihydropyridine agonists and antagonists by single amino acid substitutions in a non-L-type Ca<sup>2+</sup> channel, *Proceedings of the National Academy of Sciences of the United States of America* 94, 14906-14911.
41. Zamponi, G. W., Stotz, S. C., Staples, R. J., Andro, T. M., Nelson, J. K., Hulubei, V., Blumenfeld, A., and Natale, N. R. (2003) Unique structure-activity relationship for 4-isoxazolyl-1,4-dihydropyridines, *Journal of medicinal chemistry* 46, 87-96.
42. Richards, K. S., Swensen, A. M., Lipscombe, D., and Bommert, K. (2007) Novel CaV2.1 clone replicates many properties of Purkinje cell CaV2.1 current, *The European journal of neuroscience* 26, 2950-2961.
43. Bourinet, E., Soong, T. W., Sutton, K., Slaymaker, S., Mathews, E., Monteil, A., Zamponi, G. W., Nargeot, J., and Snutch, T. P. (1999) Splicing of alpha 1A subunit gene generates phenotypic variants of P- and Q-type calcium channels, *Nature neuroscience* 2, 407-415.
44. Adams, M. E., Myers, R. A., Imperial, J. S., and Olivera, B. M. (1993) Toxotyping rat brain calcium channels with omega-toxins from spider and cone snail venoms, *Biochemistry* 32, 12566-12570.
45. Dubel, S. J., Starr, T. V., Hell, J., Ahlijanian, M. K., Enyeart, J. J., Catterall, W. A., and Snutch, T. P. (1992) Molecular cloning of the alpha-1 subunit of an omega-conotoxin-sensitive calcium channel, *Proceedings of the National Academy of Sciences of the United States of America* 89, 5058-5062.
46. Williams, M. E., Brust, P. F., Feldman, D. H., Patthi, S., Simerson, S., Maroufi, A., McCue, A. F., Velicelebi, G., Ellis, S. B., and Harpold, M. M. (1992) Structure and functional expression of an omega-conotoxin-sensitive human N-type calcium channel, *Science* 257, 389-395.
47. Olivera, B. M., Cruz, L. J., de Santos, V., LeCheminant, G. W., Griffin, D., Zeikus, R., McIntosh, J. M., Galyean, R., Varga, J., Gray, W. R., and et al. (1987) Neuronal calcium

- channel antagonists. Discrimination between calcium channel subtypes using omega-conotoxin from *Conus magus* venom, *Biochemistry* 26, 2086-2090.
48. McCleskey, E. W., Fox, A. P., Feldman, D. H., Cruz, L. J., Olivera, B. M., Tsien, R. W., and Yoshikami, D. (1987) Omega-conotoxin: direct and persistent blockade of specific types of calcium channels in neurons but not muscle, *Proceedings of the National Academy of Sciences of the United States of America* 84, 4327-4331.
  49. Soong, T. W., Stea, A., Hodson, C. D., Dubel, S. J., Vincent, S. R., and Snutch, T. P. (1993) Structure and functional expression of a member of the low voltage-activated calcium channel family, *Science* 260, 1133-1136.
  50. Bourinet, E., Stotz, S. C., Spaetgens, R. L., Dayanithi, G., Lemos, J., Nargeot, J., and Zamponi, G. W. (2001) Interaction of SNX482 with domains III and IV inhibits activation gating of alpha(1E) (Ca(V)2.3) calcium channels, *Biophysical journal* 81, 79-88.
  51. Newcomb, R., Szoke, B., Palma, A., Wang, G., Chen, X., Hopkins, W., Cong, R., Miller, J., Urge, L., Tarczy-Hornoch, K., Loo, J. A., Dooley, D. J., Nadasdi, L., Tsien, R. W., Lemos, J., and Miljanich, G. (1998) Selective peptide antagonist of the class E calcium channel from the venom of the tarantula *Hysterocrates gigas*, *Biochemistry* 37, 15353-15362.
  52. Catterall, W. A. (2000) Structure and regulation of voltage-gated Ca<sup>2+</sup> channels, *Annual review of cell and developmental biology* 16, 521-555.
  53. Barclay, J., Balaguero, N., Mione, M., Ackerman, S. L., Letts, V. A., Brodbeck, J., Canti, C., Meir, A., Page, K. M., Kusumi, K., Perez-Reyes, E., Lander, E. S., Frankel, W. N., Gardiner, R. M., Dolphin, A. C., and Rees, M. (2001) Ducky mouse phenotype of epilepsy and ataxia is associated with mutations in the *Cacna2d2* gene and decreased calcium channel current in cerebellar Purkinje cells, *The Journal of neuroscience : the official journal of the Society for Neuroscience* 21, 6095-6104.
  54. Heron, S. E., Khosravani, H., Varela, D., Bladen, C., Williams, T. C., Newman, M. R., Scheffer, I. E., Berkovic, S. F., Mulley, J. C., and Zamponi, G. W. (2007) Extended spectrum of idiopathic generalized epilepsies associated with *CACNA1H* functional variants, *Annals of neurology* 62, 560-568.
  55. Veneziano, L., Guida, S., Mantuano, E., Bernard, P., Tarantino, P., Boccone, L., Hisama, F. M., Carrera, P., Jodice, C., and Frontali, M. (2009) Newly characterised 5' and 3' regions of *CACNA1A* gene harbour mutations associated with Familial Hemiplegic Migraine and Episodic Ataxia, *Journal of the neurological sciences* 276, 31-37.
  56. Ellis, S. B., Williams, M. E., Ways, N. R., Brenner, R., Sharp, A. H., Leung, A. T., Campbell, K. P., McKenna, E., Koch, W. J., Hui, A., and et al. (1988) Sequence and expression of mRNAs encoding the alpha 1 and alpha 2 subunits of a DHP-sensitive calcium channel, *Science* 241, 1661-1664.
  57. Varadi, G., Lory, P., Schultz, D., Varadi, M., and Schwartz, A. (1991) Acceleration of activation and inactivation by the beta subunit of the skeletal muscle calcium channel, *Nature* 352, 159-162.
  58. Bichet, D., Lecomte, C., Sabatier, J. M., Felix, R., and De Waard, M. (2000) Reversibility of the Ca(2+) channel alpha(1)-beta subunit interaction, *Biochemical and biophysical research communications* 277, 729-735.
  59. Gonzalez-Gutierrez, G., Miranda-Laferte, E., Neely, A., and Hidalgo, P. (2007) The Src homology 3 domain of the beta-subunit of voltage-gated calcium channels promotes

- endocytosis via dynamin interaction, *The Journal of biological chemistry* 282, 2156-2162.
60. Altier, C., Khosravani, H., Evans, R. M., Hameed, S., Peloquin, J. B., Vartian, B. A., Chen, L., Beedle, A. M., Ferguson, S. S., Mezghrani, A., Dubel, S. J., Bourinet, E., McRory, J. E., and Zamponi, G. W. (2006) ORL1 receptor-mediated internalization of N-type calcium channels, *Nature neuroscience* 9, 31-40.
  61. Gregg, R. G., Messing, A., Strube, C., Beurg, M., Moss, R., Behan, M., Sukhareva, M., Haynes, S., Powell, J. A., Coronado, R., and Powers, P. A. (1996) Absence of the beta subunit (cchb1) of the skeletal muscle dihydropyridine receptor alters expression of the alpha 1 subunit and eliminates excitation-contraction coupling, *Proceedings of the National Academy of Sciences of the United States of America* 93, 13961-13966.
  62. Weissgerber, P., Held, B., Bloch, W., Kaestner, L., Chien, K. R., Fleischmann, B. K., Lipp, P., Flockerzi, V., and Freichel, M. (2006) Reduced cardiac L-type Ca<sup>2+</sup> current in Ca(V)beta2<sup>-/-</sup> embryos impairs cardiac development and contraction with secondary defects in vascular maturation, *Circulation research* 99, 749-757.
  63. Murakami, M., Nakagawasai, O., Yanai, K., Nunoki, K., Tan-No, K., Tadano, T., and Iijima, T. (2007) Modified behavioral characteristics following ablation of the voltage-dependent calcium channel beta3 subunit, *Brain research* 1160, 102-112.
  64. McEnery, M. W., Vance, C. L., Begg, C. M., Lee, W. L., Choi, Y., and Dubel, S. J. (1998) Differential expression and association of calcium channel subunits in development and disease, *Journal of bioenergetics and biomembranes* 30, 409-418.
  65. Burgess, D. L., Jones, J. M., Meisler, M. H., and Noebels, J. L. (1997) Mutation of the Ca<sup>2+</sup> channel beta subunit gene Cchb4 is associated with ataxia and seizures in the lethargic (lh) mouse, *Cell* 88, 385-392.
  66. Letts, V. A., Felix, R., Biddlecome, G. H., Arikath, J., Mahaffey, C. L., Valenzuela, A., Bartlett, F. S., 2nd, Mori, Y., Campbell, K. P., and Frankel, W. N. (1998) The mouse stargazer gene encodes a neuronal Ca<sup>2+</sup>-channel gamma subunit, *Nature genetics* 19, 340-347.
  67. Rousset, M., Cens, T., Restituito, S., Barrere, C., Black, J. L., 3rd, McEnery, M. W., and Charnet, P. (2001) Functional roles of gamma2, gamma3 and gamma4, three new Ca<sup>2+</sup> channel subunits, in P/Q-type Ca<sup>2+</sup> channel expressed in *Xenopus* oocytes, *The Journal of physiology* 532, 583-593.
  68. Chemin, J., Monteil, A., Bourinet, E., Nargeot, J., and Lory, P. (2001) Alternatively spliced alpha(1G) (Ca(V)3.1) intracellular loops promote specific T-type Ca(2+) channel gating properties, *Biophysical journal* 80, 1238-1250.
  69. David, L. S., Garcia, E., Cain, S. M., Thau, E., Tyson, J. R., and Snutch, T. P. (2010) Splice-variant changes of the Ca(V)3.2 T-type calcium channel mediate voltage-dependent facilitation and associate with cardiac hypertrophy and development, *Channels* 4, 375-389.
  70. Vassort, G., Talavera, K., and Alvarez, J. L. (2006) Role of T-type Ca<sup>2+</sup> channels in the heart, *Cell calcium* 40, 205-220.
  71. Nilius, B., Talavera, K., and Verkhatsky, A. (2006) T-type calcium channels: the never ending story, *Cell calcium* 40, 81-88.
  72. Talavera, K., and Nilius, B. (2006) Evidence for common structural determinants of activation and inactivation in T-type Ca<sup>2+</sup> channels, *Pflugers Archiv : European journal of physiology* 453, 189-201.

73. Cribbs, L. L., Lee, J. H., Yang, J., Satin, J., Zhang, Y., Daud, A., Barclay, J., Williamson, M. P., Fox, M., Rees, M., and Perez-Reyes, E. (1998) Cloning and characterization of alpha1H from human heart, a member of the T-type Ca<sup>2+</sup> channel gene family, *Circulation research* 83, 103-109.
74. Perez-Reyes, E. (2003) Molecular physiology of low-voltage-activated t-type calcium channels, *Physiological reviews* 83, 117-161.
75. Perez-Reyes, E., Cribbs, L. L., Daud, A., Lacerda, A. E., Barclay, J., Williamson, M. P., Fox, M., Rees, M., and Lee, J. H. (1998) Molecular characterization of a neuronal low-voltage-activated T-type calcium channel, *Nature* 391, 896-900.
76. Lory, P., and Chemin, J. (2007) Towards the discovery of novel T-type calcium channel blockers, *Expert opinion on therapeutic targets* 11, 717-722.
77. Mesirca, P., Torrente, A. G., and Mangoni, M. E. (2014) T-type channels in the sino-atrial and atrioventricular pacemaker mechanism, *Pflugers Archiv : European journal of physiology* 466, 791-799.
78. Chiang, C. S., Huang, C. H., Chieng, H., Chang, Y. T., Chang, D., Chen, J. J., Chen, Y. C., Chen, Y. H., Shin, H. S., Campbell, K. P., and Chen, C. C. (2009) The Ca(v)3.2 T-type Ca(2+) channel is required for pressure overload-induced cardiac hypertrophy in mice, *Circulation research* 104, 522-530.
79. Lee, J., Kim, D., and Shin, H. S. (2004) Lack of delta waves and sleep disturbances during non-rapid eye movement sleep in mice lacking alpha1G-subunit of T-type calcium channels, *Proceedings of the National Academy of Sciences of the United States of America* 101, 18195-18199.
80. Tsakiridou, E., Bertollini, L., de Curtis, M., Avanzini, G., and Pape, H. C. (1995) Selective increase in T-type calcium conductance of reticular thalamic neurons in a rat model of absence epilepsy, *The Journal of neuroscience : the official journal of the Society for Neuroscience* 15, 3110-3117.
81. Molineux, M. L., McRory, J. E., McKay, B. E., Hamid, J., Mehaffey, W. H., Rehak, R., Snutch, T. P., Zamponi, G. W., and Turner, R. W. (2006) Specific T-type calcium channel isoforms are associated with distinct burst phenotypes in deep cerebellar nuclear neurons, *Proceedings of the National Academy of Sciences of the United States of America* 103, 5555-5560.
82. Huguenard, J. R. (1998) Anatomical and physiological considerations in thalamic rhythm generation, *Journal of sleep research* 7 Suppl 1, 24-29.
83. Ulrich, D., and Huguenard, J. R. (1997) GABA(A)-receptor-mediated rebound burst firing and burst shunting in thalamus, *Journal of neurophysiology* 78, 1748-1751.
84. Coulter, D. A., Huguenard, J. R., and Prince, D. A. (1989) Characterization of ethosuximide reduction of low-threshold calcium current in thalamic neurons, *Annals of neurology* 25, 582-593.
85. Destexhe, A., Neubig, M., Ulrich, D., and Huguenard, J. (1998) Dendritic low-threshold calcium currents in thalamic relay cells, *The Journal of neuroscience : the official journal of the Society for Neuroscience* 18, 3574-3588.
86. Destexhe, A., Contreras, D., and Steriade, M. (1998) Mechanisms underlying the synchronizing action of corticothalamic feedback through inhibition of thalamic relay cells, *Journal of neurophysiology* 79, 999-1016.
87. Alvina, K., Ellis-Davies, G., and Khodakhah, K. (2009) T-type calcium channels mediate rebound firing in intact deep cerebellar neurons, *Neuroscience* 158, 635-641.

88. Mangoni, M. E., Traboulsie, A., Leoni, A. L., Couette, B., Marger, L., Le Quang, K., Kupfer, E., Cohen-Solal, A., Vilar, J., Shin, H. S., Escande, D., Charpentier, F., Nargeot, J., and Lory, P. (2006) Bradycardia and slowing of the atrioventricular conduction in mice lacking CaV3.1/alpha1G T-type calcium channels, *Circulation research* 98, 1422-1430.
89. Kim, D., Song, I., Keum, S., Lee, T., Jeong, M. J., Kim, S. S., McEnery, M. W., and Shin, H. S. (2001) Lack of the burst firing of thalamocortical relay neurons and resistance to absence seizures in mice lacking alpha(1G) T-type Ca(2+) channels, *Neuron* 31, 35-45.
90. Khosravani, H., Bladen, C., Parker, D. B., Snutch, T. P., McRory, J. E., and Zamponi, G. W. (2005) Effects of Cav3.2 channel mutations linked to idiopathic generalized epilepsy, *Annals of neurology* 57, 745-749.
91. Khosravani, H., and Zamponi, G. W. (2006) Voltage-gated calcium channels and idiopathic generalized epilepsies, *Physiological reviews* 86, 941-966.
92. Anderson, M. P., Mochizuki, T., Xie, J., Fischler, W., Manger, J. P., Talley, E. M., Scammell, T. E., and Tonegawa, S. (2005) Thalamic Cav3.1 T-type Ca<sup>2+</sup> channel plays a crucial role in stabilizing sleep, *Proceedings of the National Academy of Sciences of the United States of America* 102, 1743-1748.
93. Chen, C. C., Lamping, K. G., Nuno, D. W., Barresi, R., Prouty, S. J., Lavoie, J. L., Cribbs, L. L., England, S. K., Sigmund, C. D., Weiss, R. M., Williamson, R. A., Hill, J. A., and Campbell, K. P. (2003) Abnormal coronary function in mice deficient in alpha1H T-type Ca<sup>2+</sup> channels, *Science* 302, 1416-1418.
94. Choi, S., Na, H. S., Kim, J., Lee, J., Lee, S., Kim, D., Park, J., Chen, C. C., Campbell, K. P., and Shin, H. S. (2007) Attenuated pain responses in mice lacking Ca(V)3.2 T-type channels, *Genes, brain, and behavior* 6, 425-431.
95. Bladen, C., Gadotti, V. M., Gunduz, M. G., Berger, N. D., Simsek, R., Safak, C., and Zamponi, G. W. (2014) 1,4-Dihydropyridine derivatives with T-type calcium channel blocking activity attenuate inflammatory and neuropathic pain, *Pflugers Archiv : European journal of physiology*.
96. Jagodic, M. M., Pathirathna, S., Joksovic, P. M., Lee, W., Nelson, M. T., Naik, A. K., Su, P., Jevtovic-Todorovic, V., and Todorovic, S. M. (2008) Upregulation of the T-type calcium current in small rat sensory neurons after chronic constrictive injury of the sciatic nerve, *Journal of neurophysiology* 99, 3151-3156.
97. Marger, F., Gelot, A., Alloui, A., Matricon, J., Ferrer, J. F., Barrere, C., Pizzoccaro, A., Muller, E., Nargeot, J., Snutch, T. P., Eschalier, A., Bourinet, E., and Ardid, D. (2011) T-type calcium channels contribute to colonic hypersensitivity in a rat model of irritable bowel syndrome, *Proceedings of the National Academy of Sciences of the United States of America* 108, 11268-11273.
98. Jagodic, M. M., Pathirathna, S., Nelson, M. T., Mancuso, S., Joksovic, P. M., Rosenberg, E. R., Bayliss, D. A., Jevtovic-Todorovic, V., and Todorovic, S. M. (2007) Cell-specific alterations of T-type calcium current in painful diabetic neuropathy enhance excitability of sensory neurons, *The Journal of neuroscience : the official journal of the Society for Neuroscience* 27, 3305-3316.
99. Orestes, P., Osuru, H. P., McIntire, W. E., Jacus, M. O., Salajegheh, R., Jagodic, M. M., Choe, W., Lee, J., Lee, S. S., Rose, K. E., Piro, N., Digruccio, M. R., Krishnan, K., Covey, D. F., Lee, J. H., Barrett, P. Q., Jevtovic-Todorovic, V., and Todorovic, S. M.

- (2013) Reversal of neuropathic pain in diabetes by targeting glycosylation of Ca(V)3.2 T-type calcium channels, *Diabetes* 62, 3828-3838.
100. Garcia-Caballero, A., Gadotti, V. M., Stemkowski, P., Weiss, N., Souza, I. A., Hodgkinson, V., Bladen, C., Chen, L., Hamid, J., Pizzoccaro, A., Deage, M., Francois, A., Bourinet, E., and Zamponi, G. W. (2014) The Deubiquitinating Enzyme USP5 Modulates Neuropathic and Inflammatory Pain by Enhancing Cav3.2 Channel Activity, *Neuron* 83, 1144-1158.
  101. Berjukow, S., Marksteiner, R., Gapp, F., Sinnegger, M. J., and Hering, S. (2000) Molecular mechanism of calcium channel block by isradipine. Role of a drug-induced inactivated channel conformation, *The Journal of biological chemistry* 275, 22114-22120.
  102. Hering, S., Aczel, S., Kraus, R. L., Berjukow, S., Striessnig, J., and Timin, E. N. (1997) Molecular mechanism of use-dependent calcium channel block by phenylalkylamines: role of inactivation, *Proceedings of the National Academy of Sciences of the United States of America* 94, 13323-13328.
  103. Gomora, J. C., Daud, A. N., Weiergraber, M., and Perez-Reyes, E. (2001) Block of cloned human T-type calcium channels by succinimide antiepileptic drugs, *Molecular pharmacology* 60, 1121-1132.
  104. Astori, S., Wimmer, R. D., Prosser, H. M., Corti, C., Corsi, M., Liaudet, N., Volterra, A., Franken, P., Adelman, J. P., and Luthi, A. (2011) The Ca(V)3.3 calcium channel is the major sleep spindle pacemaker in thalamus, *Proceedings of the National Academy of Sciences of the United States of America* 108, 13823-13828.
  105. Schrier, A. D., Wang, H., Talley, E. M., Perez-Reyes, E., and Barrett, P. Q. (2001) alpha1H T-type Ca<sup>2+</sup> channel is the predominant subtype expressed in bovine and rat zona glomerulosa, *American journal of physiology. Cell physiology* 280, C265-272.
  106. Trevino, C. L., Felix, R., Castellano, L. E., Gutierrez, C., Rodriguez, D., Pacheco, J., Lopez-Gonzalez, I., Gomora, J. C., Tsutsumi, V., Hernandez-Cruz, A., Fiordelisio, T., Scaling, A. L., and Darszon, A. (2004) Expression and differential cell distribution of low-threshold Ca(2+) channels in mammalian male germ cells and sperm, *FEBS letters* 563, 87-92.
  107. Kase, M., Kakimoto, S., Sakuma, S., Houtani, T., Ohishi, H., Ueyama, T., and Sugimoto, T. (1999) Distribution of neurons expressing alpha 1G subunit mRNA of T-type voltage-dependent calcium channel in adult rat central nervous system, *Neuroscience letters* 268, 77-80.
  108. Chemin, J., Monteil, A., Dubel, S., Nargeot, J., and Lory, P. (2001) The alpha1I T-type calcium channel exhibits faster gating properties when overexpressed in neuroblastoma/glioma NG 108-15 cells, *The European journal of neuroscience* 14, 1678-1686.
  109. Latour, I., Louw, D. F., Beedle, A. M., Hamid, J., Sutherland, G. R., and Zamponi, G. W. (2004) Expression of T-type calcium channel splice variants in human glioma, *Glia* 48, 112-119.
  110. McKay, B. E., McRory, J. E., Molineux, M. L., Hamid, J., Snutch, T. P., Zamponi, G. W., and Turner, R. W. (2006) Ca(V)3 T-type calcium channel isoforms differentially distribute to somatic and dendritic compartments in rat central neurons, *The European journal of neuroscience* 24, 2581-2594.

111. Klugbauer, N., Marais, E., Lacinova, L., and Hofmann, F. (1999) A T-type calcium channel from mouse brain, *Pflugers Archiv : European journal of physiology* 437, 710-715.
112. Bladen, C., Gündüz, M., Şimşek, R., Şafak, C., and Zamponi, G. (2013) Synthesis and Evaluation of 1,4-Dihydropyridine Derivatives with Calcium Channel Blocking Activity, *Pflugers Arch - Eur J Physiol*, 1-9.
113. Gadotti, V. M., You, H., Petrov, R. R., Berger, N. D., Diaz, P., and Zamponi, G. W. (2013) Analgesic effect of a mixed T-type channel inhibitor/CB2 receptor agonist, *Molecular pain* 9, 32.
114. Barbara, G., Alloui, A., Nargeot, J., Lory, P., Eschalier, A., Bourinet, E., and Chemin, J. (2009) T-type calcium channel inhibition underlies the analgesic effects of the endogenous lipoamino acids, *The Journal of neuroscience : the official journal of the Society for Neuroscience* 29, 13106-13114.
115. Traboulsie, A., Chemin, J., Chevalier, M., Quignard, J. F., Nargeot, J., and Lory, P. (2007) Subunit-specific modulation of T-type calcium channels by zinc, *The Journal of physiology* 578, 159-171.
116. Bladen, C., Gunduz, M. G., Simsek, R., Safak, C., and Zamponi, G. W. (2013) Synthesis and Evaluation of 1,4-Dihydropyridine Derivatives with Calcium Channel Blocking Activity, *Pflugers Archiv : European journal of physiology*.
117. Kang, H. W., Park, J. Y., Jeong, S. W., Kim, J. A., Moon, H. J., Perez-Reyes, E., and Lee, J. H. (2006) A molecular determinant of nickel inhibition in Cav3.2 T-type calcium channels, *The Journal of biological chemistry* 281, 4823-4830.
118. Nelson, M. T., Joksovic, P. M., Perez-Reyes, E., and Todorovic, S. M. (2005) The endogenous redox agent L-cysteine induces T-type Ca<sup>2+</sup> channel-dependent sensitization of a novel subpopulation of rat peripheral nociceptors, *The Journal of neuroscience : the official journal of the Society for Neuroscience* 25, 8766-8775.
119. Lee, C. W., Bae, C., Lee, J., Ryu, J. H., Kim, H. H., Kohno, T., Swartz, K. J., and Kim, J. I. (2012) Solution structure of kurtoxin: a gating modifier selective for Cav3 voltage-gated Ca(2+) channels, *Biochemistry* 51, 1862-1873.
120. McDonough, S. I. (2007) Gating modifier toxins of voltage-gated calcium channels, *Toxicon* 49, 202-212.
121. Catterall, W. A., Cestele, S., Yarov-Yarovoy, V., Yu, F. H., Konoki, K., and Scheuer, T. (2007) Voltage-gated ion channels and gating modifier toxins, *Toxicon* 49, 124-141.
122. Barton, M. E., Eberle, E. L., and Shannon, H. E. (2005) The antihyperalgesic effects of the T-type calcium channel blockers ethosuximide, trimethadione, and mibefradil, *European journal of pharmacology* 521, 79-85.
123. Mullins, M. E., Horowitz, B. Z., Linden, D. H., Smith, G. W., Norton, R. L., and Stump, J. (1998) Life-threatening interaction of mibefradil and beta-blockers with dihydropyridine calcium channel blockers, *JAMA : the journal of the American Medical Association* 280, 157-158.
124. Obradovic, A., Hwang, S. M., Scarpa, J., Hong, S. J., Todorovic, S. M., and Jevtovic-Todorovic, V. (2014) CaV3.2 T-Type Calcium Channels in Peripheral Sensory Neurons Are Important for Mibefradil-Induced Reversal of Hyperalgesia and Allodynia in Rats with Painful Diabetic Neuropathy, *PloS one* 9, e91467.

125. Todorovic, S. M., and Lingle, C. J. (1998) Pharmacological properties of T-type Ca<sup>2+</sup> current in adult rat sensory neurons: effects of anticonvulsant and anesthetic agents, *Journal of neurophysiology* 79, 240-252.
126. Hainsworth, A. H., McNaughton, N. C., Pereverzev, A., Schneider, T., and Randall, A. D. (2003) Actions of sipatrigine, 202W92 and lamotrigine on R-type and T-type Ca<sup>2+</sup> channel currents, *European journal of pharmacology* 467, 77-80.
127. Hildebrand, M. E., Smith, P. L., Bladen, C., Eduljee, C., Xie, J. Y., Chen, L., Fee-Maki, M., Doering, C. J., Mezeyova, J., Zhu, Y., Belardetti, F., Pajouhesh, H., Parker, D., Arneric, S. P., Parmar, M., Porreca, F., Tringham, E., Zamponi, G. W., and Snutch, T. P. (2011) A novel slow-inactivation-specific ion channel modulator attenuates neuropathic pain, *Pain* 152, 833-843.
128. Crunelli, V., and Leresche, N. (2002) Block of Thalamic T-Type Ca(2+) Channels by Ethosuximide Is Not the Whole Story, *Epilepsy currents / American Epilepsy Society* 2, 53-56.
129. Huguenard, J. R. (2002) Block of T -Type Ca(2+) Channels Is an Important Action of Succinimide Antiabsence Drugs, *Epilepsy currents / American Epilepsy Society* 2, 49-52.
130. You, H., Gadotti, V. M., Petrov, R. R., Zamponi, G. W., and Diaz, P. (2011) Functional characterization and analgesic effects of mixed cannabinoid receptor/T-type channel ligands, *Molecular pain* 7, 89.
131. Chemin, J., Monteil, A., Perez-Reyes, E., Nargeot, J., and Lory, P. (2001) Direct inhibition of T-type calcium channels by the endogenous cannabinoid anandamide, *The EMBO journal* 20, 7033-7040.
132. Chemin, J., Nargeot, J., and Lory, P. (2007) Chemical determinants involved in anandamide-induced inhibition of T-type calcium channels, *The Journal of biological chemistry* 282, 2314-2323.
133. Khosravani, H., Altier, C., Simms, B., Hamming, K. S., Snutch, T. P., Mezeyova, J., McRory, J. E., and Zamponi, G. W. (2004) Gating effects of mutations in the Cav3.2 T-type calcium channel associated with childhood absence epilepsy, *The Journal of biological chemistry* 279, 9681-9684.
134. Vitko, I., Chen, Y., Arias, J. M., Shen, Y., Wu, X. R., and Perez-Reyes, E. (2005) Functional characterization and neuronal modeling of the effects of childhood absence epilepsy variants of CACNA1H, a T-type calcium channel, *The Journal of neuroscience : the official journal of the Society for Neuroscience* 25, 4844-4855.
135. Ernst, W. L., Zhang, Y., Yoo, J. W., Ernst, S. J., and Noebels, J. L. (2009) Genetic enhancement of thalamocortical network activity by elevating alpha 1g-mediated low-voltage-activated calcium current induces pure absence epilepsy, *The Journal of neuroscience : the official journal of the Society for Neuroscience* 29, 1615-1625.
136. Su, H., Sochivko, D., Becker, A., Chen, J., Jiang, Y., Yaari, Y., and Beck, H. (2002) Upregulation of a T-type Ca<sup>2+</sup> channel causes a long-lasting modification of neuronal firing mode after status epilepticus, *The Journal of neuroscience : the official journal of the Society for Neuroscience* 22, 3645-3655.
137. Curia, G., Longo, D., Biagini, G., Jones, R. S., and Avoli, M. (2008) The pilocarpine model of temporal lobe epilepsy, *Journal of neuroscience methods* 172, 143-157.
138. Graef, J. D., Nordskog, B. K., Wiggins, W. F., and Godwin, D. W. (2009) An acquired channelopathy involving thalamic T-type Ca<sup>2+</sup> channels after status epilepticus, *The*

- Journal of neuroscience : the official journal of the Society for Neuroscience* 29, 4430-4441.
139. Lu, A. T., Dai, X., Martinez-Agosto, J. A., and Cantor, R. M. (2012) Support for calcium channel gene defects in autism spectrum disorders, *Molecular autism* 3, 18.
  140. Tai, C. H., Yang, Y. C., Pan, M. K., Huang, C. S., and Kuo, C. C. (2011) Modulation of subthalamic T-type Ca(2+) channels remedies locomotor deficits in a rat model of Parkinson disease, *The Journal of clinical investigation* 121, 3289-3305.
  141. Xiang, Z., Thompson, A. D., Brogan, J. T., Schulte, M. L., Melancon, B. J., Mi, D., Lewis, L. M., Zou, B., Yang, L., Morrison, R., Santomango, T., Byers, F., Brewer, K., Aldrich, J. S., Yu, H., Dawson, E. S., Li, M., McManus, O., Jones, C. K., Daniels, J. S., Hopkins, C. R., Xie, X. S., Conn, P. J., Weaver, C. D., and Lindsley, C. W. (2011) The Discovery and Characterization of ML218: A Novel, Centrally Active T-Type Calcium Channel Inhibitor with Robust Effects in STN Neurons and in a Rodent Model of Parkinson's Disease, *ACS chemical neuroscience* 2, 730-742.
  142. Splawski, I., Yoo, D. S., Stotz, S. C., Cherry, A., Clapham, D. E., and Keating, M. T. (2006) CACNA1H mutations in autism spectrum disorders, *The Journal of biological chemistry* 281, 22085-22091.
  143. Catterall, W. A., Dib-Hajj, S., Meisler, M. H., and Pietrobon, D. (2008) Inherited neuronal ion channelopathies: new windows on complex neurological diseases, *The Journal of neuroscience : the official journal of the Society for Neuroscience* 28, 11768-11777.
  144. Cox, J. J., Reimann, F., Nicholas, A. K., Thornton, G., Roberts, E., Springell, K., Karbani, G., Jafri, H., Mannan, J., Raashid, Y., Al-Gazali, L., Hamamy, H., Valente, E. M., Gorman, S., Williams, R., McHale, D. P., Wood, J. N., Gribble, F. M., and Woods, C. G. (2006) An SCN9A channelopathy causes congenital inability to experience pain, *Nature* 444, 894-898.
  145. Dib-Hajj, S. D., Rush, A. M., Cummins, T. R., Hisama, F. M., Novella, S., Tyrrell, L., Marshall, L., and Waxman, S. G. (2005) Gain-of-function mutation in Nav1.7 in familial erythromelalgia induces bursting of sensory neurons, *Brain : a journal of neurology* 128, 1847-1854.
  146. Dubin, A. E., and Patapoutian, A. (2010) Nociceptors: the sensors of the pain pathway, *The Journal of Clinical Investigation* 120, 3760-3772.
  147. Goldberg, Y. P., MacFarlane, J., MacDonald, M. L., Thompson, J., Dube, M. P., Mattice, M., Fraser, R., Young, C., Hossain, S., Pape, T., Payne, B., Radomski, C., Donaldson, G., Ives, E., Cox, J., Younghusband, H. B., Green, R., Duff, A., Boltshauser, E., Grinspan, G. A., Dimon, J. H., Sibley, B. G., Andria, G., Toscano, E., Kerdraon, J., Bowsher, D., Pimstone, S. N., Samuels, M. E., Sherrington, R., and Hayden, M. R. (2007) Loss-of-function mutations in the Nav1.7 gene underlie congenital indifference to pain in multiple human populations, *Clinical genetics* 71, 311-319.
  148. Theile, J. W., Jarecki, B. W., Piekarczyk, A. D., and Cummins, T. R. (2011) Nav1.7 mutations associated with paroxysmal extreme pain disorder, but not erythromelalgia, enhance Navbeta4 peptide-mediated resurgent sodium currents, *The Journal of physiology* 589, 597-608.
  149. Colovic, R. B., Grubor, N. M., Micev, M. T., Atkinson, H. D., Rankovic, V. I., and Jagodic, M. M. (2008) Cystic lymphangioma of the pancreas, *World journal of gastroenterology : WJG* 14, 6873-6875.

150. Dray, A. (2008) Neuropathic pain: emerging treatments, *British journal of anaesthesia* 101, 48-58.
151. Markman, J. D., and Dworkin, R. H. (2006) Ion channel targets and treatment efficacy in neuropathic pain, *The journal of pain : official journal of the American Pain Society* 7, S38-47.
152. Waxman, S. G., and Zamponi, G. W. (2014) Regulating excitability of peripheral afferents: emerging ion channel targets, *Nature neuroscience* 17, 153-163.
153. Woolf, C. J., and Ma, Q. (2007) Nociceptors--noxious stimulus detectors, *Neuron* 55, 353-364.
154. Zamponi, G. W., Lewis, R. J., Todorovic, S. M., Arneric, S. P., and Snutch, T. P. (2009) Role of voltage-gated calcium channels in ascending pain pathways, *Brain research reviews* 60, 84-89.
155. Abrahamsen, B., Zhao, J., Asante, C. O., Cendan, C. M., Marsh, S., Martinez-Barbera, J. P., Nassar, M. A., Dickenson, A. H., and Wood, J. N. (2008) The cell and molecular basis of mechanical, cold, and inflammatory pain, *Science* 321, 702-705.
156. Bourinet, E., Altier, C., Hildebrand, M. E., Trang, T., Salter, M. W., and Zamponi, G. W. (2014) Calcium-permeable ion channels in pain signaling, *Physiological reviews* 94, 81-140.
157. Woolf, C. J. (2000) Neuronal Plasticity: Increasing the Gain in Pain, *Science* 288, 1765-1768.
158. Moqrich, A. (2014) Peripheral pain-sensing neurons: from molecular diversity to functional specialization, *Cell Rep* 6, 245-246.
159. Moqrich, A., Hwang, S. W., Earley, T. J., Petrus, M. J., Murray, A. N., Spencer, K. S., Andahazy, M., Story, G. M., and Patapoutian, A. (2005) Impaired thermosensation in mice lacking TRPV3, a heat and camphor sensor in the skin, *Science* 307, 1468-1472.
160. Luo, Z. D. (2010) Calcium channel functions in pain processing, *Channels* 4, 52-51.
161. Lipscombe, D., and Raingo, J. (2007) Alternative splicing matters: N-type calcium channels in nociceptors, *Channels* 1, 225-227.
162. Raingo, J., Castiglioni, A. J., and Lipscombe, D. (2007) Alternative splicing controls G protein-dependent inhibition of N-type calcium channels in nociceptors, *Nature neuroscience* 10, 285-292.
163. Bourinet, E., Soong, T. W., Stea, A., and Snutch, T. P. (1996) Determinants of the G protein-dependent opioid modulation of neuronal calcium channels, *Proceedings of the National Academy of Sciences of the United States of America* 93, 1486-1491.
164. Altier, C., Dale, C. S., Kisilevsky, A. E., Chapman, K., Castiglioni, A. J., Matthews, E. A., Evans, R. M., Dickenson, A. H., Lipscombe, D., Vergnolle, N., and Zamponi, G. W. (2007) Differential role of N-type calcium channel splice isoforms in pain, *The Journal of neuroscience : the official journal of the Society for Neuroscience* 27, 6363-6373.
165. Krarup, C. (2003) An update on electrophysiological studies in neuropathy, *Current opinion in neurology* 16, 603-612.
166. Feng, Z. P., Doering, C. J., Winkfein, R. J., Beedle, A. M., Spafford, J. D., and Zamponi, G. W. (2003) Determinants of inhibition of transiently expressed voltage-gated calcium channels by omega-conotoxins GVIA and MVIIA, *The Journal of biological chemistry* 278, 20171-20178.
167. Staats, P. S., Yearwood, T., Charapata, S. G., Presley, R. W., Wallace, M. S., Byas-Smith, M., Fisher, R., Bryce, D. A., Mangieri, E. A., Luther, R. R., Mayo, M., McGuire,

- D., and Ellis, D. (2004) Intrathecal ziconotide in the treatment of refractory pain in patients with cancer or AIDS: a randomized controlled trial, *JAMA : the journal of the American Medical Association* 291, 63-70.
168. Smith, M. T., Cabot, P. J., Ross, F. B., Robertson, A. D., and Lewis, R. J. (2002) The novel N-type calcium channel blocker, AM336, produces potent dose-dependent antinociception after intrathecal dosing in rats and inhibits substance P release in rat spinal cord slices, *Pain* 96, 119-127.
169. Malmberg, A. B., and Yaksh, T. L. (1995) Effect of continuous intrathecal infusion of omega-conopeptides, N-type calcium-channel blockers, on behavior and antinociception in the formalin and hot-plate tests in rats, *Pain* 60, 83-90.
170. Lewis, R. J., Nielsen, K. J., Craik, D. J., Loughnan, M. L., Adams, D. A., Sharpe, I. A., Luchian, T., Adams, D. J., Bond, T., Thomas, L., Jones, A., Matheson, J. L., Drinkwater, R., Andrews, P. R., and Alewood, P. F. (2000) Novel omega-conotoxins from *Conus catus* discriminate among neuronal calcium channel subtypes, *The Journal of biological chemistry* 275, 35335-35344.
171. Jevtovic-Todorovic, V., and Todorovic, S. M. (2006) The role of peripheral T-type calcium channels in pain transmission, *Cell calcium* 40, 197-203.
172. Latham, J. R., Pathirathna, S., Jagodic, M. M., Choe, W. J., Levin, M. E., Nelson, M. T., Lee, W. Y., Krishnan, K., Covey, D. F., Todorovic, S. M., and Jevtovic-Todorovic, V. (2009) Selective T-type calcium channel blockade alleviates hyperalgesia in ob/ob mice, *Diabetes* 58, 2656-2665.
173. Todorovic, S., and Jevtovic-Todorovic, V. (2014) Targeting of CaV3.2 T-type calcium channels in peripheral sensory neurons for the treatment of painful diabetic neuropathy, *Pflugers Arch - Eur J Physiol* 466, 701-706.
174. Todorovic, S. M., and Jevtovic-Todorovic, V. (2011) T-type voltage-gated calcium channels as targets for the development of novel pain therapies, *British journal of pharmacology* 163, 484-495.
175. Bourinet, E., Alloui, A., Monteil, A., Barrere, C., Couette, B., Poirot, O., Pages, A., McRory, J., Snutch, T. P., Eschalier, A., and Nargeot, J. (2005) Silencing of the Cav3.2 T-type calcium channel gene in sensory neurons demonstrates its major role in nociception, *The EMBO journal* 24, 315-324.
176. Dogrul, A., Gardell, L. R., Ossipov, M. H., Tulunay, F. C., Lai, J., and Porreca, F. (2003) Reversal of experimental neuropathic pain by T-type calcium channel blockers, *Pain* 105, 159-168.
177. Matthews, E. A., and Dickenson, A. H. (2001) Effects of ethosuximide, a T-type Ca(2+) channel blocker, on dorsal horn neuronal responses in rats, *European journal of pharmacology* 415, 141-149.
178. Shin, H. S., Cheong, E. J., Choi, S., Lee, J., and Na, H. S. (2008) T-type Ca<sup>2+</sup> channels as therapeutic targets in the nervous system, *Current opinion in pharmacology* 8, 33-41.
179. Todorovic, S. M., Jevtovic-Todorovic, V., Meyenburg, A., Mennerick, S., Perez-Reyes, E., Romano, C., Olney, J. W., and Zorumski, C. F. (2001) Redox modulation of T-type calcium channels in rat peripheral nociceptors, *Neuron* 31, 75-85.
180. Pathirathna, S., Covey, D. F., Todorovic, S. M., and Jevtovic-Todorovic, V. (2006) Differential effects of endogenous cysteine analogs on peripheral thermal nociception in intact rats, *Pain* 125, 53-64.

181. Nelson, M. T., Woo, J., Kang, H. W., Vitko, I., Barrett, P. Q., Perez-Reyes, E., Lee, J. H., Shin, H. S., and Todorovic, S. M. (2007) Reducing agents sensitize C-type nociceptors by relieving high-affinity zinc inhibition of T-type calcium channels, *The Journal of neuroscience : the official journal of the Society for Neuroscience* 27, 8250-8260.
182. Plummer, N. W., and Meisler, M. H. (1999) Evolution and diversity of mammalian sodium channel genes, *Genomics* 57, 323-331.
183. Hille, B. (1977) Local anesthetics: hydrophilic and hydrophobic pathways for the drug-receptor reaction, *The Journal of general physiology* 69, 497-515.
184. Bezanilla, F. (2005) The voltage-sensor structure in a voltage-gated channel, *Trends in biochemical sciences* 30, 166-168.
185. Borjesson, S. I., and Elinder, F. (2008) Structure, function, and modification of the voltage sensor in voltage-gated ion channels, *Cell biochemistry and biophysics* 52, 149-174.
186. Yang, N., and Horn, R. (1995) Evidence for voltage-dependent S4 movement in sodium channels, *Neuron* 15, 213-218.
187. Armstrong, C. M. (2006) Na channel inactivation from open and closed states, *Proceedings of the National Academy of Sciences of the United States of America* 103, 17991-17996.
188. Tombola, F., Pathak, M. M., Gorostiza, P., and Isacoff, E. Y. (2007) The twisted ion-permeation pathway of a resting voltage-sensing domain, *Nature* 445, 546-549.
189. Villalba-Galea, C. A., Sandtner, W., Starace, D. M., and Bezanilla, F. (2008) S4-based voltage sensors have three major conformations, *Proceedings of the National Academy of Sciences of the United States of America* 105, 17600-17607.
190. Karoly, R., Lenkey, N., Juhasz, A. O., Vizi, E. S., and Mike, A. (2010) Fast- or slow-inactivated state preference of Na<sup>+</sup> channel inhibitors: a simulation and experimental study, *PLoS computational biology* 6, e1000818.
191. Patlak, J. (1991) Molecular kinetics of voltage-dependent Na<sup>+</sup> channels, *Physiological reviews* 71, 1047-1080.
192. Ulbricht, W. (2005) Sodium channel inactivation: molecular determinants and modulation, *Physiological reviews* 85, 1271-1301.
193. Hamid, J., Peloquin, J. B., Monteil, A., and Zamponi, G. W. (2006) Determinants of the differential gating properties of Cav3.1 and Cav3.3 T-type channels: a role of domain IV?, *Neuroscience* 143, 717-728.
194. Arias, O., II, Vitko, I., Fortuna, M., Baumgart, J. P., Sokolova, S., Shumilin, I. A., Van Deusen, A., Soriano-Garcia, M., Gomora, J. C., and Perez-Reyes, E. (2008) Characterization of the gating brake in the I-II loop of Ca(v)3.2 T-type Ca(2+) channels, *The Journal of biological chemistry* 283, 8136-8144.
195. Shcheglovitov, A., Vitko, I., Bidaud, I., Baumgart, J. P., Navarro-Gonzalez, M. F., Grayson, T. H., Lory, P., Hill, C. E., and Perez-Reyes, E. (2008) Alternative splicing within the I-II loop controls surface expression of T-type Ca(v)3.1 calcium channels, *FEBS letters* 582, 3765-3770.
196. Park, J. Y., Kang, H. W., Jeong, S. W., and Lee, J. H. (2004) Multiple structural elements contribute to the slow kinetics of the Cav3.3 T-type channel, *The Journal of biological chemistry* 279, 21707-21713.
197. Ono, K., and Iijima, T. (2010) Cardiac T-type Ca(2+) channels in the heart, *Journal of molecular and cellular cardiology* 48, 65-70.

198. Jarecki, B. W., Piekarz, A. D., Jackson, J. O., 2nd, and Cummins, T. R. (2010) Human voltage-gated sodium channel mutations that cause inherited neuronal and muscle channelopathies increase resurgent sodium currents, *The Journal of clinical investigation* 120, 369-378.
199. Dib-Hajj, S. D., Cummins, T. R., Black, J. A., and Waxman, S. G. (2007) From genes to pain: Na<sup>v</sup> 1.7 and human pain disorders, *Trends in neurosciences* 30, 555-563.
200. Adams, P. J., and Snutch, T. P. (2007) Calcium channelopathies: voltage-gated calcium channels, *Sub-cellular biochemistry* 45, 215-251.
201. Errington, A. C., Stohr, T., Heers, C., and Lees, G. (2008) The investigational anticonvulsant lacosamide selectively enhances slow inactivation of voltage-gated sodium channels, *Molecular pharmacology* 73, 157-169.
202. Sheets, P. L., Jackson, J. O., 2nd, Waxman, S. G., Dib-Hajj, S. D., and Cummins, T. R. (2007) A Nav1.7 channel mutation associated with hereditary erythromelalgia contributes to neuronal hyperexcitability and displays reduced lidocaine sensitivity, *The Journal of physiology* 581, 1019-1031.
203. Cummins, T. R., Sheets, P. L., and Waxman, S. G. (2007) The roles of sodium channels in nociception: Implications for mechanisms of pain, *Pain* 131, 243-257.
204. Rush, A. M., Cummins, T. R., and Waxman, S. G. (2007) Multiple sodium channels and their roles in electrogenesis within dorsal root ganglion neurons, *The Journal of physiology* 579, 1-14.
205. Nassar, M. A., Stirling, L. C., Forlani, G., Baker, M. D., Matthews, E. A., Dickenson, A. H., and Wood, J. N. (2004) Nociceptor-specific gene deletion reveals a major role for Nav1.7 (PN1) in acute and inflammatory pain, *Proceedings of the National Academy of Sciences of the United States of America* 101, 12706-12711.
206. Bender, K. J., Uebele, V. N., Renger, J. J., and Trussell, L. O. (2012) Control of firing patterns through modulation of axon initial segment T-type calcium channels, *The Journal of physiology* 590, 109-118.
207. Laird, J. M., Souslova, V., Wood, J. N., and Cervero, F. (2002) Deficits in visceral pain and referred hyperalgesia in Nav1.8 (SNS/PN3)-null mice, *The Journal of neuroscience : the official journal of the Society for Neuroscience* 22, 8352-8356.
208. Beyreuther, B. K., Callizot, N., Brot, M. D., Feldman, R., Bain, S. C., and Stohr, T. (2007) Antinociceptive efficacy of lacosamide in rat models for tumor- and chemotherapy-induced cancer pain, *European journal of pharmacology* 565, 98-104.
209. Bee, L. A., and Dickenson, A. H. (2009) Effects of lacosamide, a novel sodium channel modulator, on dorsal horn neuronal responses in a rat model of neuropathy, *Neuropharmacology* 57, 472-479.
210. Tripathi, P. K., Trujillo, L., Cardenas, C. A., Cardenas, C. G., de Armendi, A. J., and Scroggs, R. S. (2006) Analysis of the variation in use-dependent inactivation of high-threshold tetrodotoxin-resistant sodium currents recorded from rat sensory neurons, *Neuroscience* 143, 923-938.
211. Choe, Y. J., Seo, H. N., Jung, S. Y., Rhim, H., Kim, J., Choo, D. J., and Lee, J. Y. (2008) Synthesis and SAR study of T-type calcium channel blockers. Part II, *Archiv der Pharmazie* 341, 661-664.
212. Furukawa, T., Miura, R., Honda, M., Kamiya, N., Mori, Y., Takeshita, S., Isshiki, T., and Nukada, T. (2004) Identification of R(-)-isomer of efonidipine as a selective blocker of T-type Ca<sup>2+</sup> channels, *British journal of pharmacology* 143, 1050-1057.

213. Jo, M. N., Seo, H. J., Kim, Y., Seo, S. H., Rhim, H., Cho, Y. S., Cha, J. H., Koh, H. Y., Choo, H., and Pae, A. N. (2007) Novel T-type calcium channel blockers: dioxoquinazoline carboxamide derivatives, *Bioorganic & medicinal chemistry* 15, 365-373.
214. Kumar, P. P., Stotz, S. C., Paramashivappa, R., Beedle, A. M., Zamponi, G. W., and Rao, A. S. (2002) Synthesis and evaluation of a new class of nifedipine analogs with T-type calcium channel blocking activity, *Molecular pharmacology* 61, 649-658.
215. You, H., Altier, C., and Zamponi, G. W. (2010) CCR2 receptor ligands inhibit Cav3.2 T-type calcium channels, *Molecular pharmacology* 77, 211-217.
216. Edraki, N., Mehdipour, A. R., Khoshneviszadeh, M., and Miri, R. (2009) Dihydropyridines: evaluation of their current and future pharmacological applications, *Drug Discov Today* 14, 1058-1066.
217. Peterson, B. Z., Johnson, B. D., Hockerman, G. H., Acheson, M., Scheuer, T., and Catterall, W. A. (1997) Analysis of the dihydropyridine receptor site of L-type calcium channels by alanine-scanning mutagenesis, *The Journal of biological chemistry* 272, 18752-18758.
218. Tikhonov, D. B., and Zhorov, B. S. (2009) Structural model for dihydropyridine binding to L-type calcium channels, *The Journal of biological chemistry* 284, 19006-19017.
219. Moreira, F. A., Grieb, M., and Lutz, B. (2009) Central side-effects of therapies based on CB1 cannabinoid receptor agonists and antagonists: focus on anxiety and depression, *Best practice & research. Clinical endocrinology & metabolism* 23, 133-144.
220. Witkin, J. M., Tzavara, E. T., and Nomikos, G. G. (2005) A role for cannabinoid CB1 receptors in mood and anxiety disorders, *Behavioural pharmacology* 16, 315-331.
221. Bladen, C., and Zamponi, G. W. (2012) Common mechanisms of drug interactions with sodium and T-type calcium channels, *Molecular pharmacology* 82, 481-487.
222. Beedle, A. M., Hamid, J., and Zamponi, G. W. (2002) Inhibition of transiently expressed low- and high-voltage-activated calcium channels by trivalent metal cations, *The Journal of membrane biology* 187, 225-238.
223. Iftinca, M., Hamid, J., Chen, L., Varela, D., Tadayonnejad, R., Altier, C., Turner, R. W., and Zamponi, G. W. (2007) Regulation of T-type calcium channels by Rho-associated kinase, *Nature neuroscience* 10, 854-860.
224. Hylden, J. L., and Wilcox, G. L. (1980) Intrathecal morphine in mice: a new technique, *European journal of pharmacology* 67, 313-316.
225. Gadotti, V. M., and Zamponi, G. W. (2011) Cellular prion protein protects from inflammatory and neuropathic pain, *Molecular pain* 7, 59.
226. Kaster, M. P., Gadotti, V. M., Calixto, J. B., Santos, A. R., and Rodrigues, A. L. (2012) Depressive-like behavior induced by tumor necrosis factor-alpha in mice, *Neuropharmacology* 62, 419-426.
227. Şafak, C., Gündüz, M. G., İlhan, S. Ö., Şimşek, R., İşli, F., Yıldırım, Ş., Fincan, G. S. Ö., Sarioğlu, Y., and Linden, A. (2012) Synthesis and Myorelaxant Activity of Fused 1,4-Dihydropyridines on Isolated Rabbit Gastric Fundus, *Drug Development Research* 73, 332-342.
228. Armbruster, B. N., and Roth, B. L. (2005) Mining the receptorome, *The Journal of biological chemistry* 280, 5129-5132.
229. Jensen, N. H., and Roth, B. L. (2008) Massively parallel screening of the receptorome, *Combinatorial chemistry & high throughput screening* 11, 420-426.

230. Yu, F. H., Yarov-Yarovoy, V., Gutman, G. A., and Catterall, W. A. (2005) Overview of molecular relationships in the voltage-gated ion channel superfamily, *Pharmacological reviews* 57, 387-395.
231. Blair, N. T., and Bean, B. P. (2003) Role of tetrodotoxin-resistant Na<sup>+</sup> current slow inactivation in adaptation of action potential firing in small-diameter dorsal root ganglion neurons, *The Journal of neuroscience : the official journal of the Society for Neuroscience* 23, 10338-10350.
232. Waxman, S. G. (2006) Axonal conduction and injury in multiple sclerosis: the role of sodium channels, *Nature reviews. Neuroscience* 7, 932-941.
233. Isom, L. L. (2001) Sodium Channel Subunits: Anything but Auxiliary, *The Neuroscientist* 7, 42-54.
234. Cribbs, L. (2010) T-type calcium channel expression and function in the diseased heart, *Channels* 4, 447-452.
235. Wang, W., Gu, J., Li, Y. Q., and Tao, Y. X. (2011) Are voltage-gated sodium channels on the dorsal root ganglion involved in the development of neuropathic pain?, *Molecular pain* 7, 16.
236. Cregg, R., Momin, A., Rugiero, F., Wood, J. N., and Zhao, J. (2010) Pain channelopathies, *The Journal of physiology* 588, 1897-1904.
237. McGaraughty, S., Chu, K. L., Scanio, M. J., Kort, M. E., Faltynek, C. R., and Jarvis, M. F. (2008) A selective Nav1.8 sodium channel blocker, A-803467 [5-(4-chlorophenyl-N-(3,5-dimethoxyphenyl)furan-2-carboxamide)], attenuates spinal neuronal activity in neuropathic rats, *The Journal of pharmacology and experimental therapeutics* 324, 1204-1211.
238. Browne, L. E., Blaney, F. E., Yusaf, S. P., Clare, J. J., and Wray, D. (2009) Structural determinants of drugs acting on the Nav1.8 channel, *The Journal of biological chemistry* 284, 10523-10536.
239. Browne, L. E., Clare, J. J., and Wray, D. (2009) Functional and pharmacological properties of human and rat Nav1.8 channels, *Neuropharmacology* 56, 905-914.
240. Jarvis, M. F., Honore, P., Shieh, C. C., Chapman, M., Joshi, S., Zhang, X. F., Kort, M., Carroll, W., Marron, B., Atkinson, R., Thomas, J., Liu, D., Krambis, M., Liu, Y., McGaraughty, S., Chu, K., Roeloffs, R., Zhong, C., Mikusa, J. P., Hernandez, G., Gauvin, D., Wade, C., Zhu, C., Pai, M., Scanio, M., Shi, L., Drizin, I., Gregg, R., Matulenko, M., Hakeem, A., Gross, M., Johnson, M., Marsh, K., Wagoner, P. K., Sullivan, J. P., Faltynek, C. R., and Krafte, D. S. (2007) A-803467, a potent and selective Nav1.8 sodium channel blocker, attenuates neuropathic and inflammatory pain in the rat, *Proceedings of the National Academy of Sciences of the United States of America* 104, 8520-8525.
241. Sheets, P. L., Heers, C., Stoehr, T., and Cummins, T. R. (2008) Differential block of sensory neuronal voltage-gated sodium channels by lacosamide [(2R)-2-(acetylamino)-N-benzyl-3-methoxypropanamide], lidocaine, and carbamazepine, *The Journal of pharmacology and experimental therapeutics* 326, 89-99.
242. Lipkind, G. M., and Fozzard, H. A. (2010) Molecular model of anticonvulsant drug binding to the voltage-gated sodium channel inner pore, *Molecular pharmacology* 78, 631-638.

243. Ragsdale, D. S., McPhee, J. C., Scheuer, T., and Catterall, W. A. (1994) Molecular determinants of state-dependent block of Na<sup>+</sup> channels by local anesthetics, *Science* 265, 1724-1728.
244. Yarov-Yarovoy, V., Brown, J., Sharp, E. M., Clare, J. J., Scheuer, T., and Catterall, W. A. (2001) Molecular determinants of voltage-dependent gating and binding of pore-blocking drugs in transmembrane segment IIS6 of the Na<sup>(+)</sup> channel alpha subunit, *The Journal of biological chemistry* 276, 20-27.
245. Yarov-Yarovoy, V., McPhee, J. C., Idsvoog, D., Pate, C., Scheuer, T., and Catterall, W. A. (2002) Role of amino acid residues in transmembrane segments IS6 and IIS6 of the Na<sup>+</sup> channel alpha subunit in voltage-dependent gating and drug block, *The Journal of biological chemistry* 277, 35393-35401.
246. Ikeda, H., Heinke, B., Ruscheweyh, R., and Sandkuhler, J. (2003) Synaptic plasticity in spinal lamina I projection neurons that mediate hyperalgesia, *Science* 299, 1237-1240.
247. Prescott, S. A., and De Koninck, Y. (2005) Integration time in a subset of spinal lamina I neurons is lengthened by sodium and calcium currents acting synergistically to prolong subthreshold depolarization, *The Journal of neuroscience : the official journal of the Society for Neuroscience* 25, 4743-4754.
248. Bosmans, F., Rash, L., Zhu, S., Diochot, S., Lazdunski, M., Escoubas, P., and Tytgat, J. (2006) Four novel tarantula toxins as selective modulators of voltage-gated sodium channel subtypes, *Molecular pharmacology* 69, 419-429.
249. Gurevitz, M. (2012) Mapping of scorpion toxin receptor sites at voltage-gated sodium channels, *Toxicon* 60, 502-511.
250. Rogers, J. C., Qu, Y., Tanada, T. N., Scheuer, T., and Catterall, W. A. (1996) Molecular determinants of high affinity binding of alpha-scorpion toxin and sea anemone toxin in the S3-S4 extracellular loop in domain IV of the Na<sup>+</sup> channel alpha subunit, *The Journal of biological chemistry* 271, 15950-15962.
251. Saucedo, A. L., Flores-Solis, D., Rodriguez de la Vega, R. C., Ramirez-Cordero, B., Hernandez-Lopez, R., Cano-Sanchez, P., Noriega Navarro, R., Garcia-Valdes, J., Coronas-Valderrama, F., de Roodt, A., Brieba, L. G., Domingos Possani, L., and del Rio-Portilla, F. (2012) New tricks of an old pattern: structural versatility of scorpion toxins with common cysteine spacing, *The Journal of biological chemistry* 287, 12321-12330.
252. Smith, J. J., Cummins, T. R., Alphy, S., and Blumenthal, K. M. (2007) Molecular interactions of the gating modifier toxin ProTx-II with NaV 1.5: implied existence of a novel toxin binding site coupled to activation, *The Journal of biological chemistry* 282, 12687-12697.
253. Wang, J., Yarov-Yarovoy, V., Kahn, R., Gordon, D., Gurevitz, M., Scheuer, T., and Catterall, W. A. (2011) Mapping the receptor site for alpha-scorpion toxins on a Na<sup>+</sup> channel voltage sensor, *Proceedings of the National Academy of Sciences of the United States of America* 108, 15426-15431.
254. Xiao, Y., Blumenthal, K., Jackson, J. O., 2nd, Liang, S., and Cummins, T. R. (2010) The tarantula toxins ProTx-II and huwentoxin-IV differentially interact with human Nav1.7 voltage sensors to inhibit channel activation and inactivation, *Molecular pharmacology* 78, 1124-1134.
255. Xiao, Y., Jackson, J. O., 2nd, Liang, S., and Cummins, T. R. (2011) Common molecular determinants of tarantula huwentoxin-IV inhibition of Na<sup>+</sup> channel voltage sensors in domains II and IV, *The Journal of biological chemistry* 286, 27301-27310.

256. Zhang, J. Z., Yarov-Yarovoy, V., Scheuer, T., Karbat, I., Cohen, L., Gordon, D., Gurevitz, M., and Catterall, W. A. (2011) Structure-function map of the receptor site for beta-scorpion toxins in domain II of voltage-gated sodium channels, *The Journal of biological chemistry* 286, 33641-33651.
257. Chuang, R. S., Jaffe, H., Cribbs, L., Perez-Reyes, E., and Swartz, K. J. (1998) Inhibition of T-type voltage-gated calcium channels by a new scorpion toxin, *Nature neuroscience* 1, 668-674.
258. Sidach, S. S., and Mintz, I. M. (2002) Kurtoxin, a gating modifier of neuronal high- and low-threshold Ca channels, *The Journal of neuroscience : the official journal of the Society for Neuroscience* 22, 2023-2034.
259. Kim, J. I., Konishi, S., Iwai, H., Kohno, T., Gouda, H., Shimada, I., Sato, K., and Arata, Y. (1995) Three-dimensional solution structure of the calcium channel antagonist omega-agatoxin IVA: consensus molecular folding of calcium channel blockers, *Journal of molecular biology* 250, 659-671.
260. Kim, J. I., Takahashi, M., Martin-Moutot, N., Seagar, M. J., Ohtake, A., and Sato, K. (1995) Tyr13 is essential for the binding of omega-conotoxin MVIIC to the P/Q-type calcium channel, *Biochemical and biophysical research communications* 214, 305-309.
261. Gui, J., Liu, B., Cao, G., Lipchik, A. M., Perez, M., Dekan, Z., Mobli, M., Daly, N. L., Alewood, P. F., Parker, L. L., King, G. F., Zhou, Y., Jordt, S. E., and Nitabach, M. N. (2014) A tarantula-venom peptide antagonizes the TRPA1 nociceptor ion channel by binding to the S1-S4 gating domain, *Current biology : CB* 24, 473-483.
262. Priest, B. T., and Kaczorowski, G. J. (2007) Subtype-selective sodium channel blockers promise a new era of pain research, *Proceedings of the National Academy of Sciences of the United States of America* 104, 8205-8206.
263. Middleton, R. E., Warren, V. A., Kraus, R. L., Hwang, J. C., Liu, C. J., Dai, G., Brochu, R. M., Kohler, M. G., Gao, Y. D., Garsky, V. M., Bogusky, M. J., Mehl, J. T., Cohen, C. J., and Smith, M. M. (2002) Two tarantula peptides inhibit activation of multiple sodium channels, *Biochemistry* 41, 14734-14747.
264. Ohkubo, T., Yamazaki, J., and Kitamura, K. (2010) Tarantula Toxin ProTx-I Differentiates Between Human T-type Voltage-Gated Ca<sup>2+</sup> Channels Cav3.1 and Cav3.2, *Journal of Pharmacological Sciences* 112, 452-458.
265. Kim, D., Park, D., Choi, S., Lee, S., Sun, M., Kim, C., and Shin, H. S. (2003) Thalamic control of visceral nociception mediated by T-type Ca<sup>2+</sup> channels, *Science* 302, 117-119.
266. Edgerton, G. B., Blumenthal, K. M., and Hanck, D. A. (2010) Inhibition of the activation pathway of the T-type calcium channel Ca(V)<sub>3.1</sub> by ProTxII, *Toxicon* 56, 624-636.
267. Triggle, D. J., and Rampe, D. (1989) 1,4-Dihydropyridine activators and antagonists: structural and functional distinctions, *Trends in pharmacological sciences* 10, 507-511.
268. Jacques, D., Bkaily, G., Jasmin, G., D'Orleans-Juste, P., and Chahine, M. (2003) Isradipine prevents the development of spontaneously occurring cardiac necrosis in cardiomyopathic hamster, *Canadian journal of physiology and pharmacology* 81, 120-124.
269. Chen, X. L., Bayliss, D. A., Fern, R. J., and Barrett, P. Q. (1999) A role for T-type Ca<sup>2+</sup> channels in the synergistic control of aldosterone production by ANG II and K<sup>+</sup>, *The American journal of physiology* 276, F674-683.
270. Lang, F., Capasso, G., Schwab, M., and Waldegger, S. (2005) Renal tubular transport and the genetic basis of hypertensive disease, *Clinical and experimental nephrology* 9, 91-99.

271. Subramanya, A. R., Yang, C. L., McCormick, J. A., and Ellison, D. H. (2006) WNK kinases regulate sodium chloride and potassium transport by the aldosterone-sensitive distal nephron, *Kidney international* 70, 630-634.
272. Lipkind, G. M., and Fozzard, H. A. (2003) Molecular modeling of interactions of dihydropyridines and phenylalkylamines with the inner pore of the L-type Ca<sup>2+</sup> channel, *Molecular pharmacology* 63, 499-511.
273. Peterson, B. Z., Tanada, T. N., and Catterall, W. A. (1996) Molecular determinants of high affinity dihydropyridine binding in L-type calcium channels, *The Journal of biological chemistry* 271, 5293-5296.
274. Goldmann, S., Born, L., Kazda, S., Pittel, B., and Schramm, M. (1990) Synthesis, pharmacological effects, and conformation of 4,4-disubstituted 1,4-dihydropyridines, *Journal of medicinal chemistry* 33, 1413-1418.
275. Gordeev, M. F., Patel, D. V., England, B. P., Jonnalagadda, S., Combs, J. D., and Gordon, E. M. (1998) Combinatorial synthesis and screening of a chemical library of 1,4-dihydropyridine calcium channel blockers, *Bioorganic & medicinal chemistry* 6, 883-889.
276. Miri, R., Javidnia, K., Sarkarzadeh, H., and Hemmateenejad, B. (2006) Synthesis, study of 3D structures, and pharmacological activities of lipophilic nitroimidazolyl-1,4-dihydropyridines as calcium channel antagonist, *Bioorganic & medicinal chemistry* 14, 4842-4849.
277. Goldmann, S., Stoltefuss, J., and Born, L. (1992) Determination of the absolute configuration of the active amlodipine enantiomer as (-)-S: a correction, *Journal of medicinal chemistry* 35, 3341-3344.
278. Carosati, E., Ioan, P., Micucci, M., Broccatelli, F., Cruciani, G., Zhorov, B. S., Chiarini, A., and Budriesi, R. (2012) 1,4-Dihydropyridine scaffold in medicinal chemistry, the story so far and perspectives (part 2): action in other targets and antitargets, *Current medicinal chemistry* 19, 4306-4323.
279. Triggle, D. J. (2003) Drug targets in the voltage-gated calcium channel family: why some are and some are not, *Assay and drug development technologies* 1, 719-733.
280. Houston, J. B. (1994) Utility of in vitro drug metabolism data in predicting in vivo metabolic clearance, *Biochemical pharmacology* 47, 1469-1479.
281. Powell, K. L., Cain, S. M., Ng, C., Sirdesai, S., David, L. S., Kyi, M., Garcia, E., Tyson, J. R., Reid, C. A., Bahlo, M., Foote, S. J., Snutch, T. P., and O'Brien, T. J. (2009) A Cav3.2 T-type calcium channel point mutation has splice-variant-specific effects on function and segregates with seizure expression in a polygenic rat model of absence epilepsy, *The Journal of neuroscience : the official journal of the Society for Neuroscience* 29, 371-380.
282. Snutch, T. P., and David, L. S. (2006) T-type calcium channels: an emerging therapeutic target for the treatment of pain, *Drug Development Research* 67, 404-415.
283. Di Marzo, V., De Petrocellis, L., and Bisogno, T. (2005) The biosynthesis, fate and pharmacological properties of endocannabinoids, *Handbook of experimental pharmacology*, 147-185.
284. Huang, S. M., Bisogno, T., Trevisani, M., Al-Hayani, A., De Petrocellis, L., Fezza, F., Tognetto, M., Petros, T. J., Krey, J. F., Chu, C. J., Miller, J. D., Davies, S. N., Geppetti, P., Walker, J. M., and Di Marzo, V. (2002) An endogenous capsaicin-like substance with

- high potency at recombinant and native vanilloid VR1 receptors, *Proceedings of the National Academy of Sciences of the United States of America* 99, 8400-8405.
285. De Petrocellis, L., and Di Marzo, V. (2010) Non-CB1, non-CB2 receptors for endocannabinoids, plant cannabinoids, and synthetic cannabimimetics: focus on G-protein-coupled receptors and transient receptor potential channels, *Journal of neuroimmune pharmacology : the official journal of the Society on NeuroImmune Pharmacology* 5, 103-121.
  286. De Petrocellis, L., and Di Marzo, V. (2009) Role of endocannabinoids and endovanilloids in Ca<sup>2+</sup> signalling, *Cell calcium* 45, 611-624.
  287. Zygmunt, P. M., Petersson, J., Andersson, D. A., Chuang, H., Sorgard, M., Di Marzo, V., Julius, D., and Hogestatt, E. D. (1999) Vanilloid receptors on sensory nerves mediate the vasodilator action of anandamide, *Nature* 400, 452-457.
  288. Petrov, R. R., Knight, L., Chen, S. R., Wager-Miller, J., McDaniel, S. W., Diaz, F., Barth, F., Pan, H. L., Mackie, K., Cavasotto, C. N., and Diaz, P. (2013) Mastering tricyclic ring systems for desirable functional cannabinoid activity, *Eur J Med Chem* 69, 881-907.
  289. Francois, A., Kerckhove, N., Meleine, M., Alloui, A., Barrere, C., Gelot, A., Uebele, V. N., Renger, J. J., Eschalier, A., Ardid, D., and Bourinet, E. (2013) State-dependent properties of a new T-type calcium channel blocker enhance Ca(V)<sub>3.2</sub> selectivity and support analgesic effects, *Pain* 154, 283-293.
  290. Khosravani, H. (2003) Gating Effects of Mutations in the Cav3.2 T-type Calcium Channel Associated with Childhood Absence Epilepsy, *Journal of Biological Chemistry* 279, 9681-9684.
  291. Zamponi, G. W., Lory, P., and Perez-Reyes, E. (2010) Role of voltage-gated calcium channels in epilepsy, *Pflugers Archiv : European journal of physiology* 460, 395-403.
  292. King, G. F., Escoubas, P., and Nicholson, G. M. (2008) Peptide toxins that selectively target insect Na(V) and Ca(V) channels, *Channels* 2, 100-116.
  293. Doyle, D. A., Morais Cabral, J., Pfuetzner, R. A., Kuo, A., Gulbis, J. M., Cohen, S. L., Chait, B. T., and MacKinnon, R. (1998) The structure of the potassium channel: molecular basis of K<sup>+</sup> conduction and selectivity, *Science* 280, 69-77.
  294. Payandeh, J., Scheuer, T., Zheng, N., and Catterall, W. A. (2011) The crystal structure of a voltage-gated sodium channel, *Nature* 475, 353-358.
  295. Bladen, C., Hamid, J., Souza, I. A., and Zamponi, G. W. (2014) Block of T-type calcium channels by protoxins I and II, *Molecular brain* 7, 36.
  296. Katz, B. (1979) Elementary components of synaptic transmission, *Die Naturwissenschaften* 66, 606-610.
  297. Catterall, W. A. (1984) The molecular basis of neuronal excitability, *Science* 223, 653-661.
  298. Olivera, B. M., Miljanich, G. P., Ramachandran, J., and Adams, M. E. (1994) Calcium channel diversity and neurotransmitter release: the omega-conotoxins and omega-agatoxins, *Annual review of biochemistry* 63, 823-867.
  299. King, G. F. (2011) Venoms as a platform for human drugs: translating toxins into therapeutics, *Expert opinion on biological therapy* 11, 1469-1484.
  300. Schmalhofer, W. A., Calhoun, J., Burrows, R., Bailey, T., Kohler, M. G., Weinglass, A. B., Kaczorowski, G. J., Garcia, M. L., Koltzenburg, M., and Priest, B. T. (2008) ProTx-II, a selective inhibitor of NaV1.7 sodium channels, blocks action potential propagation in nociceptors, *Molecular pharmacology* 74, 1476-1484.

301. McGivern, J. G. (2007) Ziconotide: a review of its pharmacology and use in the treatment of pain, *Neuropsychiatric disease and treatment* 3, 69-85.
302. Miljanich, G. P. (2004) Ziconotide: neuronal calcium channel blocker for treating severe chronic pain, *Current medicinal chemistry* 11, 3029-3040.
303. Minett, M. S., Nassar, M. A., Clark, A. K., Passmore, G., Dickenson, A. H., Wang, F., Malcangio, M., and Wood, J. N. (2012) Distinct Nav1.7-dependent pain sensations require different sets of sensory and sympathetic neurons, *Nature communications* 3, 791.
304. Yang, Y. C., Hsieh, J. Y., and Kuo, C. C. (2009) The external pore loop interacts with S6 and S3-S4 linker in domain 4 to assume an essential role in gating control and anticonvulsant action in the Na(+) channel, *The Journal of general physiology* 134, 95-113.

## APPENDIX A: PUBLICATIONS OVER THE SPAN OF THIS THESIS

- Bladen, Chris**; McDaniel, Steven; Gadotti, Vinicius; Petrov, Ravil; Berger, N.; Diaz, Philippe; Zamponi, Gerald. Characterization of novel cannabinoid based selective T-type calcium channel ligands with analgesic effects." ACS Chem Neurosci 2014. Oct 14. Epub 2014 Oct 14.
- Agustin Garcia-Caballero, Vinicius M Gadotti, Patrick Stemkowski, Norbert Weiss, Ivana Souza, Victoria Hodgkinson, **Chris Bladen**, Lina Chen, Jawed Hamid, Anne Pizzoccaro, Mickael Deage, Amaury Francois, Emmanuel Bourinet and Gerald W Zamponi. The deubiquitinating enzyme USP5 modulates neuropathic and inflammatory pain by enhancing Cav3.2 channel activity. Neuron 2014 Sep;83(5):1144-58
- Chris Bladen**, Vinicius M. Gadotti, Miyase G. Gündüz, N. Daniel Berger, Rahime Şimşek, Cihat Şafak and Gerald W. Zamponi. 1,4-Dihydropyridine derivatives with T-type calcium channel blocking activity attenuate inflammatory and neuropathic pain. Pflügers Archiv 2014. Jul 3. Epub 2014 Jul 3.
- Chris Bladen**, Jawed Hamid, Ivana Assis-Souza, and Gerald W. Zamponi 2014. Block of T-type calcium channels by protoxins I and II. Mol Brain 2014. 9;7:36. Epub 2014 May 9.
- Bladen C**, Gündüz MG, Şimşek R, Şafak C and Zamponi GW. 2013. Synthesis and evaluation of 1,4-Dihydropyridine derivatives with calcium channel blocking activity. Pflügers Archiv 2014. Jul 23;466(7):1355-63. Epub 2013 Oct 23 <http://dx.doi.org/10.1007/s00424-013-1376-z>
- Bladen C**, Taking a bite out of pain: Snake venom can be both a curse and a cure when targeting acid sensing ion channels (ASICs) in the pain pathway. Channels 2013 7:1-2.
- Norbert Weiss, Stefanie A.G. Black, **Chris Bladen**, Lina Chen and Gerald W. Zamponi. Surface expression and function of Cav3.2 T-type calcium channels is controlled by asparagine-linked glycosylation. Pflügers Archiv 2013. 465(8):1159-70.
- Bladen C**, Zamponi GW. Common mechanisms of drug interactions with sodium and T-type calcium channels. Mol Pharmacol 2012. 82:481-7.
- Michael E. Hildebrand, PhD, Paula Smith, PhD, **Chris Bladen**, BSc, Cyrus Eduljee, PhD, Jennifer Xie, PhD, Clint Doering, PhD, Janette Mezeyova, BSc, Molly Fee-Maki, BSc, Yongbao Zhu, PhD, F. Belardetti, PhD, Hassan Pajouhesh, PhD, David Parker, PhD, Manjeet Parmar, PhD, Frank Porreca, PhD, Elizabeth Tringham, PhD, Gerald Zamponi, PhD, Terrance P. Snutch, PhD. A novel slow-inactivation specific ion channel modulator attenuates neuropathic pain in rats. PAIN 2011. 152: 833–843.